

**Study of Advanced Drug Delivery of Liposomes
by Maleimide Modification**

マレイミド修飾によるリポソームの先進的薬物運搬に関する研究

A Thesis
Presented to
Waseda University

July 2013

Tianshu LI

李 天舒

**Study of Advanced Drug Delivery of Liposomes
by Maleimide Modification**

マレイミド修飾によるリポソームの先進的薬物運搬に関する研究

A Thesis

Presented to

Waseda University

July 2013

Waseda University

Graduate School of Advanced Science and Engineering

Major in Life Science and Medical Bioscience

Research on Biomolecular-Assembly

Tianshu LI

李 天舒

Promoter: Prof. Dr. Shinji Takeoka

Referees: Prof. Dr. Yasuo Ikeda

Prof. Dr. Nobuhito Goda

Preface

Drug side-effects or adverse drug reactions especially in anticancer therapy, are severe problems that have caused public attention. It has been reported that serious drug-side effects are estimated to be one of the major causes of death in the United States, leading to over 100,000 deaths per year. This issue has also resulted in many cases of drug withdrawal in the early period of their reaching the market. In order to overcome these disadvantages, many efforts have been made to reverse this awkward situation in drug R&D. One of the successful strategies is the drug carrier design with ‘smart’ system to prevent the drug from directly attaching to the organs and control the drug release under specific conditions or at target site. For example, the bilayer structural liposome, which is capable to encapsulate or carry nearly any kind of drug, can be functionalized with stimuli-sensitive lipids or moieties, thus the drug release is selective and efficient.

However, there is an important issue that has hindered the further application of most of the nanoparticle-based drug delivery systems. It is the low cellular uptake efficiency and subsequently inadequate dosage at target site after the administration of nanoparticles. Therefore, there is a need for more efficient drug carrier design with enhanced cellular uptake.

Recently, cellular thiols have got a lot of attention for their promoting role on enhanced cellular uptake of a series of thiol-reactive compounds, nanoparticles and peptides. Due to the extensive and considerable existence of thiols on cell surface, this enhanced effect has great potential on biological and pharmaceutical applications. Nevertheless, the mechanism of thiol-mediated enhanced cellular uptake is still not clear yet. That whether it is independent from the conventional endocytosis or it just facilitates the regular internalization routes, requires thorough investigation.

In this research, the author utilized this novel strategy on the design of a ‘smart’ liposome to obtain an advanced drug delivery system both *in vitro* and *in vivo*. Maleimide, which is a thiol-reactive compound, was applied as the key factor of the enhanced cellular uptake. Through this study, the author reveals a successful example of the application of maleimide on liposomal drug carrier in anticancer therapy, and further discusses about the mechanisms of the maleimide-mediated enhanced cellular uptake effect. It is promising that the thorny issue that has hampered the development of nano-sized drug carrier can be conquered by this novel technique.

Tianshu Li

Contents

PREFACE

CHAPTER 1	PREPARATION AND CHARACTERIZATION OF MALEIMIDE-MODIFIED LIPOSOMES	OF 1
1.1.	Introduction	3
1.1.1.	Overview	3
1.1.2.	Preparation of liposomes	5
1.1.2.1.	Classification of liposomes	5
1.1.2.2.	Preparation methods	6
1.1.3.	Chracterization of liposomes	8
1.1.3.1.	Size distribution	8
1.1.3.2.	Drug encapsulation efficiency	8
1.1.3.3.	Drug-lipid ratio	8
1.1.3.4.	Stability	8
1.1.3.5.	Stimuli-sensitivity	9
1.2.	Preparation of maleimide-modified liposomes	9
1.2.1.	Methods and materials	9
1.2.2.	Preparation	10
1.3.	Characterization of maleimide-modified liposomes	11
1.3.1.	Methods	11
1.3.1.1.	Size of the liposomes	11
1.3.1.2.	Stability of liposomal DOX	11
1.3.1.3.	Zeta potential of the liposomes	11
1.3.2.	Results	12
1.3.2.1.	Size distribution and dispersibility of the liposomes	12
1.3.2.2.	Stability of liposomal DOX	13
1.3.2.3.	Zeta potential of the liposomes	14
1.4.	Summary	15
	References	15

5.3.1. Methods	86
5.3.1.1. Study for the influence of thiol-reactive compounds on cell surface thiols	86
5.3.1.2. Study for the influence of NEM on cellular uptake of liposomes	86
5.3.2. Results	87
5.3.2.1. Study for the influence of thiol-reactive compounds on cell surface thiols	87
5.3.2.2. Study for the influence of NEM on cellular uptake of liposomes	88
5.4. Summary	88
References	90
CHAPTER 6 CONCLUSIONS AND PROSPECT	93
6.1. Conclusions	94
6.1.1. Physical and biological evaluation of maleimide-modified liposome	94
6.1.2. Mechanisms of maleimide-mediated enhanced drug delivery	95
6.2. Propsect	97
6.2.1. Application of thiol-reactive moieties on advanced drug delivery system	97
6.2.2. Further investigation of the biological function of cellular thiols	98

ACADEMIC ACHIEVEMENTS

ACKNOWLEDGEMENT

Chapter 1 Preparation and characterization of maleimide-modified liposomes

1.1. Introduction

1.1.1. Overview

1.1.2. Preparation of liposomes

1.1.2.1. Classification of liposomes

1.1.2.2. Preparation methods

1.1.3. Characterization of liposomes

1.1.3.1. Size distribution

1.1.3.2. Drug encapsulation efficiency

1.1.3.3. Drug-lipid ratio

1.1.3.4. Stability

1.1.3.5. Stimuli-sensitivity

1.2. Preparation of maleimide-modified liposomes

1.2.1. Methods and materials

1.2.2. Preparation

1.3. Characterization of maleimide-modified liposomes

1.3.1. Methods

1.3.1.1. Size distribution of the liposomes

1.3.1.2. Stability of liposomal DOX

1.3.1.3. Zeta potential of the liposomes

1.3.2. Results

1.3.2.1. Size distribution and dispersibility of the liposomes

1.3.2.2. Stability of liposomal DOX

1.3.2.3. Zeta potential of the liposomes

1.4. Summary

References

1.1. Introduction

1.1.1. Overview

Liposome is a spherical vesicle which is composed of natural or synthesized amphiphilic lipids to form a bilayer structure. It is one of the most commonly used and well investigated carrier for drug delivery. [1] Water-soluble and water-insoluble low molecular weight drugs, DNA, RNA, magnetic particles, ligands, stimuli-sensitive lipids or moieties, and coated lipids such as polyethylene glycol (PEG) can be encapsulated or embedded in the bilayer of liposomes. (Fig.1-1)



Fig. 1-1. Structural illustration of liposome designs.

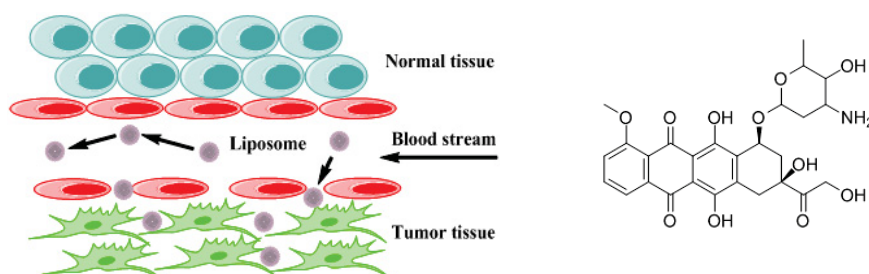


Fig. 1-2. (Left) Illustration of EPR effect; (Right) Chemical structure of doxorubicin (DOX).

Due to its nano-scale size range (usually 50 to 300 nm in diameter), liposomes can extravasate from tumor blood vessels and accumulate in tumors, infarcted or inflamed regions instead of normal tissues *via* the enhanced permeability and retention (EPR) effect (Fig.1-2). [2] Well known examples of liposome preparations include Doxil[®] and Caelyx[®], which are doxorubicin (DOX) delivery systems in clinical use for anticancer therapy such as ovarian cancer, breast cancer, lung cancer, bladder cancer, multiple myeloma, leukemia, and *et al.*

Chapter 1

Unfortunately, however, rapid clearance of liposomes from the blood circulation by the mononuclear phagocyte system (MPS)* often reduces the drug concentration at the target site to the level much below its effective range. Therefore, a new generation of so called 'long-circulating liposomes' has been developed. [3] These 'long-circulating liposomes' include protective polymer chains (e.g., PEG) that modify the outer surface of the liposomes to shield them from opsonization, and subsequently slow down their clearance by MPS.

*Notes: *Mononuclear phagocyte system (MPS) composes of phagocytic cells mainly located in the reticular connective tissue in lymph nodes and the spleen, which belong to the immune system. It also contains the Kupffer cells of the liver and tissue histiocytes.*

Over the past few decades, stimuli-sensitive liposomes have attracted a great deal of attention due to the requirement for controllable drug delivery and release systems. [4] For example, pH-responsive GGLG-liposomes, which is an amino acid-based zwitterionic liposome containing 1,5-dihexadecyl *N,N*-diglutamyl-lysyl-L-glutamate (Fig.1-3) developed in our laboratory, exhibit enhanced drug release from endosomes by comparison with conventional DPPC-liposomes. [5] As such, pH-responsive GGLG-liposomes display enhanced potency during anticancer therapy. In addition to pH, [5, 6] liposome delivery systems sensitive to other environmental stimuli such as temperature, [7] magnetic fields, [8] redox potential, [9, 10] light, [11, 12] ultrasound [13, 14] or shear [15] have also been developed. The more recent trends in liposome technology might also include the multiple functionalization of liposomes. [16] Strategies such as the conjugation of liposomal surfaces with antibodies or ligands, which increase their selectivity to a specific target, are also widely utilized in the design of functional liposomes. [17-19] However, most of these liposomal modifications are both complicated and expensive. Hence, there is a need for a simple and efficient design method for improved liposomal delivery systems.

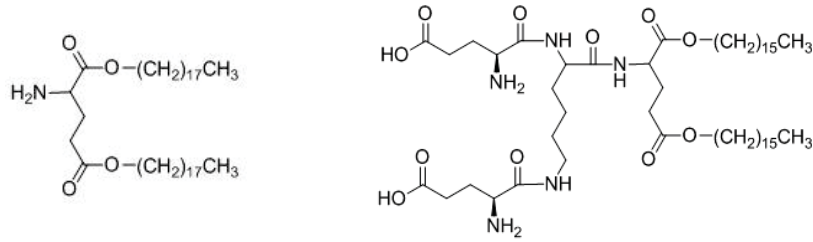


Fig. 1-3. Chemical structure of lipid (left) Glu2C₁₈ and (right) GGLG.

1.1.2. Preparation of liposomes

1.1.2.1. Classification of liposomes

According to the method of liposome preparation or the number of bilayers contained in the liposome, or the size distribution, there are several classifications and definitions of liposomes (Fig.1-4). [20] By the preparation methods, liposomes can be classified to reverse-phase evaporation vesicles (REV), French press vesicle (FPV), and ether injection vesicles (EIV). Based on the number of bilayer, liposomes can be described as unilamellar vesicles (ULV) or multilamellar vesicles (MLV). When unilamellar liposomes are expressed by their size, they can be defined as small unilamellar vesicles (SUV) or large unilamellar vesicles (LUV).

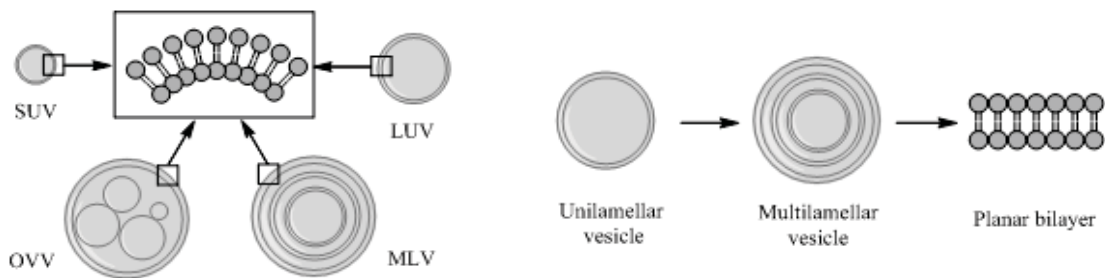


Fig. 1-4. (Left) Illustration of vesicles structures with respect to the shape, size and number of bilayers; SUV, small unilamellar vesicle; LUV; large unilamellar vesicle; MLV, multilamellar vesicle; OVV, oligovesicular vesicle; (Right) Illustration of structure transitions from unilamellar vesicles to multilamellar vesicles, and further to planar bilayers by increasing the lipid concentration. [21]

The transition of ULV to MLV was observed by Regev as shown in Fig.1-4 (right). [22] By comparison to ULV, MLV are usually found in a more concentrated system, while ULV are usually formed in a relatively diluted surfactant solution.

1.1.2.2. Preparation methods

Generally, one key step of the preparation of liposomes is the hydration of homogeneously mixed lipids. In order to mix the lipids homogeneously, all the lipid was first dissolved in organic solvent (e.g., CHCl_3), which is subsequently removed by evaporation. Then the mixed lipid was dissolved in *t*-BuOH, following freeze drying to get a homogeneous mixture in a round bottom flask. After the hydration of the mixed lipids in aqueous buffer/drug solution, bilayer structure can be formed/drugs can be encapsulated in a MLV. The size and drug encapsulation efficiency can be controlled by the rate of hydration and stirring speed. Using this method, the drug encapsulation efficiency is always as low as 10-20%.

Another method for MLV preparation is to mix a two phase systems vigorously, which consists of equal volumes of ether dissolved lipids and an aqueous phase. And then remove the organic (e.g., ether) phase by ventilating nitrogen over the mixture. This technique can receive an increased drug encapsulation efficiency of around 40%, but the disadvantage is that a large amount of organic solvent will be left in the liposome solution, which is not suitable for the further biological and pharmaceutical applications of the liposomes.

Technically, because of the high lipid/drug ratio, less volume for drug encapsulating and low drug release efficiency, MLV is not a preferred vesicle to delivery drugs. Therefore, ULV is more practically employed in liposome researches and clinical applications. Especially, ULV with a diameter less than 500 nm is more often used biologically and pharmaceutically for the increased cellular uptake efficiency in comparison to larger particles.

The preparation of SUV is similar with that of MLV, but needs external energy to reduce the vesicle size and layer such as heat, pressure or sonication. Sonicator can be a bath type or

probe type instruments. For the probe type, unfortunately, the shedding of metal particles in the solution leads to the contamination of liposomes, which is an inevitable problem that has limited the application. On the contrary, the bath type has the advantage of contamination-free, however, the ultrasonic energy is much lower than the probe type and the heat produced during the bath sonication also has to be considered.

Regarding to the drug encapsulation efficiency, LUV, which has a diameter of more than 50 nm is capable of providing larger volume for drug encapsulating than SUV. On the other hand, LUV formation is more economic of lipids usage to carry drugs. Thus it is more commonly used in drug delivery system, which is also preferred in this study for advanced drug delivery.

LUV can be produced from MLV by subsequent extrusion through small size polycarbonate membranes (e.g., 800 nm, 400 nm, 200 nm, 100 nm and 50 nm) under high pressure of nitrogen gas using an extruder.

The encapsulation of drugs in liposomes using pH-gradient method is practical to a variety of drugs. For example, daunorubicin, doxorubicin, epirubicin, mitoxanthrone, vinblastine, chlorpromazine, dibucaine, lidocaine, quinidine, dopamine, serotonin, imipramine, diphenhydramine, quinine, and chloroquine. These organic drugs can become water-soluble by being prepared into hydrochloride salt form, which are stable in acidic aqueous solution. Hence, the formation of pH gradient across the liposome bilayer is a key process for drug encapsulation. In order to create the pH difference (inside acidic), LUV was first prepared in acidic solution, following the exchange of the exterior solution with neutral buffer. The hydrochloride salts of the drugs were then incubated with the liposomes solution in neutral pH at the transition temperature of the liposomes, so that the drugs can more easily penetrate the liposome bilayer to form a stable hydrophilic phase inside the liposomes. The pH-gradient loading is an efficient method for encapsulating water soluble drugs (usually with a more than 90% of the encapsulation efficiency) and practical in scale-up scheme.

1.1.3. Characterization of liposomes

1.1.3.1. Size distribution

The average diameter and size distribution of liposomes are important parameters that contribute to the stability, drug encapsulation efficiency, cellular uptake efficiency and pathway and so on. Dynamic light scattering is always used for the measurement of liposome size when particles are suspended in a solution. Through illumination by light, the scatters light of the particle provide a refraction index which reflects the particle size and can be varied from the suspending solvent.

1.1.3.2. Drug encapsulation efficiency

The proportion of drugs encapsulated in the liposomes can be evaluated after the purification by column chromatography or ultracentrifugation to separate the 'free' drugs that have not been entrapped in liposomes from the drug encapsulating liposomes. The data shows the percentage of encapsulating drugs comparing with the original drug concentration used in the initial stage of drug encapsulation.

1.1.3.3. Drug-lipid ratio

The drug-lipid ratio reflects the encapsulation potency of liposomes. LUV often exhibits higher drug-lipid ratio than SUV due to its larger cavity for drug carrying. The ratio is expressed as the total weight of drug to that of lipids which compose liposomes.

1.1.3.4. Stability

The stability or dispersibility of liposomes is a major consideration that is involved in all steps of the production and administration. On one hand, the aggregation of liposomes results in an increased size which will lead reduced cellular uptake efficiency and accelerated destabilization of liposomes. Therefore, liposomes are preferred to be stored at low

temperature such as 4 °C to retard the aggregation. Moreover, the components of stock solution, pH, and ionic strength might also influence the stability of liposomes. It has been reported that the lipid peroxidation and hydrolysis are two main routes of degradation. Strategies such as removing heavy metals by adding EDTA and protecting liposomes from light, are beneficial to lipid preservation.

On the other hand, drug leakage rate is also an important factor to evaluate the stability of liposomes. For those drugs that are unstable in aqueous solution, freeze drying-thaw or lyophilization-reconstitution is recommended to preserve the liposomes before administration.

1.1.3.5. Stimuli-sensitivity

‘Smart’ design of liposomes includes the insertion of stimuli-sensitive lipids or moieties into liposomes, which trigger drug release in specific milieu. For instance, lipid that is sensitive to pH, temperature, redox potential, magnetic field, or light. To evaluate the pH-sensitivity of these liposomes, the characterization of zeta potential is often employed, which reflects the electric potential of nanoparticle surface.

1.2. Preparation of maleimide-modified liposomes

1.2.1. Methods and materials

The following reagents were purchased: maleimide-PEG₅₀₀₀-carboxyl-NHS from NOF Corporation (Tokyo, Japan); 1,2-dipalmitoyl-sn-glycero-3-phosphocholine (DPPC), 1,2-distearoyl-sn-glycero-3-phosphoethanolamine (DSPE) and cholesterol from Nippon Fine Chemicals (Osaka, Japan); doxorubicin hydrochloride from Sigma-Aldrich (St Louis, MO); XenoLight DiR from Caliper Life Sciences (Hopkinton, MA); and NBD-PE lipid from Avanti Polar Lipids Inc. (Alabaster, Alabama). 1,5-dioctadecyl L-glutamate (Glu2C₁₈), PEG₅₀₀₀-Glu2C₁₈, PEG₅₀₀₀-DSPE, 1,5-dihexadecyl *N,N*-diglutamyl-lysyl-L-glutamate (GGLG) and maleimide-PEG₅₀₀₀-Glu2C₁₈ (Figure 1) were synthesized in our laboratory using

previously published methods [5, 23].

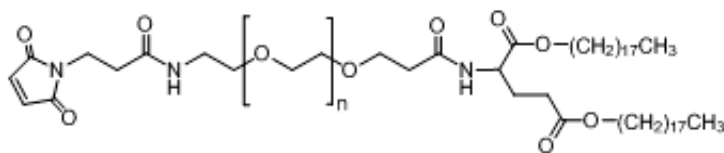
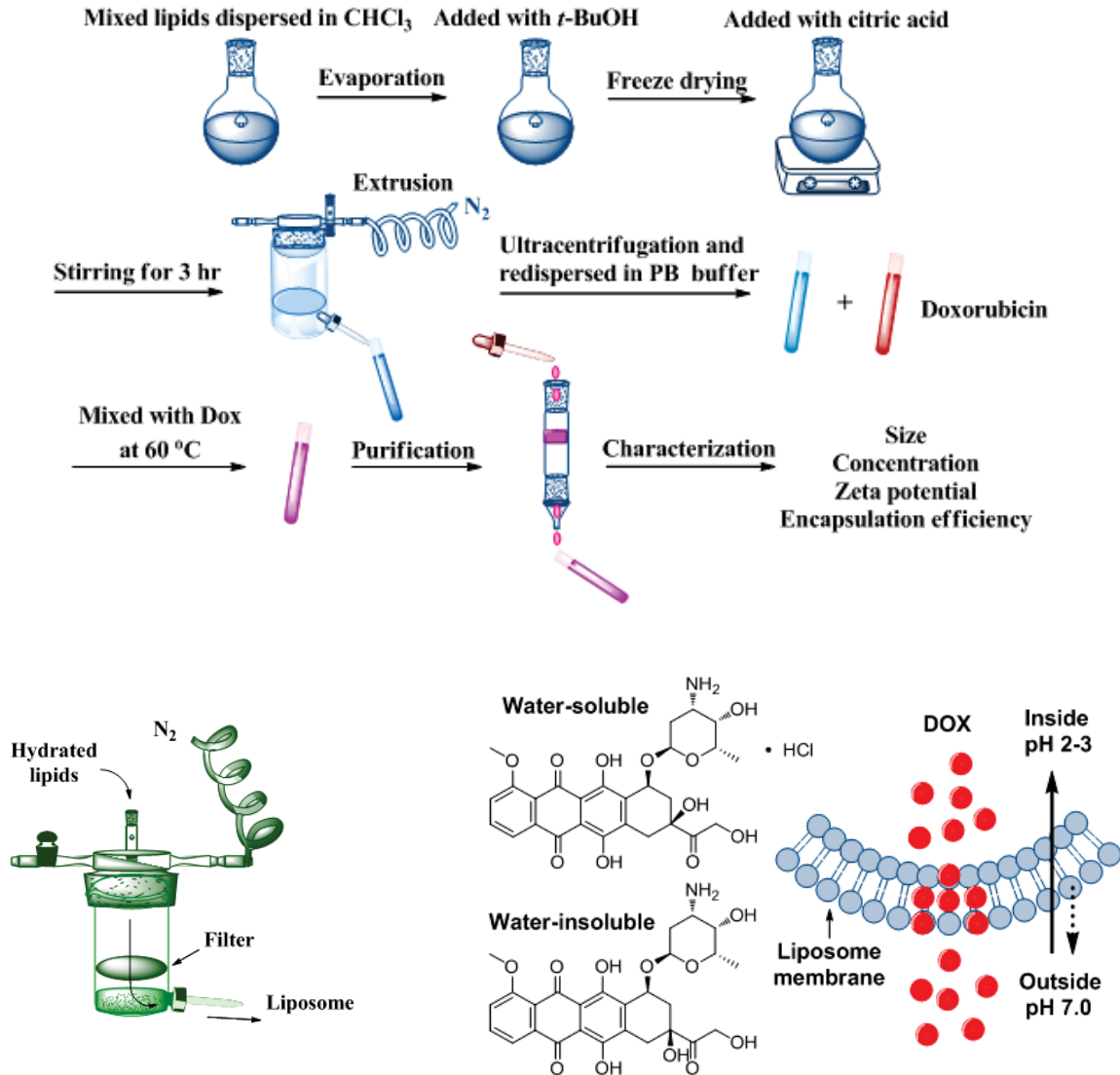


Fig. 1-5. Chemical structure of Mal-PEG₅₀₀₀-Glu2C₁₈.

1.2.2. Preparation

M-GGLG-liposomes were prepared from GGLG, cholesterol, PEG₅₀₀₀-DSPE, maleimide-PEG₅₀₀₀-Glu2C₁₈ at a molar ratio of 5:5:0.03:0.03, stirring at room temperature (rt) for 2-4 hr in a citrate solution (pH 2.2) according to the referenced method. [5] For preparation of GGLG-liposomes, the lipid PEG₅₀₀₀-Glu2C₁₈ was used instead of maleimide-PEG₅₀₀₀-Glu2C₁₈ with the molar ratio of 5:5:0.03:0.03. After hydration and extrusion (Picture 1-1), the liposome dispersion was subject to ultracentrifugation at 49,000 rpm for 30 min. The supernatant was then removed and the pellet was re-dispersed in DPBS for further characterization. Doxorubicin (DOX), a potent anticancer drug, has a limited clinical application due to its severe side effects, such as myelosuppression, cardiotoxicity and gastrointestinal toxicity. [24, 25] We utilized the liposomes as a carrier of DOX to protect the drug from rapid metabolism and reduce its side effects by enhancing selectivity for tumor tissues. For the preparation of DOX-encapsulating liposomes, a liposome suspension ([lipid]=3 mg/mL, 1 mL) and a DOX solution (300 µg/mL, 1 mL) were pre-heated at 60°C for 15 min and then mixed at 60°C for a further 15 min. The resulting mixed solution was allowed to cool to rt overnight and the DOX-encapsulated liposomes were separated from free DOX by gel filtration chromatography using a Sephadex G-25 column. The lipid concentration of the liposomes was calculated from the concentration of cholesterol using a Cholesterol kit from WAKO Pure Chemical Industries, Ltd (Osaka, Japan) according to the manufacturer's instructions. The concentration of DOX encapsulated in the liposomes was

calculated from fluorescent measurements after solubilization of the DOX-liposomes in 0.5% Triton X-100 solution (excitation wavelength, 485 nm; emission wavelength, 590 nm).



Picture 1-1. Illustration of the preparation of liposome and pH-gradient loading of DOX.

1.3. Characterization of maleimide-modified liposomes

1.3.1. Methods

1.3.1.1. Size distribution of the liposomes

The dispersion of liposomes (2 μ L) containing 3 mg/mL of total lipids was diluted in DPBS (1 mL). The mean particle diameter was measured in a disposable plastic cuvette using a

Chapter 1

dynamic light scattering spectrophotometer (N4 PLUS Submicro Particle Size Analyzer, Beckman-Coulter, Fullerton, FL). All measurements were performed in triplicate.

1.3.1.2. Stability of liposomal DOX

The stability of DOX-liposomes was evaluated by the DOX leakage from liposomes in saline at 37 °C. After column purification and ultracentrifugation, GGLG-DOX- and M-GGLG-DOX-liposomes (fc [DOX]=15 µg/mL) were dispersed in saline (5mL) and incubated at 37 °C for 1, 4, 24, 48, 168 and 720 hr. At each time point, 0.5 mL of a solution of DOX-liposomes was drawn and subject to ultrafiltration at 14,000 g for 20 min using an Amicon Ultra-100k tube according to the manufacture's instruction. The leakage rate of DOX was calculated using the eq showed below:

$$\% \text{ Rate of DOX leakage} = [\text{DOX}]_{\text{leaked}}/[\text{DOX}]_{\text{initial}} \times 100\%$$

1.3.1.3. Zeta potential of the liposomes

Zeta potentials of the liposomes at various pH values were calculated with a Zetasizer (Zetasizer4, Malvern, UK). The liposome dispersion in acetic acid-sodium acetate buffers (pH 3.0, 3.5, 4.0, 4.5, 5.0, 5.5, 6.0) or disodium hydrogen phosphate-sodium dihydrogen phosphate buffer (pH 6.5, 7.0, 7.5, 8.0, 8.5, 9.0) was loaded in a capillary cell mounted on the apparatus and measured in triplicate at 37 °C.

1.3.2. Results

1.3.2.1. Size distribution and dispersibility of the liposomes

The size of liposome is an important factor for its physical and biological properties, such as stability, cellular uptake pathway, and metabolism *in vivo*. Nanoparticles, with a mean diameter around 200 nm, are thought to have a similar mechanism of cellular uptake. [26]

As shown in Table 1-1, similar size distributions of M-GGLG- and GGLG-liposomes

were observed, and the mean diameters were around 160-190 nm before and after encapsulation of DOX. Therefore, it was suggested that the particle size would not result in significant change in physical or biological functions of maleimide-modified liposomes. Moreover, M-GGLG-liposomes were as stable as the GGLG-liposomes during storage (ie, 4°C in refrigerator). Specifically, after two months storage at 4°C, no aggregation of the liposomes was detected by measuring the size distribution (Table 1-2). Furthermore, the drug encapsulation efficiency of M-GGLG-DOX-liposomes was as high as 95%, and the leakage ratio of DOX at 37°C one month after drug encapsulation was around 10%, which was slightly lower than that of GGLG-DOX-liposomes (Fig.1-6). Thus, we judged the M-GGLG-DOX-liposomes to be sufficiently stable to conduct further *in vitro* and *in vivo* measurements.

Table 1-1. Size and characteristics of empty liposomes and DOX-encapsulating liposomes. The composition of GGLG-liposome was GGLG/cholesterol/PEG₅₀₀₀-DSPE/PEG₅₀₀₀-Glu2C₁₈ whereas that of M-GGLG-liposome was GGLG/cholesterol/PEG₅₀₀₀-DSPE/ Mal-PEG₅₀₀₀-Glu2C₁₈ at a molar ratio of 5:5:0.03:0.03 in DPBS at room temperature (n=3)

Samples	Size (nm)	DOX-lipid [μg/mg]	Encapsulation efficiency [%]
GGLG-liposome	167.5 ±56.03	-	-
GGLG-DOX-liposome	175.9 ±53.40	94.2	93.3
M-GGLG-liposome	178.6 ±68.79	-	-
M-GGLG-DOX-liposome	188.6 ±66.41	99.2	95.0

Notes: M-GGLG-liposomes showed similar size distribution, ratio of DOX-lipid and drug-encapsulation efficiency with GGLG-liposomes.

Abbreviations: GGLG, pH sensitive lipid 1,5-dihexadecyl *N,N*-diglutamyl-lysyl-L-glutamate; DOX,

anticancer drug doxorubicin; Mal/M, maleimide moiety

Table 1-2. Size distribution of GGLG- and M-GGLG-liposomes after preparation for 30 days storage at 4 °C. (n=3)

Time (d)	GGLG-liposome	M-GGLG-liposome
30	167.9 ±72.3	173.7 ±81.33

1.3.2.2. Stability of liposomal DOX

As shown in Fig. 1-6, the drug leakage of both GGLG-DOX- and M-GGLG-DOX-liposomes was around 5% within 100 hr storage at 37 °C in saline, which indicated the liposomal DOX was relatively stable for short time (i.e., 4 days) incubation. Then the leakage started to accelerate, however, the final leakage rate after one month incubation was only around 15% for GGLG-DOX-liposomes and 10% for M-GGLG-DOX-liposomes. This result suggested that the pH-gradient loading of DOX was efficient and stable, and under physiological conditions (i.e., saline solution at 37 °C), drug release from GGLG- and M-GGLG-liposomes could not be triggered non-specifically.

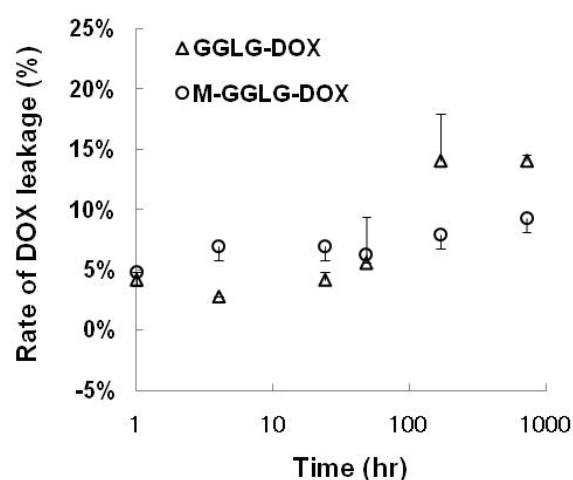


Fig. 1-6. Stability of GGLG-DOX- and M-GGLG-DOX-liposomes in saline at 37 °C. Errors mean SEM. (n=3).

1.3.2.3. Zeta potential of the liposomes

As we reported previously, the GGLG-liposomes are pH-sensitive owing to the presence of zwitterionic lipid GGLG on the liposomal surface. [5]

Zeta potentials of GGLG- and M-GGLG-liposomes increased from negative to positive by decreasing pH value from 9.0 to 3.0 (Fig.1-7). The amount of maleimide in the M-GGLG-liposomes was so low (0.3 mol%) that the zeta potential of M-GGLG-liposomes showed similar values to those of GGLG-liposomes at various pHs, and M-GGLG-liposomes were still sensitive to pH change.

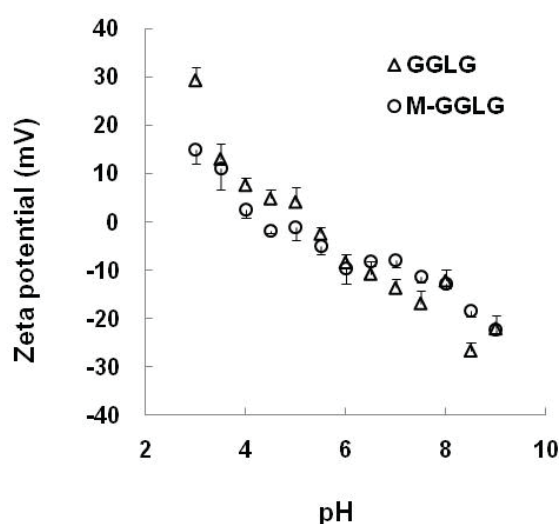


Fig. 1-7. Zeta potentials of GGLG- and M-GGLG liposomes under various pH values at 37 °C. Errors mean SEM. (n=5).

The zeta potentials of both GGLG- and M-GGLG-liposomes became 0 at around pH 5.5, in which condition the aggregation/self-fusion of these liposomes accelerated the most due to the disappearance of the electrostatic repulsion on liposome surfaces. The increasing ratios of the mean diameter of GGLG-liposomes at pH 5.5 were 1.58, 2.09 and 2.35 by comparison to those at physiological pH after preservation at 4 °C for 0.5 hr, 6 hr and 12 hr, respectively. Likewise, the increasing ratios of the mean diameter of M-GGLG-liposomes at the same condition showed above were 1.34, 1.64 and 1.88, respectively.

1.4. Summary

Maleimide-modified liposome (M-GGLG-liposome) was prepared and characterized for its size distribution, drug encapsulation efficiency, drug-lipid ratio, stability, drug leakage rate and pH-sensitivity. The results suggested that with a small amount (0.3 mol%) of maleimide-modification, the physical properties shown above were not influenced significantly, thus physical indexes would not be the key factors that lead a differentiated biological behavior between maleimide-modified and non-modified liposomes.

References

- [1] Torchilin VP. Recent advances with liposomes as pharmaceutical carriers. *Nat Rev Drug Discov.* 2005;4:145-60.
- [2] Maeda H. The enhanced permeability and retention (EPR) effect in tumor vasculature: the key role of tumor-selective macromolecular drug targeting. *Advances in enzyme regulation.* 2001;41:189-207.
- [3] Allen TM. Long-circulating (sterically stabilized) liposomes for targeted drug delivery. *Trends in pharmacological sciences.* 1994;15:215-20.
- [4] Sawant RR, Torchilin VP. Liposomes as 'smart' pharmaceutical nanocarriers. *Soft Matter.* 2010;6:4026-44.
- [5] Obata Y, Tajima S, Takeoka S. Evaluation of pH-responsive liposomes containing amino acid-based zwitterionic lipids for improving intracellular drug delivery in vitro and in vivo. *Journal of Controlled Release.* 2010;142:267-76.
- [6] Connor J, Yatvin MB, Huang L. Ph-Sensitive Liposomes - Acid-Induced Liposome Fusion. *P Natl Acad Sci-Biol.* 1984;81:1715-8.
- [7] Needham D, Anyarambhatla G, Kong G, Dewhirst MW. A new temperature-sensitive liposome for use with mild hyperthermia: characterization and testing in a human tumor xenograft model. *Cancer research.* 2000;60:1197-201.

- [8] Kikumori T, Kobayashi T, Sawaki M, Imai T. Anti-cancer effect of hyperthermia on breast cancer by magnetite nanoparticle-loaded anti-HER2 immunoliposomes. *Breast cancer research and treatment*. 2009;113:435-41.
- [9] Ong W, Yang Y, Cruciano AC, McCarley RL. Redox-triggered contents release from liposomes. *Journal of the American Chemical Society*. 2008;130:14739-44.
- [10] Meng F, Hennink WE, Zhong Z. Reduction-sensitive polymers and bioconjugates for biomedical applications. *Biomaterials*. 2009;30:2180-98.
- [11] Liang X, Yue X, Dai Z, Kikuchi J. Photoresponsive liposomal nanohybrid cerasomes. *Chemical communications*. 2011;47:4751-3.
- [12] Ohya Y, Okuyama Y, Fukunaga A, Ouchi T. Photo-sensitive lipid membrane perturbation by a single chain lipid having terminal spiropyran group. *Supramol Sci*. 1998;5:21-9.
- [13] Huang SL. Liposomes in ultrasonic drug and gene delivery. *Advanced drug delivery reviews*. 2008;60:1167-76.
- [14] Schroeder A, Honen R, Turjeman K, Gabizon A, Kost J, Barenholz Y. Ultrasound triggered release of cisplatin from liposomes in murine tumors. *Journal of Controlled Release*. 2009;137:63-8.
- [15] Holme MN, Fedotenko IA, Abegg D, Althaus J, Babel L, Favarger F, et al. Shear-stress sensitive lenticular vesicles for targeted drug delivery. *Nat Nanotechnol*. 2012;7:536-43.
- [16] Sukhorukov GB, Rogach AL, Garstka M, Springer S, Parak WJ, Munoz-Javier A, et al. Multifunctionalized polymer microcapsules: Novel tools for biological and pharmacological applications. *Small*. 2007;3:944-55.
- [17] Manjappa AS, Chaudhari KR, Venkataraju MP, Dantuluri P, Nanda B, Sidda C, et al. Antibody derivatization and conjugation strategies: Application in preparation of stealth immunoliposome to target chemotherapeutics to tumor. *Journal of Controlled Release*. 2011;150:2-22.
- [18] Huwyler J, Wu DF, Pardridge WM. Brain drug delivery of small molecules using

immunoliposomes. *P Natl Acad Sci USA*. 1996;93:14164-9.

[19] Peeters PA, Oussoren C, Eling WM, Crommelin DJ. Immunospecific targeting of immunoliposomes, F(ab')₂ and IgG to red blood cells in vivo. *Biochimica et biophysica acta*. 1988;943:137-47.

[20] Vemuri S, Rhodes CT. Preparation and characterization of liposomes as therapeutic delivery systems: a review. *Pharmaceutica acta Helvetiae*. 1995;70:95-111.

[21] Segota S, Tezak D. Spontaneous formation of vesicles. *Advances in colloid and interface science*. 2006;121:51-75.

[22] Regev O, Guillemet F. Various bilayer organizations in a single-tail nonionic surfactant: Unilamellar vesicles, multilamellar vesicles, and flat-stacked lamellae. *Langmuir : the ACS journal of surfaces and colloids*. 1999;15:4357-64.

[23] Okamura Y, Maekawa I, Teramura Y, Maruyama H, Handa M, Ikeda Y, et al. Hemostatic effects of phospholipid vesicles carrying fibrinogen gamma chain dodecapeptide in vitro and in vivo. *Bioconjugate chemistry*. 2005;16:1589-96.

[24] Voute PA, Souhami RL, Nooij M, Somers R, Cortes-Funes H, van der Eijken JW, et al. A phase II study of cisplatin, ifosfamide and doxorubicin in operable primary, axial skeletal and metastatic osteosarcoma. *Ann Oncol*. 1999;10:1211-8.

[25] Bruynzeel AME, Niessen HWM, Bronzwaer JGF, van der Hoeven JJMD, Berkhof J, Bast A, et al. The effect of monohydroxyethylrutoside on doxorubicin-induced cardiotoxicity in patients treated for metastatic cancer in a phase II study. *Brit J Cancer*. 2007;97:1084-9.

[26] Rejman J, Oberle V, Zuhorn IS, Hoekstra D. Size-dependent internalization of particles via the pathways of clathrin- and caveolae-mediated endocytosis. *Biochem J*. 2004;377:159-69.

Chapter 2 *In vitro* evaluation of maleimide-modified liposomes

2.1. Introduction

2.2. Study of the cellular uptake properties of maleimide-modified liposomes

2.2.1. Methods

2.2.1.1. Cell culture

2.2.1.2. Cellular uptake of liposomes

2.2.1.3. Confocal laser scanning microscopic observation of cellular internalization of DOX-liposomes

2.2.2. Results

2.3. Study of the intracellular drug release properties of drug encapsulated liposomes

2.3.1. Methods

2.3.1.1. Intracellular drug delivery of DOX-liposomes

2.3.1.2. Cytotoxicity of DOX-liposomes

2.3.2. Results

2.3.2.1. Intracellular drug delivery of DOX-liposomes

2.3.2.2. Cytotoxicity of DOX-liposomes

2.4. Study of the biocompatibility properties of maleimide-modified liposomes

2.4.1. Methods

2.4.2. Results

2.4.2.1. Biocompatibility of empty liposomes

2.4.2.2. Cytotoxicity of NEM

2.5. Discussion and summary

References

2.1. Introduction

The interaction of nanoparticles with cells is well known to be greatly affected by particle size, shape and surface chemistry. These characteristics also influence the intracellular trafficking and biodistribution of nanoparticles. [1-3] However, little is known about the interdependent relationship that these factors have with the biological and pharmaceutical behaviors of nanoparticles. For example, nonspherical particles as large as 3 μm can be internalized into HeLa cells by using several diverse mechanisms of endocytosis; and rod-like particles can show a remarkable superiority on internalization rates. [4] Moreover, nanoparticles with a diameter as large as 500 nm can be internalized by cells via an energy-dependent process. When the diameter is less than 200 nm, the cellular internalization involves clathrin-coated pits. Following the size increasing, the mechanism shifts to caveolae-mediated endocytic pathway, which becomes a predominant intracellular trafficking pathway for the nanoparticles with a diameter of 500 nm. With the increasing size (e.g., > 500 nm) of nanoparticles, the intracellular delivery to lysosomes is no longer apparent. [2]

However, it is ambiguous to define the relationship between the nanoparticle size and cellular uptake efficiency, since the cellular uptake efficiency is also related to the cell species and the components of the nanoparticle. For example, a golden particle can show highest cellular uptake efficiency with a size of 50 nm by comparison to the ones with a diameter of 14 nm and 74 nm. [5] While in a biodegradable polylactic polyglycolic acid (50:50) co-polymer system, gastrointestinal uptake of the particles performs a significantly decreasing efficiency by increasing the size of the particle (i.e., 100 nm, 500 nm, 1 μm , and 10 μm). [6]

In this research, spherical shaped GGLG-liposome and M-GGLG-liposome were prepared with a uniform size distribution and same lipid composition except for the maleimide modification on M-GGLG-liposomes. Therefore, it is expected that only surface chemistry would influence the intracellular trafficking and biodistribution of the liposomes.

Chapter 2

2.2. Study of the cellular uptake properties of maleimide-modified liposomes

2.2.1. Methods

2.2.1.1. Cell culture

HeLa, HCC1954 and MDA-MB-468 cells were maintained in Dulbecco's Modified Eagle's Medium (DMEM) supplemented with 10% fetal bovine serum (FBS) and 1% penicillin-streptomycin. The cells were grown at 37°C in an atmosphere containing 5% CO₂ and passaged by trypsinization with 0.1% trypsin-EDTA.

2.2.1.2. Cellular uptake of liposomes

To quantify the concentration of liposomes internalized in the cells, NBD-PE lipids were homogeneously inserted into liposomes during the preparation of the lipid mixture using a molar ratio of 2%. A standard fluorescence curve for each type of liposome was made to calculate the concentration of liposomes.

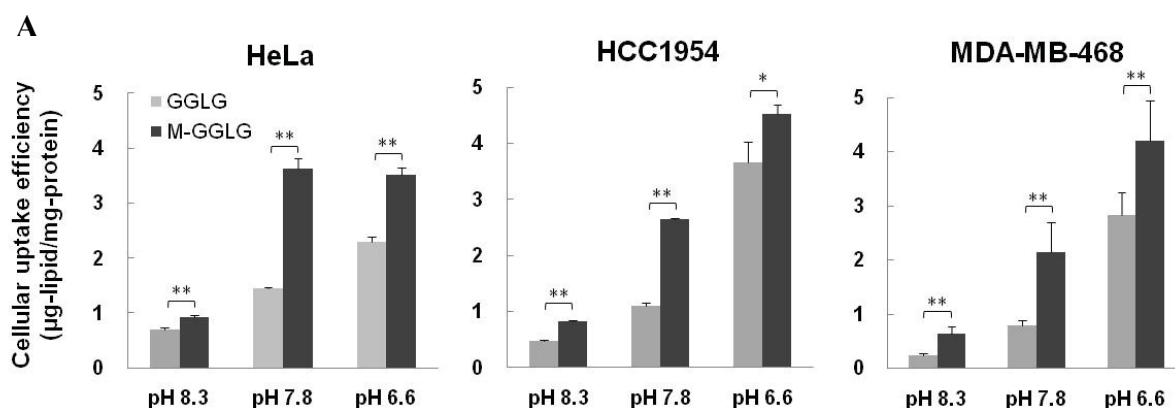
Cells were seeded in 24-well cell culture plates (5×10^4 cells/well) and incubated in an atmosphere of 5% CO₂ at 37°C for 24 hr. Then the medium in the cell culture dish was exchanged with 500 μ L of fresh DMEM (pH 8.3, 7.8 and 6.6, respectively) containing 72 μ g/mL NBD-liposomes in the presence of 10% FBS. Upon incubation at 37°C for 2 hr, the cells were washed twice with PBS and 350 μ L of 0.5% Triton X-100 buffer was added. The amount of liposomes in the cells was fluorometrically determined from the lysate using a fluorescence spectrometer (excitation wavelength, 485 nm; emission wavelength, 590 nm). The protein concentration of the lysate was determined by a standard protein assay (660 nm Pierce Protein Assay, Pierce Biotechnology, Rockford, IL). The cellular uptake efficiency of the liposomes was expressed as lipid- μ g per cellular protein-mg.

2.2.1.3. Confocal laser scanning microscopic observation of cellular internalization of DOX-liposomes

HeLa cells (1×10^5 cells/well) were seeded in a 35-mm cell glass bottom dish and incubated in an atmosphere of 5% CO₂ at 37°C for 24 hr. After removing the medium, fresh DMEM medium containing DOX-liposomes ([DOX]=150 µg/mL) was added to the dish and incubated for 5 min. The cells were then washed three times with DPBS and observed under a confocal laser scanning microscope (FV1000, Olympus, Japan).

2.2.2. Results

The surface charge of nanoparticles is an important factor in terms of their cellular internalization. Positively charged nanoparticles have a tendency to attach themselves to the negatively charged cell membrane. For HCC1954 and MDA-MB-468 cells, GGLG- and M-GGLG-liposomes showed the highest cellular uptake efficiencies at pH 6.6 rather than pH 7.8 or 8.3 (Fig.2-1A). The surfaces of the M-GGLG and GGLG-liposomes were less negatively charged at pH 6.6 than at the higher pH values (Fig.1-7). Thus, the liposomes were more likely to attach to the cell surface and be internalized by cells at the lower pH (ie, pH 6.6). It should be noted that the M-GGLG-liposomes showed significantly increased cellular uptake efficiencies over the GGLG-liposomes in all three cell lines and pH conditions tested.



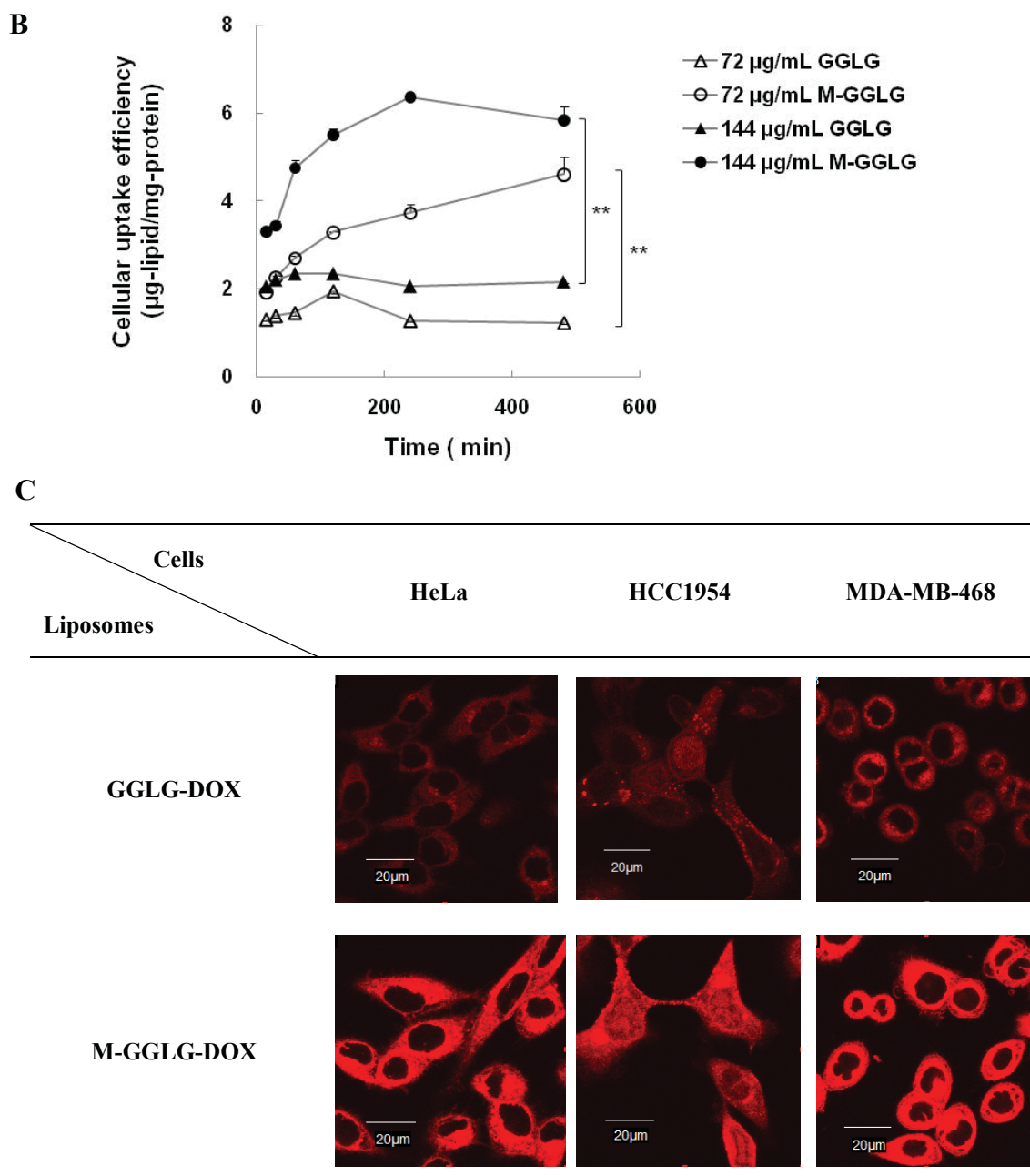


Fig. 2-1. Cellular internalization of liposomes. (A) Cellular uptake efficiency of M-GGLG- and GGLG-liposomes for 2 hr incubation in HeLa, HCC1954, and MDA-MB-468 cells at various pH medium. (B) Time dependence of cellular uptake efficiency of GGLG- and M-GGLG-liposomes in different initial concentrations in HeLa cells at pH 7.8. (n=4). Errors mean SEM. * $p < 0.05$, ** $p < 0.01$. (C) Confocal microscopic observation of rapid cellular uptake of M-GGLG-DOX- and GGLG-DOX-liposomes ([DOX]=150 µg/mL) after 5 min incubation with HeLa, HCC1954 and MDA-MB-468 cells. No morphological change of cells was confirmed after short-time incubation

Chapter 2

with M-GGLG-DOX- and GGLG-DOX-liposomes.

Notes: Both empty and DOX-encapsulating M-GGLG-liposome showed significantly increased cellular uptake efficiency by comparison with that of GGLG-liposome.

The internalization of liposomes occurred as soon as the liposomes were attached to the cell surface. For example, M-GGLG-liposomes exhibited a rapid cellular internalization within a short time of attaching to the cell surface (Fig.2-1C), which then continued for at least 8 hr (Fig.2-1B). By contrast, the cellular internalization of GGLG-liposomes was much lower, reaching a maximum after 2 hr.

2.3. *Study of the intracellular drug release properties of drug encapsulated liposomes*

Doxorubicin (DOX) is a broadly used anticancer drug, which is an anthracycline antibiotic, closely related to the natural product daunomycin. It is commonly used in the treatment of a wide range of cancers, including hematological malignancies, various types of carcinoma, and soft tissue sarcomas. Like all anthracyclines, it works by intercalating DNA (Fig.2-2A), and may lead the most serious adverse effect of life-threatening damage such as myelosuppression, cardiotoxicity, and gastrointestinal toxicity. [7, 8] Therefore, the liposomal formulation for DOX delivery is extremely needed for the controlled drug release to reduce the side effect.

There is another issue subsequently emerged however, that the efficient intracellular drug release after liposome trafficking into the target tissue or cells. One of the obstacles is the destabilization and metabolism of the cargos by the degradative enzymes lysosomes such as lipase, carbohydrates, proteases, and nucleases in. For most of the nanoparticles, endocytosis is a main pathway for the intracellular trafficking. Others include penetration, membrane fusion and destabilization and so on. Thus, efficient escape of liposomes and/or drug release from lysosomes is a key factor that determines the intracellular drug delivery efficiency of liposomal delivery system, which needs to be well investigated for further application.

Chapter 2

2.3.1. Methods

2.3.1.1. Intracellular drug delivery of DOX-liposomes

HeLa cells (1×10^5 cells/well) were seeded in a 35-mm cell glass bottom dish and incubated in an atmosphere of 5% CO₂ at 37°C for 48 hr. After removing the medium, fresh DMEM medium containing DOX-liposomes ([DOX]=100 µg/mL) was added to the dish and incubated for 8 hr. The cells were then washed three times with DPBS and fixed with 4% formalin solution at room temperature for 20 min. The fluorescent intensity of DOX was measured through a confocal laser scanning microscope (FV1000, Olympus, Japan). The intracellular drug release efficiency was calculated by calculating the total fluorescent intensity of DOX internalized in the whole cell and DOX released into the nucleus. The ratio of [DOX] released into the nucleus was expressed as the percentage of [DOX]nucleus/[DOX]cell.

2.3.1.2. Cytotoxicity of DOX-liposomes

HeLa, HCC1954 and MDA-MB-468 cells were seeded in 96-well cell culture plates (1×10^4 cells/well) and incubated in an atmosphere of 5% CO₂ at 37°C for 24 hr. Then the medium in the cell culture dish was exchanged with 100 µL fresh DMEM containing the DOX-liposomes ([DOX] = 0.01, 0.05, 0.1, 0.5, 1.0, 5.0, 10.0 µg/mL) in the presence of 10% FBS. After incubation at 37°C for 24 hr, the cells were washed twice with DPBS and 100 µL of fresh DMEM medium was then added. The cells were then incubated for a further 24 hr. Cell viability was tested using a WST-8 assay kit (Cell Counting Kit-8, Dojindo Molecular Technologies, Inc, Osaka, Japan), according to the manufacturer's instructions. After adding 10 µL WST-8 to each well followed by a 2 hr incubation, the absorbance of each sample was measured at a wavelength of 450 nm using a microplate reader (Benchmark Plus, Bio-Rad). The cell viability was calculated using following eq:

$$\% \text{ Cell viability} = (\text{Abs}[\text{cells+liposome+WST}] - \text{Abs}[\text{cells}]) / (\text{Abs}[\text{cells+WST}] - \text{Abs}[\text{cells}])$$

x100%

2.3.2. Results

2.3.2.1. Intracellular drug delivery of DOX-liposomes

In my experiments, the intracellular drug release of DOX-liposomes was evaluated by calculating the DOX concentration in nucleus, which is the final subcellular location for DOX to exert its cytotoxicity through Confocal Microscopic observation. The results were expressed as the average proportion of [DOX] in nucleus to that in the whole cell after 8 hr incubation of DOX-liposomes in HeLa cells. The number of samples was 70 cells for each experimental group.

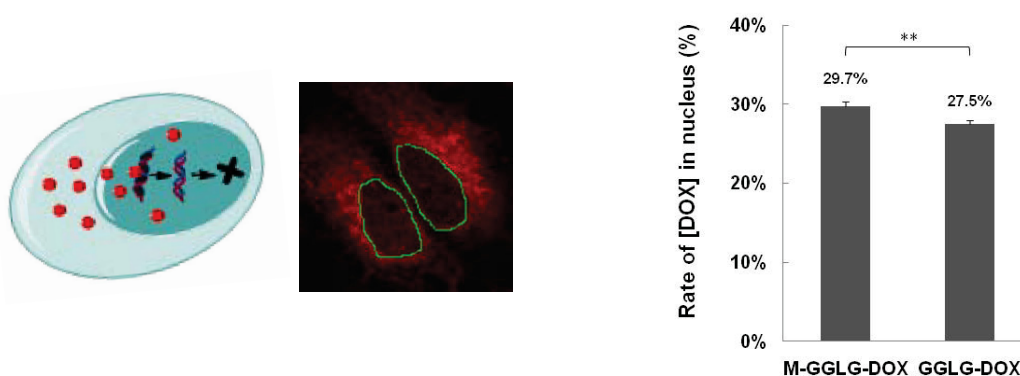


Fig. 2-2. (A) The cytotoxic mechanism of DOX and confocal microscopic observation of subcellular distribution of DOX delivered by M-GGLG-liposomes; (B) Rate of [DOX] in nucleus after incubation of DOX-liposomes with HeLa cells at 37 °C for 8 hr. The drug release efficiency was calculated by measuring the total fluorescent intensity of DOX internalized in the whole cell and DOX released into the nucleus using Confocal Microscopy. The ratio of [DOX] released into the nucleus was expressed as the percentage of [DOX]_{nucleus}/[DOX]_{cell}. Errors mean SEM. n=70. ***p* < 0.01.

As shown in Fig.2-2B, the nuclear distribution of DOX exhibited a slightly but significantly increase for M-GGLG-DOX-liposomes by comparison with that of GGLG-DOX-liposomes. It was suggested again that the maleimide-modification of liposomes

did not influence the pH-sensitivity of liposomes under subcellular milieu, and the drug release from lysosome to nucleus was not impeded. Interestingly, the slight increasing of the intracellular delivery efficiency of M-GGLG-DOX-liposomes also indicated a more potent membrane fusion capability with endosomes/lysosomes by the maleimide-modification of liposome.

2.3.2.2. Cytotoxicity of DOX-liposomes

Doxorubicin is a low molecular weight compound that enters the cell nucleus, intercalates into the DNA and thereby triggers apoptosis. Thus, the drug delivery efficiency of DOX-liposomes could be evaluated in terms of cytotoxicity caused by the release of DOX from the liposomes into the cytosol and ultimately the nucleus. As shown in Fig.2-3, the cytotoxicity of M-GGLG-DOX-liposomes was significantly higher than that of GGLG-DOX-liposomes in all the cell lines tested. The IC_{50} of GGLG-DOX-liposomes was estimated to be $>18.4 \mu\text{M}$ ($10 \mu\text{g/mL}$), while that of M-GGLG-DOX-liposomes was approximately $9.2 \mu\text{M}$ ($5 \mu\text{g/mL}$) for HeLa and HCC1954 cells, and $1.84 \mu\text{M}$ ($1 \mu\text{g/mL}$) for MDA-MB-468 cells.

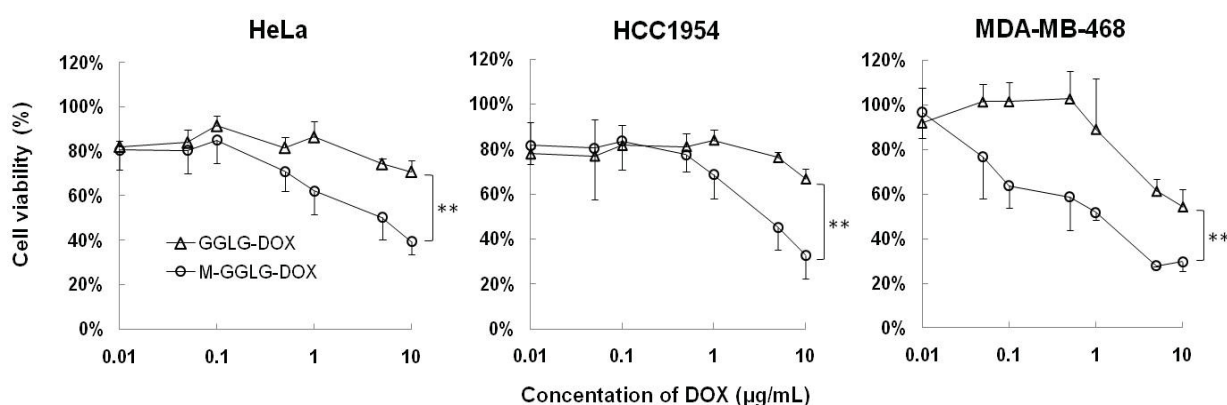


Fig. 2-3. Cytotoxicity of DOX-liposomes for 24 hr incubation with HeLa, HCC1954 and MDA-MB-468 cells at 37 °C. Errors mean SD. (n=4). ** $p < 0.01$.

Chapter 2

Notes: Empty liposomes of both M-GGLG- and GGLG-liposomes were biocompatible at all experimental concentrations which were applied for drug delivery. The significant increased cytotoxicity of DOX-encapsulating M-GGLG-liposomes revealed an advanced *in vitro* drug delivery by maleimide-modification.

2.4. Study of the biocompatibility properties of maleimide-modified liposomes

2.4.1. Methods

HeLa, HCC1954, MDA-MB-468 and COS-7 cells were seeded in 96-well cell culture plates (1×10^4 cells/well) and incubated in an atmosphere of 5% CO₂ at 37°C for 24 hr. Then the medium in the cell culture dish was exchanged with 100 µL fresh DMEM containing empty liposomes (0.72, 7.2, 72, 720 and 1440 mg/L) in the presence of 10% FBS or NEM (1 nM, 10 nM, 100 nM, 1 µM, 10 µM, 20 µM, 50 µM, 100 µM and 1 mM) in the absence of FBS. After incubation at 37°C for 24 hr, the cells were washed twice with DPBS and 100 µL of fresh DMEM medium was then added. The cells were then incubated for a further 24 hr. Cell viability was tested using a WST-8 assay kit (Cell Counting Kit-8, Dojindo Molecular Technologies, Inc, Osaka, Japan), according to the manufacturer's instructions. After adding 10 µL WST-8 to each well followed by a 2 hr incubation, the absorbance of each sample was measured at a wavelength of 450 nm using a microplate reader (Benchmark Plus, Bio-Rad). The cell viability was calculated using the following eq:

$$\% \text{ Cell viability} = \frac{(\text{Abs}[\text{cells} + \text{liposome} + \text{WST}] - \text{Abs}[\text{cells}])}{(\text{Abs}[\text{cells} + \text{WST}] - \text{Abs}[\text{cells}])} \times 100\%$$

2.4.2. Results

2.4.2.1. Biocompatibility of empty liposomes

The cytotoxicity of empty liposomes was observed after a relatively long (i.e., 48 hr) incubation period with the cells (Fig.2-4). The IC₁₀ of empty liposomes was estimated to be

720, 200 and 730 mg/L for GGLG-liposomes, and 1000, 500 and 600 mg/L for M-GGLG-liposomes in HeLa, HCC1954 and MDA-MB-468 cells, respectively. The maximum concentration of the lipids used in the cytotoxicity experiments of DOX-liposomes was around 100 mg/L (calculated by [DOX] and DOX-lipid rate), which was much lower than the IC₁₀ values of empty liposomes (shown above). Therefore, in the cytotoxicity experiments of DOX-liposomes, liposomes alone did not lead to cell death *in vitro* after 24 h incubation, suggesting the observed cytotoxicity was caused by the encapsulated DOX.

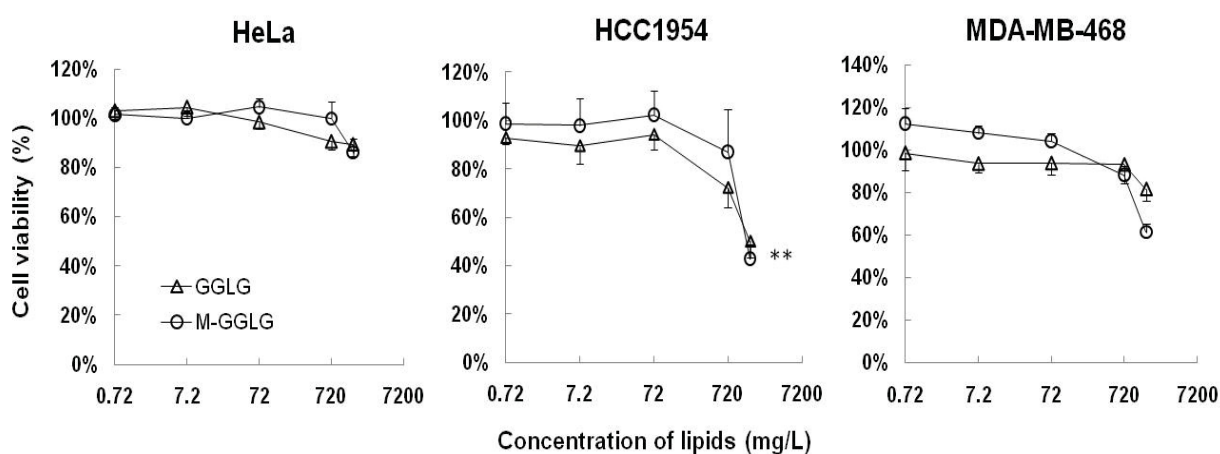


Fig. 2-4. Cytotoxicity of empty liposomes for 48 hr incubation with HeLa, HCC1954 and MDA-MB-468 cells at 37 °C. Errors mean SD. (n=4). ** $p < 0.01$.

Notes: Empty liposomes of both M-GGLG- and GGLG-liposomes were biocompatible at all experimental concentrations which were applied for drug delivery. The significant increased cytotoxicity of DOX-encapsulating M-GGLG-liposomes revealed an advanced drug delivery by maleimide-modification.

2.4.2.2. Cytotoxicity of NEM

As shown in Fig.2-5, no significant cytotoxicity of *N*-ethylmaleimide (NEM) was confirmed within the concentration of 1.25 mg/L (10 μ M) in HeLa, HCC1954 and MDA-MB-468 cells.

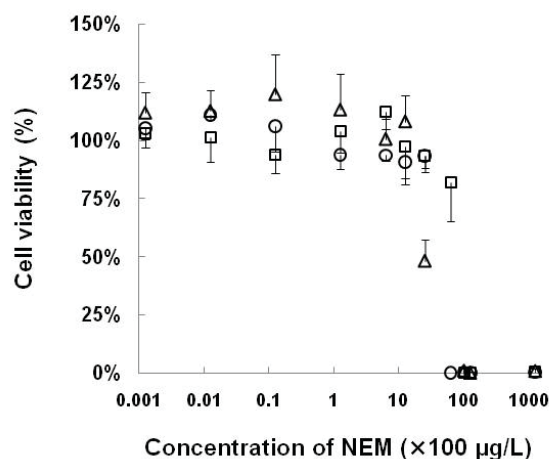


Fig. 2-5. Cell viability of (square) HeLa, (circle) HCC1954, and (triangle) MDA-MB-468 cells after incubation with *N*-ethylmaleimide (NEM) for 24 hr at 37 °C. Errors mean SD (n=4).

Table 2-1. IC₅₀ of NEM in HeLa, HCC1954 and MDA-MB-468 cell lines for 24 hr incubation. The cytotoxicity was tested by Cell Counting Kit-8 according to the manufacturer's instruction.

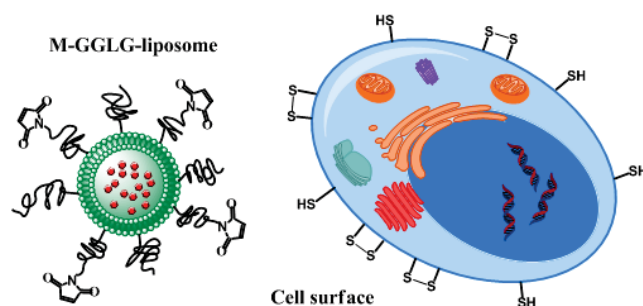
Cell lines	HeLa	HCC1954	MDA-MB-468
IC ₅₀ (mg/L)	6.8	3.7	3.5

2.5. Discussion and summary

The surface structure of the liposome is an important factor that influences their physical and biological properties such as stimuli-sensitivity, stability, cellular uptake efficiency, drug release rate and biodegradation rate. Maleimide is a thiol-reactive moiety that rapidly, covalently and specifically conjugates with the thiol group of cysteine residues. Thus, surface modification with maleimide-PEG provides the liposomes with reactive sites to the cell membrane thiols. We reasoned such a modification might strengthen the association of liposomes with the cell surface. This concept was introduced into the design of liposomes with the expectation of enhanced cellular uptake. [9]

Maleimide-modification at a level of 0.3 mol% of total lipids in the liposomes did not

affect their physical characteristics such as size, drug encapsulation efficiency (Table 1-1), stability (Table 1-2), drug leakage rate (Fig.1-6) and pH-sensitivity (Fig.1-7). Therefore, M-GGLG-liposomes exhibit a similar pH-responsive characteristic upon cellular uptake (Fig.2-1A) and drug release *in vitro* (Fig.2-2) to that of pH-responsive GGLG-liposomes. If we consider that the liposomes are composed of 68.2% GGLG lipid and 4.2% PEG of total lipid weight, 0.3 mol% of maleimide moiety represents only 0.05% of total lipid weight. Thus, it is not surprising that our maleimide modification did not influence the physical properties of the liposomes to any significant extent.



Picture 2-1. Illustration of estimated interaction of M-GGLG-liposome and cell surface thiols.

Nonetheless, the maleimide moiety furnished the liposomes with new biological properties and/or functions. The maleimide moiety on the outer surface of the M-GGLG-liposomes could recognize and conjugate with thiol groups on the cell surface (Picture 2-1). The more rapid and increased duration of cellular uptake observed for the M-GGLG-liposomes (Fig.2-1) implied that the conjugation of maleimide moieties to the cell surface thiols facilitated their cellular internalization. Given that liposomes with a mean size of 100 to 200 nm enter cells mainly *via* clathrin- and/or caveolae-mediated endocytosis, [10] it is possible the thiol-reactive maleimide moiety strengthens the recognition and/or interaction between liposomes and coat proteins on the plasma membrane. It is also hypothesized that the thiol-mediated cellular uptake is independent from conventional

endocytosis. Some other factors such as PDI (protein disulfide isomerase) might also be involved in this movement.

The intracellular DOX release efficiency by M-GGLG-liposomes delivery was slightly but significantly increased in comparison with that by GGLG-liposomes (Fig.2-2B). Thus, it was suggested that maleimide-modification of liposomes has no influence on the subcellular membrane fusion ability. In other words, maleimide-modification did not weaken the fusion ability of M-GGLG-DOX-liposomes with lysosomes, and encapsulating DOX could release into the cytosol and ultimately locate in nucleus as efficiently as non-modified GGLG-DOX-liposomes.

The drug delivery efficiency of DOX-liposomes can be evaluated as the cytotoxicity of DOX-liposomes. First, to estimate the safety of the maleimide moiety applied on M-GGLG-liposomes, the cytotoxicity of empty M-GGLG-liposomes was investigated. Cytotoxicity was only observed after incubation for 48 hr at extremely high concentrations of total lipid i.e., more than 1000, 500 and 600 mg/L for HeLa, HCC1954 and MDA-MB-468 cells, respectively (Fig.2-4). These findings were similar to those obtained for GGLG-liposomes. The concentration of total lipid used for the experiments of cellular uptake efficiency and cytotoxicity of DOX-liposomes were 72 mg/L and 100 mg/L for no more than 24 hr incubation *in vitro*. Hence, we considered the biocompatibilities of GGLG- and M-GGLG-liposomes were sufficiently high in all the cell lines tested to evaluate their biological functions *in vitro*. Furthermore, the concentration of the maleimide moiety on M-GGLG-liposomes used in the studies of tumor growth inhibition and biodistribution were 1.25 mg/L and 41.7 μ g/L, respectively. Both these concentrations were within the safe concentration limit of *N*-ethylmaleimide for cells (Fig.2-5 and Table 2-1). We therefore concluded that the modification of liposomes using 0.3 mol% of maleimide moiety on M-GGLG-liposomes was also biocompatible *in vivo*. Moreover, the increased cytotoxicity of DOX-liposomes *in vitro* (Fig.2-3) was a result of enhanced cellular uptake (Fig.2-1) and

Chapter 2

efficient drug (DOX) release of the M-GGLG-DOX-liposomes (Fig. 2-2). Our experiments show that the maleimide moiety did not contribute to the observed cytotoxicity of the modified liposomes and M-GGLG-DOX-liposomes are more efficient to deliver anticancer drugs *in vitro*.

References

- [1] Geng Y, Dalhaimer P, Cai S, Tsai R, Tewari M, Minko T, et al. Shape effects of filaments versus spherical particles in flow and drug delivery. *Nat Nanotechnol.* 2007;2:249-55.
- [2] Rejman J, Oberle V, Zuhorn IS, Hoekstra D. Size-dependent internalization of particles via the pathways of clathrin- and caveolae-mediated endocytosis. *Biochem J.* 2004;377:159-69.
- [3] Zauner W, Farrow NA, Haines AM. In vitro uptake of polystyrene microspheres: effect of particle size, cell line and cell density. *Journal of controlled release : official journal of the Controlled Release Society.* 2001;71:39-51.
- [4] Gratton SE, Ropp PA, Pohlhaus PD, Luft JC, Madden VJ, Napier ME, et al. The effect of particle design on cellular internalization pathways. *Proc Natl Acad Sci U S A.* 2008;105:11613-8.
- [5] Chithrani BD, Ghazani AA, Chan WC. Determining the size and shape dependence of gold nanoparticle uptake into mammalian cells. *Nano letters.* 2006;6:662-8.
- [6] Desai MP, Labhsetwar V, Amidon GL, Levy RJ. Gastrointestinal uptake of biodegradable microparticles: effect of particle size. *Pharmaceutical research.* 1996;13:1838-45.
- [7] Voute PA, Souhami RL, Nooij M, Somers R, Cortes-Funes H, van der Eijken JW, et al. A phase II study of cisplatin, ifosfamide and doxorubicin in operable primary, axial skeletal and metastatic osteosarcoma. European Osteosarcoma Intergroup (EOI). *Ann Oncol.* 1999;10:1211-8.
- [8] Bruynzeel AM, Niessen HW, Bronzwaer JG, van der Hoeven JJ, Berkhof J, Bast A, et al. The effect of monohydroxyethylrutoside on doxorubicin-induced cardiotoxicity in patients

Chapter 2

treated for metastatic cancer in a phase II study. *Br J Cancer*. 2007;97:1084-9.

[9] Aubry S, Burlina F, Dupont E, Delaroche D, Joliot A, Lavielle S, et al. Cell-surface thiols affect cell entry of disulfide-conjugated peptides. *FASEB journal : official publication of the Federation of American Societies for Experimental Biology*. 2009;23:2956-67.

[10] Rejman J, Oberle V, Zuhorn IS, Hoekstra D. Size-dependent internalization of particles via the pathways of clathrin-and caveolae-mediated endocytosis. *Biochem J*. 2004;377:159-69.

Chapter 3 *In vivo* evaluation of maleimide-modified liposomes

3.1. Introduction

3.1.1. Overview

3.1.2. EPR effect

3.1.3. Intravenous administration

3.1.4. Local administration

3.2. Study of the tumor growth inhibition of drug encapsulating liposomes

3.2.1. Methods

3.2.2. Results

3.3. Study of the biodistribution of maleimide-modified liposomes

3.3.1. Methods

3.3.2. Results

3.4. Summary

References

Chapter 3

3.1. Introduction

3.1.1. Overview

During the past two decades, clinically application of liposomal drug delivery system has been investigated for the treatment of a variety of cancers and sarcomas showed in Table 3-1.

Table 3-1. Approved and emerging liposomal drug delivery system [1]

Product name (active agent)	Composition	Stealth	Application	Trial phase
DaunoXome [®] (daunorubicin)	DSPC/CHOL	No	Kaposi's sarcoma	Approved
DOXIL [®] /Caelyx [®] (doxorubicin)	SoyHPC/CHOL/ DSPE-PEG	Yes	Kaposi's sarcoma	Approved
Myocet [®] /Evacet [®] (doxorubicin)	EPC/CHOL	No	Metastatic breast cancer	Approved
SPI-007 (cisplatin)	SoyHPC/CHOL/ DSPE-PEG	Yes	Head and neck cancer; Lung cancer	Phase I/II
Lipoplatin [™] (cisplatin)	SoyPC/DPPG/CHOL	Yes	Several cancer type	Phase II/III
S-CKD602 (camptothecin analogue)	–	Yes	Several cancer type	Phase I
Aroplatin (oxaliplatin analogue)	DMPC/DMPG	No	Colorectal cancer	Phase II
Depocyt	DOPC/DPPG/CHOL/ triolein	No	Lymphomatous meningitis	Approved
LEP-ETU (paclitaxel)	DOPE/CHOL/cardioliapon	No	Ovarian, breast and lung cancer	Phase I
LEM-ETU (mitoxantrone)	DOPE/CHOL/cardioliapon	No	Leukemia, breast, stomach, liver and ovarian cancer	Phase I
LE-SN38 (irinotecan)	DOPE/CHOL/cardioliapon	No	Advanced cancer	Phase I
MBT-0206 (paclitaxel)	DOPE/DO-trimethyl- ammoniumpropane	No	Anti-angiogenic properties; Breast cancer	Phase I
OSI-211 (lurtotecan)	SoyHPC/CHOL	No	Ovarian cancer; Head and neck cancer	Phase II
Marqibo [®] (vincristine)	DSPPC/CHOL/sphingosine	No	Non-Hodgkin's lymphoma	Phase II/III
Atragen [®] (t-retinoic acid)	DMPC, and soybean oil	No	Advanced renal cell carcinoma; Acute pro-myelocytic leukemia	Phase I/II

Chapter 3

INX-0125 (vinorelbine)	DSPPC/CHOL/sphingosine	No	Breast, colon and lung cancer	Preclinical Phase I
INX-0076 (topotecan)	DSPPC/CHOL/sphingosine	No	Advanced cancer	Preclinical
Liposomal- Annamycin [®]	DSPC/DSPG/Tween	No	Breast cancer	Phase II
Ambisome [®] (amphotericin)	SoyHPC/DSPPC/CHOL	No	Fungal infections in immune-compromised patients	Approved
Nyotran [®] (nistatin)	DMPC/DMPG/CHOL	No	Fungal infections in immune-compromised patients	Phase II/III

Most of the liposomal drug delivery system is applied by intravenous (iv) injection. However, the iv injection of liposomes in blood circulation may challenge the stability and fast metabolism of liposomes by mononuclear phagocyte system (MPS) mainly in liver, spleen and lymph nodes. Another concern is the side effect of drug encapsulating liposomes after circulating in the whole body. The accumulation of liposomes and subsequently drug release at the normal organs might lead severe damage to the normal tissue and cause pain or even death of patients. Therefore, proper drug carrier design and administration method are important issues to investigate the clinical application of liposomal drug delivery system.

On the other hand, subcutaneous (sc) administration of PEGylated liposomes appears to be important to target the lymph nodes for administration of antitumor, antibacterial, and antiviral drugs. This administration route is able to achieve sustained drug release *in vivo* and reduce/eliminate the drugs in blood circulatory system. The lymphatic targeting is thought to be beneficial to suppress tumor metastasis since the tumor cells tend to penetrate the lymphatic capillaries to spread in the circulatory system and migrate to other tissues/organs. It has also been reported that sc administration of liposomes can be employed in the field of vaccination and rheumatism, with the aim to form a local drug depot locally and prolong the release of antigens. [2, 3]

3.1.2. *EPR effect*

It was first reported by Prof. Hiroshi Maeda [4] that the tumor vascular permeability is higher than that of normal tissue vascular, which facilitates nanoparticles to penetrate the tumor vessel instead of normal vessel to get an increased retention at tumor site, known as enhanced permeation and retention (EPR) effect. [5]

Most solid tumors have been reported to have elevated levels of vascular permeability factors such as bradykinin, nitric oxide (NO), and peroxynitrite (ONOO⁻). [6-9] Proteinaceous vascular permeability factor (VPF), identified to vascular endothelial growth factor (VEGF), is also actively produced in tumor tissue, whose effect is probably indirectly mediated by extensive production of NO. [10] Besides solid tumor, enhanced vascular permeability can also be observed in granuloma and inflammatory and infected tissues, with resultant extravasation of plasma proteins as well as macromolecules and lipid particles into the interstitial space and clearance via the lymphatic system. [11-14]

3.1.3. *Intravenous administration*

The route of administration of liposomes apparently influenced the distribution, metabolism, and elimination of drugs. Thus, the pharmacodynamics and tissue damage (side effect) can be diverse by different administration routes. Intravenous (iv) injection is mostly applied for a series of drugs clinically for the thoroughly circulation in blood and drug delivery in the whole body. However, nanoparticles such as liposomes can quickly bind to opsonin proteins in the blood serum which leads the rapid clearance from the mononuclear phagocytic system (MPS) after intravenous (iv) injection. [15] Therefore, a new generation of so called 'long-circulating liposomes' has been developed. [16] These 'long-circulating liposomes' include protective polymer chains (eg, PEG) that modify the outer surface of the liposomes to shield them from opsonization, and subsequently slow down their clearance by MPS and increase the blood circulation time. Unfortunately, this PEGylation effect is still limited for

clinical application. Usually only about 5% of the administrated nanoparticles remains to circulate in the blood after iv injection for 12 hr, whereas the majority is eliminated within a few hours by liver, spleen and other organs. [17] There is no doubt that PEGylation is beneficial in most of the iv cases, but the mechanism is still not fully understood. Therefore, the EPR effect of nanoparticles for drug delivery to solid tumor is not always very effective to exert pharmacodynamic effect.

3.1.4. Local administration

By comparison to intravenous (iv) administration, local injection such as subcutaneous (sc), intradermal (id), intraperitoneal (ip) and intramuscular (im) injections, of a high concentration of antineoplastic agents is considered as a relatively effective therapeutic method due to the partial absorption of injected drugs by lymphatic capillaries and subsequently delivery to regional lymph nodes. However, it should be noted that most of the antineoplastic agents have vesicant properties, and tissue damage such as necrosis can be caused. Thus, local administration of the free drug is not feasible. [18] Liposome has a bilayer structure which can separate drugs from directly contact with interstitial tissues and release drug “smartly”, therefore, it is often used to encapsulate antineoplastic agents in order to protect surrounding tissue from the cytotoxic effects of the drugs after local injection.

The nanoparticle with a diameter of less than 100 nm, is suggested to enter blood circulation after sc injection, while with a diameter of more than 100 nm, it is retained and destabilized locally and subsequently flow into lymphatic capillaries and metabolized by macrophages at regional lymph nodes. Thus, the side effect or tissue damage resulted from sc injection of larger liposome encapsulating drug can be eliminated in comparison to that by iv injection.

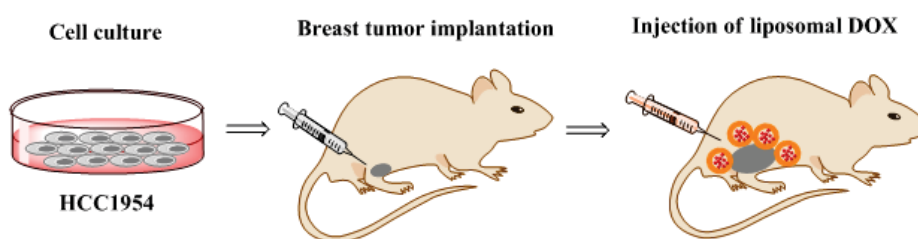
The anatomical site of injection, liposome composition, size and dosage and surface modification, can significantly or slightly influence the lymphatic uptake of liposomes.

[19-21] Generally speaking, following the increasing of the particle size, the lymphatic uptake of nanoparticles becomes slower and the retention at local site becomes longer. Furthermore, saturation of lymphatic uptake and lymph node localization does not occur over a large liposomal lipid dose range, illustrating the efficient performance of lymph nodes in capturing sc administered particles.

3.2. Study of the tumor growth inhibition of drug encapsulating liposomes

3.2.1. Methods

The antitumor effects of DOX-liposomes were evaluated by using tumor-bearing mice (Picture 3-1). HCC1954 cells (5×10^5) in 50 μ L DPBS were mixed with 50 μ L BD Matrigel™ on ice, and then subcutaneously injected into the flank of female BALB/c *nu/nu* mice (5 weeks old, 17-19 g) purchased from Sankyo Labo Service Corp. (Tokyo, Japan). The mice were fed and housed under standard conditions with free access to water and food. In order to distinguish the subtle differences of antitumor effects among various DOX-liposomes, the injection amount, times and frequency were limited. After confirming that the tumor size had increased to 250 mm³, 2 mg DOX/kg was subcutaneously administered twice around the tumor tissue with a two week interval between treatments.



Picture 3-1. Construction of breast cancer model using nude mice.

DPPC-DOX-liposome was applied as a positive control and saline was used as a negative control. The tumor volume (V) was measured and calculated using the eq. below:

$$V (\text{mm}^3) = LW^2/2$$

where L and W indicated the long and short diameters of the tumor tissue, respectively. All the animal experiments were supervised and approved by the local ethical committee of Waseda University

3.2.2. Results

The tumor growth inhibition by DPPC-DOX-, GGLG-DOX- and M-GGLG-DOX-liposomes was evaluated against breast cancer using nude mice. As shown in Fig.3-1, the M-GGLG-DOX-liposomes exhibited an enhanced antitumor effect over GGLG-DOX-liposomes throughout the observation period. In the early stage of tumor growth, the DPPC-DOX-liposomes exerted a relatively strong antitumor activity within a short period after s.c. injections. However, this inhibition of tumor growth was not maintained and the tumor restarted to grow after the second administration of drug. By comparison, the M-GGLG-DOX-liposomes elicited a slightly weaker inhibition of tumor growth than the DPPC-DOX-liposomes in the early stage of treatment. However, the anticancer effect of M-GGLG-DOX-liposomes was more sustained and became more potent than that of DPPC-DOX-liposomes after the final administration. Moreover, the inhibition of tumor growth continued for a further 20 days without any additional injection of M-GGLG-DOX-liposomes, and no increase in tumor volume was observed. Our results suggested that the inhibition of tumor growth by M-GGLG-DOX-liposomes was delayed but more prolonged than that brought about by an equivalent treatment with DPPC-DOX-liposomes.

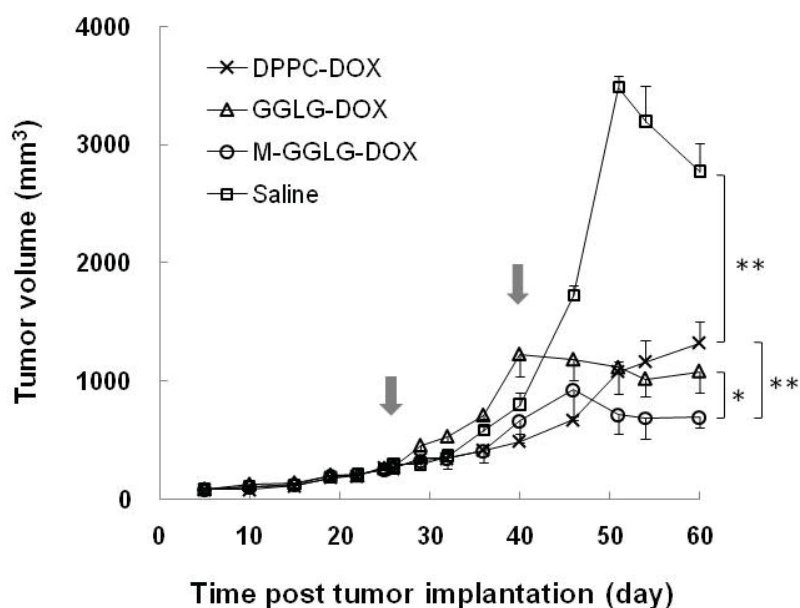


Fig. 3-1. Tumor growth inhibition by sc injection of DOX-liposomes around breast cancer tissues.

Arrows indicated the injection dates. Errors mean SEM. n=4. * $p < 0.05$, ** $p < 0.01$.

Abbreviations: sc, subcutaneous; DPPC, 1,2-dipalmitoyl-sn-glycero-3-phosphocholine.

3.3. Study of the biodistribution of maleimide-modified liposomes

3.3.1. Methods

To visualize the biodistribution and measure the removal rate of liposomes at the injection site, fluorescent liposomes were prepared by adding XenoLight DiR (1,1'-dioctadecyltetramethyl indotricarbocyanine iodide) to the mixed lipids at a molar ratio of 1% of the lipid mixture. The fluorescent liposomes of GGLG or M-GGLG (16 μg) in a volume of 200 μL were injected subcutaneously or intravenously across the longer diameter of the tumor. The biodistribution of liposomes was observed using an IVIS Imaging System (Caliper Lifesciences). The proportion of remaining liposomes at the injection site was expressed as the ratio of residual fluorescence efficiency, calculated using the eq. below:

$$\% \text{ Ratio of residual fluorescence efficiency} = \frac{[\text{total fluorescence efficiency}]_t}{[\text{total fluorescence efficiency}]_{t=0}} \times 100\%$$

3.3.2. Results

After sc injection, the liposomes with a mean diameter of more than 100 nm were mostly accumulated at the injection site (shown in Fig.3-2A), following the recognition and metabolism by the local lymph nodes. [20]

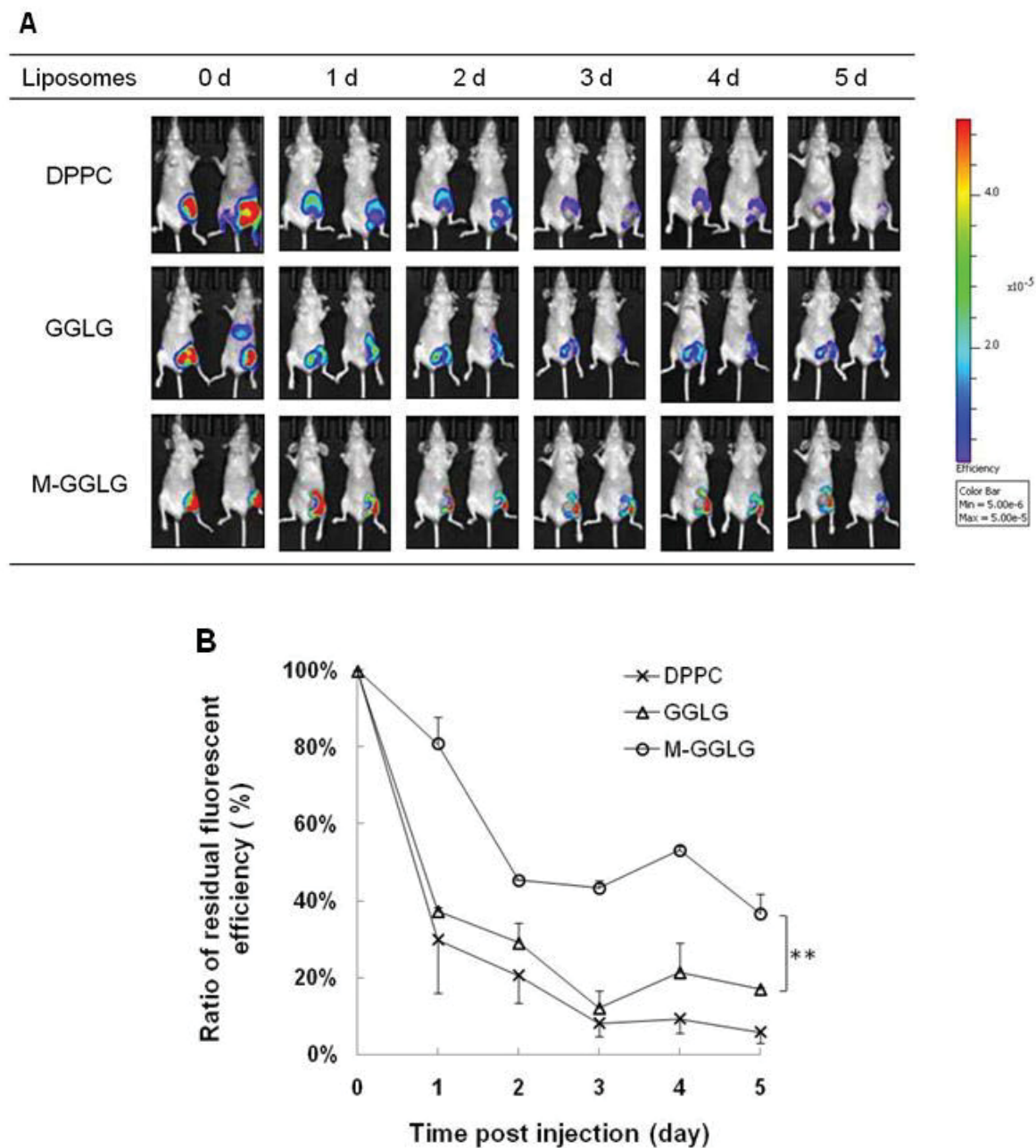


Fig. 3-2. (A) IVIS observation of the biodistribution of DiR-liposomes after s.c. injection around breast cancer tissue. (B) The ratio of residual liposomes at injection site post injection. Errors mean SEM. $n=2$. $**p < 0.01$.

Chapter 3

Notes: M-GGLG-liposomes showed a significant enhanced retention after sc injection for 5 days.

Abbreviations: IVIS, *in vivo* imaging system; DiR, 1,1'-dioctadecyltetramethyl indotricarbocyanine iodide

Within 24 hr after injection, the concentration of DPPC- and GGLG-liposomes sharply decreased with more than half of the liposomes eliminated at the local site. Subsequently, the decomposition of DPPC- and GGLG-liposomes slowed down, and finally, almost 90% of the liposomes were eliminated at the 5th day post injection (Fig.3-2B). By contrast, M-GGLG-liposomes exhibited a significantly slower clearance rate over the entire period i.e., >30% of liposomes were retained five days after sc injection. Our results suggest that M-GGLG-liposomes are retained for much longer at the injection site by comparison with DPPC- and GGLG-liposomes.

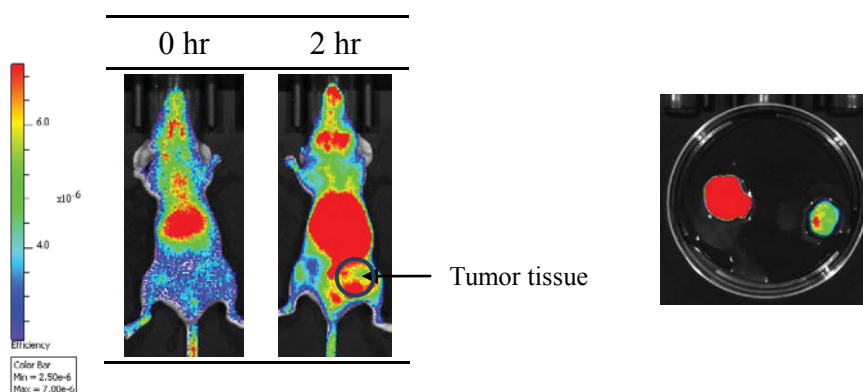


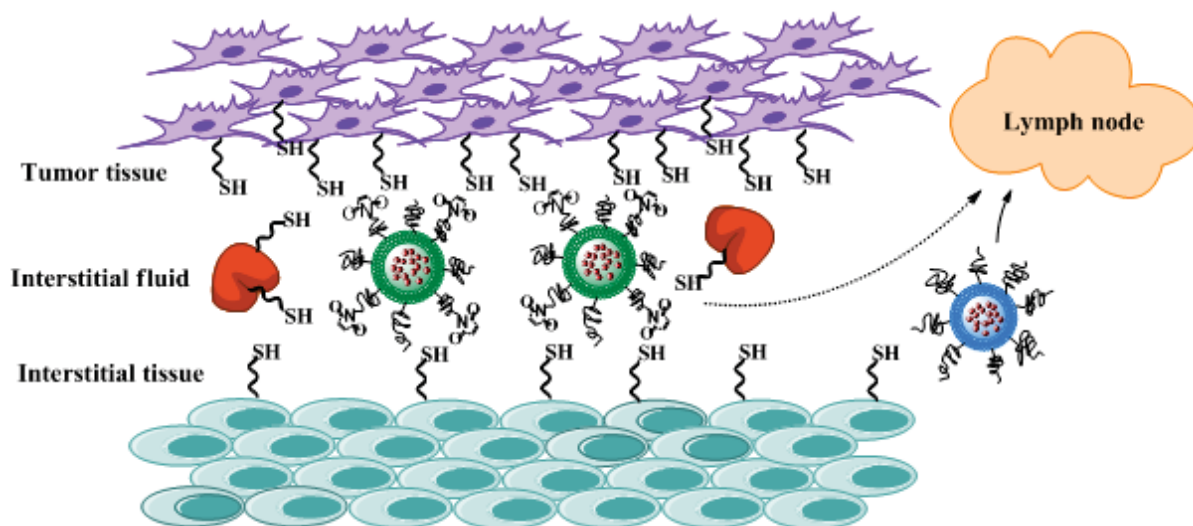
Fig. 3-3. Biodistribution of M-GGLG-liposomes after intravenous injection for 2 hr. The organs showed in the plate are (left) liver and (right) tumor after sacrificing the same mouse in the same period.

For most of the nanoparticle, the fast clearance from MPS in the main digestive organs such as liver and spleen after blood circulation is inevitable, which lead to an extremely low concentration of administrated agents at target site, e.g., solid tumor site. As showed in

Fig.3-3, after iv injection of M-GGLG-liposomes for 2 hr in blood circulation, nearly 90% of the M-GGLG-liposomes were accumulated in the liver or spleen. Although the liposomes can retain at tumor site via the EPR effect, the amount is always not high enough to exert pharmacodynamic effect.

3.4. Summary

By contrast to iv injection (Fig.3-3), sc injection can prevent the liposomes with a mean diameter of above 100 nm from entering the blood circulation directly (Fig.3-2A) and thereby reduce the side effect on normal organs and avoid the rapid clearance of liposomes by MPS in the liver and spleen. Therefore, we considered sc injection as a proper usage of M-GGLG-liposomes to study the in vivo effect. Upon sc injection around the tumor site, liposomes directly diffuse into a limited interstitial area and are either taken up by the tumor tissues or pass through a system of lymphatic vessels to arrive at one or more lymph nodes, and then are taken up and degraded by macrophages via phagocytosis. [21] Shortly after sc injection of liposomes, the concentration of liposomes in the subcutaneous tissues was high, leading to a high rate of degradation by lymph nodes. Gradually, the liposomes were assimilated and the concentration decreased, resulting in a decrease in the degradation rate. Although the clearance of DPPC- and GGLG-liposomes occurred via logarithmic elimination (Fig.3-2B), the M-GGLG-liposomes exhibited a more complicated and slower mode of degradation. Because the lipid composition of M-GGLG- and GGLG-liposomes was the same and the size distribution and other physical properties were similar (Table 1-1), thus only maleimide-moiety was considered as a key factor that resulted in the different biological properties of M-GGLG-liposomes.



Picture 3-2. Schematic of the estimated *in vivo* interactions of liposomes with surrounding tissues and interstitial fluid. Green vesicles, M-GGLG-liposomes; Blue vesicles, GGLG-liposomes; Orange particles, interstitial fluid proteins/factors; Red dots (inside liposomes), DOX.

It is hypothesized that due to the high reactivity of maleimide to thiols on cysteines, after sc injection around breast tumor, M-GGLG-liposomes could conjugate with thiols on tumor and interstitial tissue (mainly adipose tissue) surface, and/or proteins in the interstitial fluid such as albumin, transferrin and globulin (Picture 3-2). In the first case, maleimides immobilize the liposomes to the tissues at the injection site and consequently decrease the absorption of liposomes from lymphatic drainage system. In the second case, maleimide-conjugation with proteins lead to an increase on particle size, which is not beneficial for the liposomes to pass through the interstitium and permeate into the lymphatic capillaries. [22] Therefore, the conjugation of maleimide moiety on the liposome surface might prevent liposomes from lymphatic absorption and destabilization, which resulted in an extended subcutaneous retention of the M-GGLG-liposomes at the injection site. Hence, the extended inhibition of tumor growth elicited by M-GGLG-DOX-liposomes (Fig.3-1) appears to be due to the high retention rate of liposomes around tumor tissue as well as the subsequent enhanced cellular uptake and efficient drug release.

Chapter 3

References

- [1] Immordino ML, Dosio F, Cattel L. Stealth liposomes: review of the basic science, rationale, and clinical applications, existing and potential. *International journal of nanomedicine*. 2006;1:297-315.
- [2] Babai I, Samira S, Barenholz Y, Zakay-Rones Z, Kedar E. A novel influenza subunit vaccine composed of liposome-encapsulated haemagglutinin/neuraminidase and IL-2 or GM-CSF. II. Induction of TH1 and TH2 responses in mice. *Vaccine*. 1999;17:1239-50.
- [3] Corvo ML, Boerman OC, Oyen WJ, Van Bloois L, Cruz ME, Crommelin DJ, et al. Intravenous administration of superoxide dismutase entrapped in long circulating liposomes. II. In vivo fate in a rat model of adjuvant arthritis. *Biochimica et biophysica acta*. 1999;1419:325-34.
- [4] Maeda H. The enhanced permeability and retention (EPR) effect in tumor vasculature: the key role of tumor-selective macromolecular drug targeting. *Advances in enzyme regulation*. 2001;41:189-207.
- [5] Maeda H, Wu J, Sawa T, Matsumura Y, Hori K. Tumor vascular permeability and the EPR effect in macromolecular therapeutics: a review. *Journal of Controlled Release*. 2000;65:271-84.
- [6] Maruo K, Akaike T, Ono T, Maeda H. Involvement of bradykinin generation in intravascular dissemination of *Vibrio vulnificus* and prevention of invasion by a bradykinin antagonist. *Infection and immunity*. 1998;66:866-9.
- [7] Maeda H, Noguchi Y, Sato K, Akaike T. Enhanced vascular permeability in solid tumor is mediated by nitric oxide and inhibited by both new nitric oxide scavenger and nitric oxide synthase inhibitor. *Japanese journal of cancer research : Gann*. 1994;85:331-4.
- [8] Doi K, Akaike T, Horie H, Noguchi Y, Fujii S, Beppu T, et al. Excessive production of nitric oxide in rat solid tumor and its implication in rapid tumor growth. *Cancer*. 1996;77:1598-604.

Chapter 3

- [9] Wu J, Akaike T, Maeda H. Modulation of enhanced vascular permeability in tumors by a bradykinin antagonist, a cyclooxygenase inhibitor, and a nitric oxide scavenger. *Cancer research*. 1998;58:159-65.
- [10] Papapetropoulos A, Garcia-Cardena G, Madri JA, Sessa WC. Nitric oxide production contributes to the angiogenic properties of vascular endothelial growth factor in human endothelial cells. *J Clin Invest*. 1997;100:3131-9.
- [11] Maeda H, Wu J, Okamoto T, Maruo K, Akaike T. Kallikrein-kinin in infection and cancer. *Immunopharmacology*. 1999;43:115-28.
- [12] Maeda H. Role of microbial proteases in pathogenesis. *Microbiol Immunol*. 1996;40:685-99.
- [13] Molla A, Yamamoto T, Akaike T, Miyoshi S, Maeda H. Activation of Hageman-Factor and Prekallikrein and Generation of Kinin by Various Microbial Proteinases. *Journal of Biological Chemistry*. 1989;264:10589-94.
- [14] Peterson HI, Appelgre.KI. Experimental Studies on Uptake and Retention of Labeled Proteins in a Rat Tumor. *European journal of cancer*. 1973;9:543-7.
- [15] Owens DE, 3rd, Peppas NA. Opsonization, biodistribution, and pharmacokinetics of polymeric nanoparticles. *International journal of pharmaceutics*. 2006;307:93-102.
- [16] Allen TM. Long-circulating (sterically stabilized) liposomes for targeted drug delivery. *Trends in pharmacological sciences*. 1994;15:215-20.
- [17] Bae YH, Park K. Targeted drug delivery to tumors: myths, reality and possibility. *Journal of controlled release : official journal of the Controlled Release Society*. 2011;153:198-205.
- [18] Oussoren C, Eling WMC, Crommelin DJA, Storm G, Zuidema J. The influence of the route of administration and liposome composition on the potential of liposomes to protect tissue against local toxicity of two antitumor drugs. *Bba-Biomembranes*. 1998;1369:159-72.
- [19] Oussoren C, Storm G. Lymphatic uptake and biodistribution of liposomes after subcutaneous injection: III. Influence of surface modification with poly(ethyleneglycol).

Chapter 3

Pharmaceutical research. 1997;14:1479-84.

[20] Oussoren C, Zuidema J, Crommelin DJ, Storm G. Lymphatic uptake and biodistribution of liposomes after subcutaneous injection. II. Influence of liposomal size, lipid composition and lipid dose. *Biochimica et biophysica acta*. 1997;1328:261-72.

[21] Oussoren C, Velinova M, Scherphof G, van der Want JJ, van Rooijen N, Storm G. Lymphatic uptake and biodistribution of liposomes after subcutaneous injection - IV. Fate of liposomes in regional lymph nodes. *Bba-Biomembranes*. 1998;1370:259-72.

[22] Oussoren C, Storm G. Liposomes to target the lymphatics by subcutaneous administration. *Advanced drug delivery reviews*. 2001;50:143-56.

Chapter 4 Study of the endocytic mechanism of maleimide-modified liposomes

4.1. Introduction

4.1.1. Overview

4.1.2. Classification of the mechanisms of endocytosis

4.1.3. Inhibitors of endocytosis

4.2. Study of the influence of conventional endocytosis inhibitors on the cellular uptake of maleimide-modified liposomes

4.2.1. Methods

4.2.1.1. Cell culture

4.2.1.2. Study for the endocytic mechanism of liposomes

4.2.1.3. Confocal laser scanning microscopic observation of subcellular distribution of liposomes after cellular internalization

4.2.2. Results

4.2.2.1. Study for the endocytic mechanism of liposomes

4.2.2.2. Lysosomal distribution of liposomes

4.3. Study of the influence of other factors on the cellular uptake of maleimide-modified liposomes

4.3.1. Methods

4.3.1.1. Study for the influence of serum on the cellular uptake of liposomes

4.3.1.2. Study for the influence of temperature block on the cellular uptake of liposomes

4.3.2. Results

4.3.2.1. Study for the influence of serum on the cellular uptake of liposomes

4.3.2.2. Study for the influence of temperature block on the cellular uptake of

liposomes

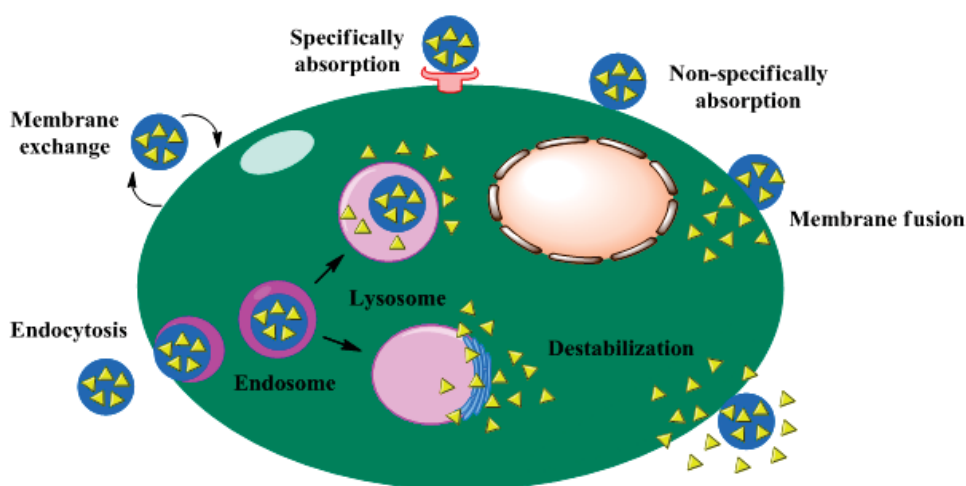
4.4. Summary

References

4.1. Introduction

4.1.1. Overview

Cell membranes are the protective frontiers of cytoplasm and organelles against surrounding stressful milieus. They play a key role in the compartmentalization of cellular chemistry through specific accumulation of proteins on the surfaces (e.g., increasing the affinity of protein to protein interactions) or by the formation of diffusion barriers between their lumina and the cytoplasm. Plasma membrane participates in the exocytosis of secretory proteins and other cellular metabolites, and the endocytosis of exogenous nutrients or cargos. They control and regulate the intracellular trafficking and drug release behavior of nanoparticle-based drug carriers.



Picture 4-1. Illustration of the mechanisms of intracellular drug release from nanoparticles.[1]

As shown in Picuture 4-1, the mechanisms of intracellular trafficking and drug release of nanoparticle-based drug carrier are varied from specifically or non-specifically absorption, membrane exchange, membrane fusion to endocytosis.[1] The trafficking can be energy-dependent or independent. However, it should be noted that for most of the nanoparticles with a diameter of more than 50 nm such as liposomes, active transportation (i.e., endocytosis) is a main intracellular trafficking pathway. Therefore, both efficient

Chapter 4

endocytosis and subsequently drug release from lysosomes are important issues to increase the *in vitro* drug delivery efficiency of liposomes.

Endocytosis is a process of reproduction of internal membranes from the plasma membrane lipid bilayer during the cellular internalization of extracellular fluid together with plasma membrane lipids and integral proteins. Endocytic mechanisms control the composition of lipid and protein on the plasma membrane and thereby determine the interaction of cells with extracellular environments. It can be considered the morphological opposite of exocytosis, which describes the fusion of entirely internal membranes with the plasma membrane, and during which specific chemicals are expelled to the extracellular milieu and transport lipids and proteins are exported to the plasma membrane.

The endocytosis is manipulated by cellular proteins on the plasma membrane which make the achievement of precise regulation of the interactions between the cell and its environment. For example, during the endocytosis of transmembrane receptors, long-term sensitivity of cells to their specific ligands can be simultaneously regulated. Moreover, endocytosis does not simply regulate cellular interactions with the external milieu passively, but also the regulations of endocytosis tend to relate to some seemingly disparate processes such as cell migration, mitosis and antigen presentation. Therefore, it is becoming quite obvious that endocytosis plays important roles in the regulation of a series of intracellular signaling cascades [2]. Additionally, pathogens often employ endocytic pathways to mediate their intracellular internalization [3]. Unfortunately, although the endocytic structures of the cargoes are well studied, the specific mechanisms which are employed by the cargoes in the endocytic processes are less known yet.

4.1.2. *Classification of the mechanisms of endocytosis*

Up to now, many mechanisms of endocytosis has been revealed according to the proteins involved and/or the morphology during the endocytosis. Some of the putative mechanisms of

endocytosis have been shown as below (Fig.4-1). However, there are still some mechanisms left to be further investigated.

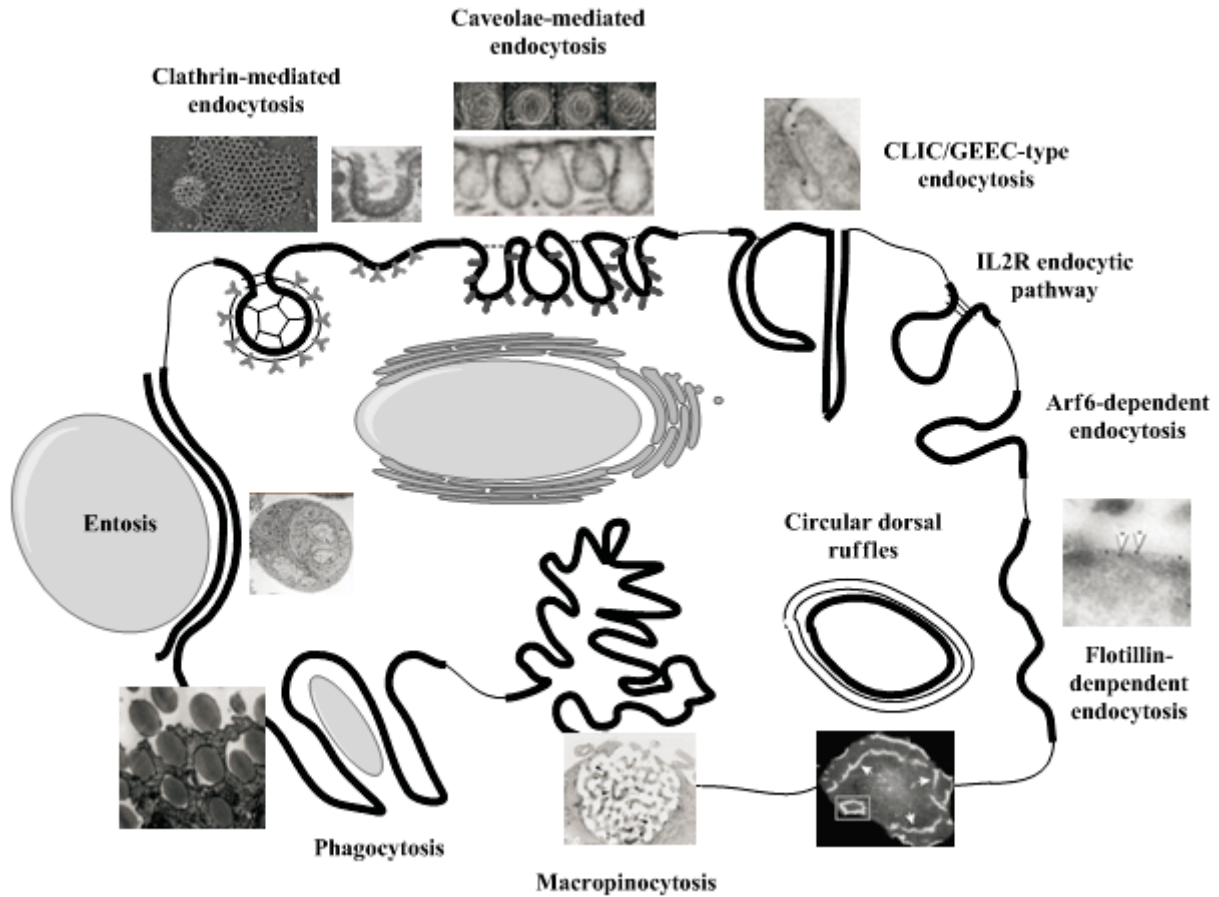


Fig. 4-1. Illustrations of putative endocytic pathways by the implicated protein and morphology.[4] The pictures show the transmission and scanning electron micrographs (TEM and SEM) and fluorescence micrographs of endocytic membrane structures that are considered to be involved in these endocytic events, including clathrin-mediated endocytosis [5], caveolae-type endocytosis [6], CLIC/GEEC-type endocytosis [7, 8], the flotillin-dependent endocytosis [9], phagocytosis, macropinocytosis [10], circular dorsal ruffles [11], and entosis [12]. A summary of each endocytic pathway has been categorized in Table 4-1.

Table 4-1. The putative classifications of endocytosis and morphological and molecular characteristics of each of the endocytic pathways. [4]

Chapter 4

Mechanism	Morphology	Implicated cargos	Small G-protein dependence	Dynamin implicated	Other proteins implicated
Clathrin-mediated	Vesicular	RTKs, GPCRs, transferring receptors, anthrax toxin	Rab5, Arf6 implicated	Well established	Clathrin, AP2, epsin, SNX9, synaptojanin, actin, amphiphysin, plus many others
Caveolae-mediated	Vesicular/tubulovesicular	CTxB, SV40, GPI-linked proteins	Unclear	Some evidence	Caveolins, PTRF, src, PKC, actin
CLIC/GEEC	Tubular/ring like	Fluid phase markers, CTxB, GPI-linked proteins	Cdc42, Arf1	Not as yet	ARHGAP10, actin, GRAF1, other GRAFs
IL2R β pathway	Vesicular?	IL2R β , FC ϵ RI, Kir3,4, γ c-cytokine receptor	RhoA, Rac1	Implicated	PAK1, PAK2
Arf6 dependent	Vesicular/tubular	MHC class I proteins, CD59, carboxypeptidase E	Arf6	Not as yet	Unclear as yet
Flotillin dependent	Vesicular	CTxB, CD59, proteoglycans	Unclear	Implicated but unclear	Flotillin 1 and 2
Phagocytosis	Cargo shaped	Pathogens, apoptotic remnants	Arf6/cdc42/rac1/rhoA	Implicated	Actin, IQGAP1, amphiphysin1, Rho kinase, adhesion proteins
Macro-pinocytosis	Highly ruffled	Fluid phase markers, RTKs	Rac1	Not as yet	Actin, PAK1, PI3K, Ras, Src, HDAC6
Circular dorsal ruffles	Highly ruffled	Fluid phase markers, RTKs	Unclear	Implicated	Cortactin, actin
Entosis	Cell shaped	Matrix-deligated cells	RhoA	Not as yet	Adherens junctions

Abbreviations: CLIC, clathrin-independent carrier; MHC, major histocompatibility complex; GEEC, GPI-AP enriched early endosomal compartment; GPI, glycosylphosphatidylinositol; GPCRs, G protein-coupled

Chapter 4

receptors; RTK, receptor tyrosine kinase.

There are three endocytic pathways that have been extensively investigated. The first pathway includes the assembly of clathrin, a specific coat protein located on the internal surface of the plasma membrane, to form a clathrin-coated pit. Besides clathrin, a number of adaptor and accessory molecules are also involved in this pathway to control the assembly and maturation of the coated pits. For example, an already known adaptor protein (AP)2 complex, is indispensable for cargo molecules to link clathrin in the initial step, and amphiphysin and dynamin guanosine triphosphatase (GTPase) are responsible for the regulation of vesicle invagination during the conversion of membrane in the later step. [13, 14] Receptor-mediated endocytosis depends highly on this pathway. The second pathway describes the invagination of cholesterol-enriched microdomains within the plasma membrane through a coat protein, so-called caveolin, the structures of which are usually referred to caveolae or lipid rafts. [15] Caveolae-mediated endocytosis serves the internalization of glycosylphosphatidylinositol (GPI)-anchored proteins and intracellular cholesterol trafficking. Cholera toxin entry is also facilitated by this pathway. The molecular mechanisms may include tyrosine kinase signaling and dynamin activity of the plasma membrane. The third major internalization pathway is the formation of large F-actin-coated vacuoles that participate in the cellular uptake of either solid particles (phagosome) or liquid (macropinosomes) from the extracellular milieu. [16-18] Macropinocytosis can be induced universally in many cell types on stimulation with mitogens and growth factors. Comparingly, phagocytosis is a characteristic of particular cells, for example leukocytes. Nevertheless, both macropinocytosis and phagocytosis are initiated by the dynamic changes of cortical actin, and are controlled by intracellular protein machinery that regulates actin polymerization.

Chapter 4

4.1.3. *Inhibitors of endocytosis*

The most well investigated and important endocytic routes include clathrin-mediated endocytosis (CME), caveolae-mediated endocytosis and macropinocytosis. For the inhibition of these endocytic routes, inhibitors are often used. For example, chlorpromazine (CPZ) for the inhibition of clathrin-mediated endocytosis, Nystatin (Nys) and methyl- β -cyclodextrin (M β CD) for the inhibition of caveolae-dependent endocytosis, and cytochalasin D (Cyto D) and wortmannin (Wort) for the inhibition of macropinocytosis.

CPZ is a cationic amphiphilic agent which is considered to inhibit the conformation of clathrin-coated pit on the plasma membrane into invaginated vesicles. [19] Nystatin is polyene antibiotics which readily interact with cholesterol in mimic and biological membranes to interfere the cholesterol-rich membrane domains. M β CD is a cyclic oligomer of glucopyranoside which reversibly deplete the steroid away from the plasma membrane to suppress the cholesterol-dependent endocytic process. [20] It is often used to determine whether endocytosis is dependent on the integrity of lipid rafts/caveolae. Cyto D is a cell permeable alkaloid which is a potent inhibitor of actin polymerization, including actin-dependent phagocytosis and macropinocytosis. Wort is an inhibitor of phosphoinositide 3-kinase (PI3K), which is a key enzyme related to the metabolism of phosphoinositide. It is used to block constitutive or stimulated macropinocytosis and phagocytosis in macrophages, fibroblasts, and epithelial cells. [21-24]

4.2. *Study of the influence of conventional endocytosis inhibitors on the cellular uptake of maleimide-modified liposomes*

4.2.1. *Methods*

4.2.1.1. *Cell culture*

HeLa, HCC1954, MDA-MB-468 and COS-7 cells were maintained in Dulbecco's Modified Eagle's Medium (DMEM) supplemented with 10% fetal bovine serum (FBS) and 1%

Chapter 4

penicillin-streptomycin. The cells were grown at 37 °C in an atmosphere containing 5% CO₂ and passaged by trypsinization with 0.1% trypsin-EDTA.

4.2.1.2. Study for the endocytic mechanism of liposomes

Cells were seeded in 24-well plates (5.0×10^4 cells/well) and incubated in an atmosphere of 5% CO₂ at 37 °C for 24 hr. Then the medium in the cell culture dish was exchanged with 400 µL fresh complete DMEM containing 72 µg/mL Rho-liposomes. Upon incubation at 37 °C for 2 hr, the cells were washed once with DPBS containing 20 U/mL heparin sulfate and twice with DPBS, then added with 200 µL of 0.5% Triton X-100 buffer to lyse cells. For endocytosis inhibition groups, cells were pre-incubated with one of the following inhibitors: 10 µg/mL chlorpromazine (CPZ) as an inhibitor of clathrin-mediated endocytosis, 10 µg/mL Nystatin (Nys) and 1 mM methyl-β-cyclodextrin (MβCD) as inhibitors of caveolae-dependent endocytosis, 10 µg/mL cytochalasin D (Cyto D) and 20 µM wortmannin (Wort) as inhibitors of macropinocytosis for 30 min at 37 °C under a 5% CO₂ atmosphere. For the comprehensive inhibition of the above endocytic pathways, a mixture of 4 µg/mL CPZ, 4 µg/mL Nys, 0.4 mM MβCD, 4 µg/mL Cyto D and 5 µM Wort in DMEM was applied for 30 min pre-incubation at 37 °C under a 5% CO₂ atmosphere. The relative cellular uptake efficiency was calculated using the following formula:

$$\% \text{ Relative cellular uptake efficiency} = \frac{[\text{Cellular uptake efficiency}]_{\text{inhibitory group}}}{[\text{Cellular uptake efficiency}]_{\text{control group}}} \times 100\%$$

4.2.1.3. Confocal laser scanning microscopic observation of subcellular distribution of liposomes after cellular internalization

Cells were seeded in 6-well glass plates (1.0×10^5 cells/well) and incubated in an atmosphere of 5% CO₂ at 37 °C for 24 hr. Culture medium was exchanged with fresh DMEM medium containing 100 µM Rho-M-GGLG- or Rho-GGLG-liposomes for 30 min incubation. Then

Chapter 4

cells were washed once by DPBS containing 20 U/mL heparin sulfate and twice by DPBS, and then added with 50 nM LysoTracker[®] Green DND-26 (Molecular probes[®], Life Technologies Corp., Eugene, OR) for a further 30 min incubation. Finally, cells were washed three times by DPBS, added with transparent DMEM medium, and observed under confocal laser scanning microscope (FV1000, Olympus, Japan).

4.2.2. Results

4.2.2.1. Study for the endocytic mechanism of liposomes

Well known endocytic pathway includes clathrin-mediated endocytosis (CME), caveolae-dependent endocytosis and macropinocytosis. Herein, we utilized chlorpromazine (CPZ) to inhibit CME, Nystatin (Nys) and methyl- β -cyclodextrin (M β CD) to inhibit caveolae-dependent endocytosis, and cytochalasin D (Cyto D) and wortmannin (Wort) to inhibit macropinocytosis.

As shown in Fig.4-2, the cellular endocytic pathway of liposomes can be varied according to the species of the cells and liposomes. For GGLG-liposomes, the endocytic rate of was reduced to around 50% by each of the inhibitors applied in HeLa, MDA-MB-468 and COS-7 cells, indicating that the endocytic pathways in the above cell lines includes CME, caveolae-dependent endocytosis and macropinocytosis. In HCC1954 cells, the endocytosis of GGLG-liposomes was mainly caveolae-dependent, with an inhibition of cellular uptake by Nys and M β CD around 50%. By comparison, the cellular uptake of M-GGLG-liposomes by CPZ and/or Nys in HeLa, HCC1954 and COS-7 cells only showed a slight inhibition, with the inhibitory rates ranging from 10% to 25% in the above cell lines. No inhibition of cellular uptake of M-GGLG-liposome's by M β CD, Cyto D or Wort was confirmed in all the cell lines tested. On the contrary, the cellular uptake of M-GGLG-liposomes was stimulated by M β CD, Cyto D and Wort in HeLa, MDA-MB-468 and COS-7 cells.

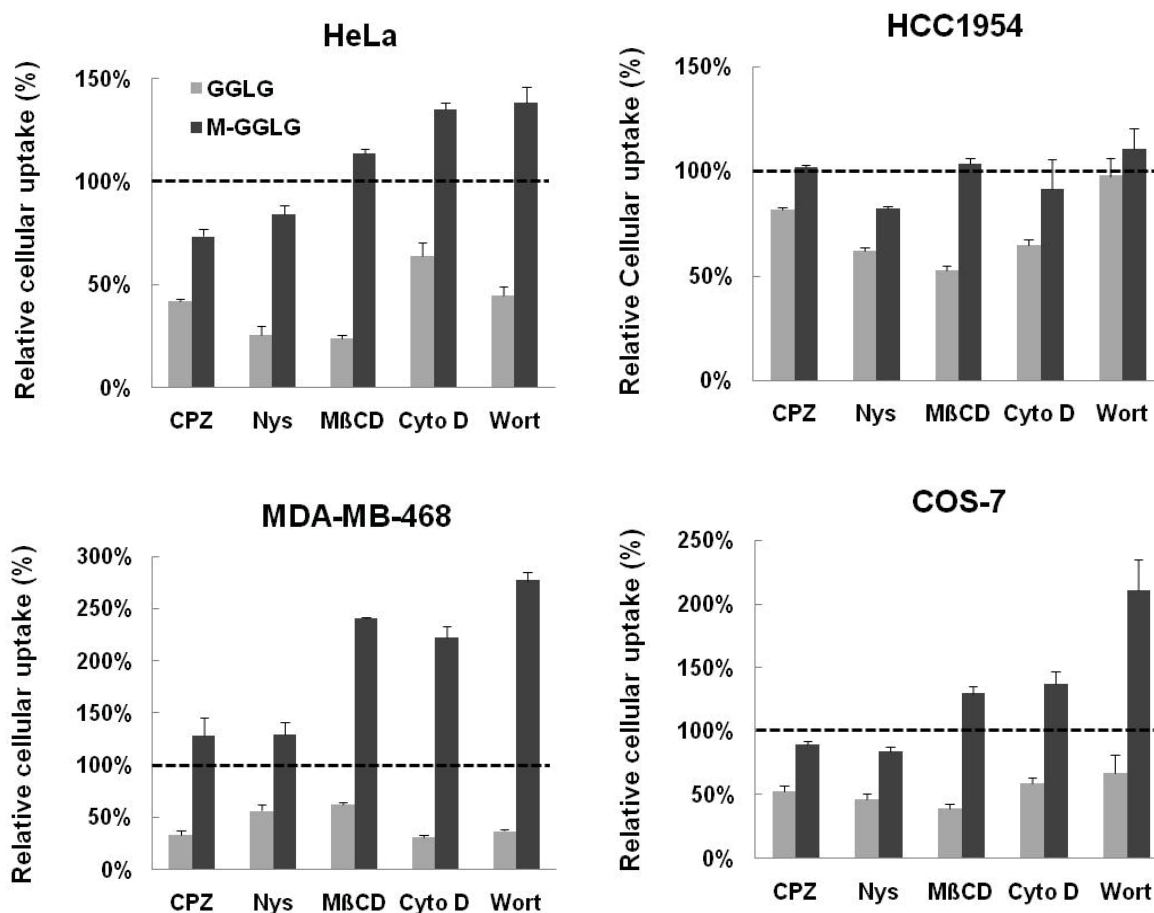


Fig. 4-2. Influence of endocytosis inhibitors on cellular uptake of M-GGLG- and GGLG-liposomes. HeLa, HCC1954, MDA-MB-468 and COS-7 cells were pre-incubated with each inhibitor for 30 min and subsequently incubated with 72 $\mu\text{g}/\text{mL}$ M-GGLG- or GGLG-liposomes in complete DMEM. Error bars mean S.E. (n=4).

In a separate experiment (shown in Fig.4-3), a mixture of all the above endocytosis inhibitors was employed to comprehensively inhibit the conventional endocytic pathways of liposomes (i.e., CME, caveolae-dependent endocytosis and macropinocytosis). The experimental conditions were the same with that showed in Fig.4-2 except a decreased (i.e., 40% of the original) concentration of each inhibitor in consideration of the cytotoxicity. The cellular uptake efficiency of M-GGLG-liposomes did not inhibited by the mixture of the endocytosis inhibitors in HeLa, HCC1954 and COS-7 cells, and a stimulated internalization

was confirmed in MDA-MB-468 cells.

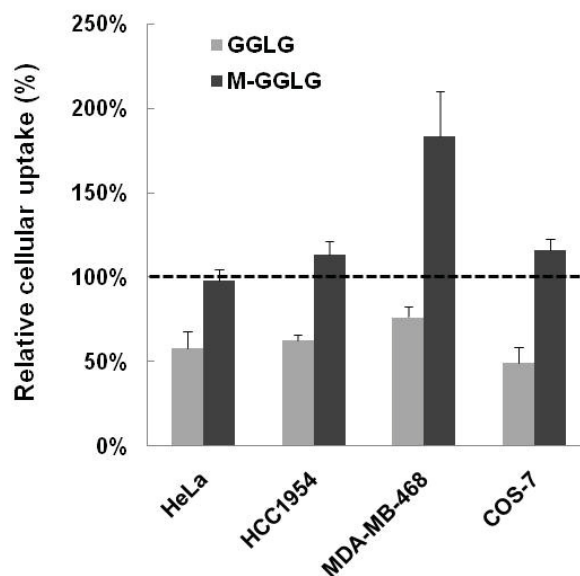


Fig. 4-3. Relative cellular uptake efficiency of GGLG- and M-GGLG-liposomes after the inhibition of endocytosis by the treatment with a mixture of inhibitors, including 4 $\mu\text{g/mL}$ CPZ, 4 $\mu\text{g/mL}$ Nys, 0.4 mM M β CD, 4 $\mu\text{g/mL}$ Cyto D and 5 μM Wort in DMEM for 30 min pre-incubation with the HeLa, HCC1954, MDA-MB-468 and COS-7 cells. Error bars mean SEM. (n=3).

4.2.2.2. Lysosomal distribution of liposomes

In general, the mechanism of cell membrane trafficking of nanoparticles can be divided into active transports such as endocytosis, and passive transport such as membrane fusion. [25-27] In the process of endocytosis of the nanoparticles, endocytic vesicles will be formed for the transportation of the nanoparticles, and thus there is no direct delivery of the nanoparticles to the cytosol. By contrary, the passive trafficking results in the cell membrane penetration of the attached nanoparticles, which directly releases the cargo into the cytosol.

Herein, we utilized LysoTracker[®] to visualize the distribution of lysosomes (green dots) and Rhodamine-PE, a component of liposome bilayer, to trace the liposome trafficking (red dots). The yellow dots in the overlay pictures mean the co-localization of liposomes and lysosomes, while the red dots show a cytoplasmic distribution.

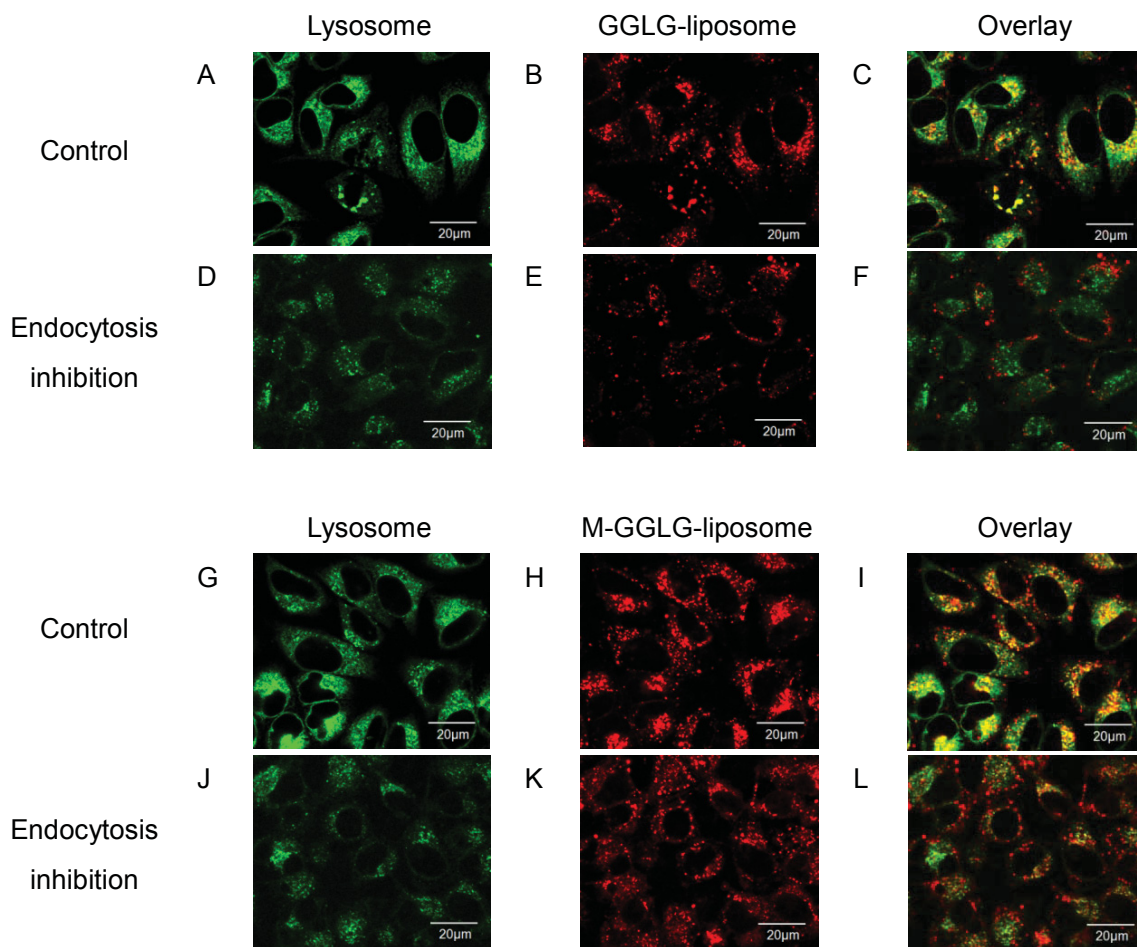


Fig. 4-4. Confocal microscopic observation of intracellular distribution of Rho-GGLG- and Rho-M-GGLG-liposomes after treatment with a mixture of endocytosis inhibitors (4 μg/mL CPZ, 4 μg/mL Nys, 0.4 mM MβCD, 4 μg/mL Cyto D and 5 μM Wort) in HeLa cells. Red: Rhodamine-PE 559 nm/571 nm; Green: Lysosome-tracker Green 473 nm/511 nm.

As shown in Fig.4-4C, after cellular internalization without endocytosis inhibition, a majority of GGLG-liposomes located in lysosomes and a minority distributed in the cytoplasm, which revealed that endocytosis was a dominant cellular internalization pathway for GGLG-liposomes. By contrast, a slightly increased cytoplasmic distribution of M-GGLG-liposomes was observed (red dots in Fig.4-4I), suggesting an enhanced cellular uptake through passive trafficking. However, it should be noted that endocytosis was still a

main cellular internalization pathway for M-GGLG-liposomes.

Endocytosis inhibition was practiced by treating the HeLa cells with a mixture of conventional endocytosis inhibitors for the inhibition of CME, caveolae-dependent endocytosis and macropinocytosis before the cellular uptake of liposomes. As shown in Fig.4-4F, endocytosis inhibition resulted in a decreased cellular internalization for GGLG-liposomes and no localization in lysosomes was confirmed, which indicated that a complete endocytosis inhibition by the mixture of conventional endocytosis inhibitors occurred, and the cytoplasmic distribution of GGLG-liposomes disclosed the cellular uptake through membrane fusion. For M-GGLG-liposomes, however, the regular endocytosis inhibitors did not totally suppress the subcellular distribution of liposomes in lysosomes, which hinted that the endocytosis of M-GGLG-liposomes included an alternative pathway.

4.3. Study of the influence of other factors on the cellular uptake of maleimide-modified liposomes

4.3.1. Methods

4.3.1.1. Study for the influence of serum on the cellular uptake of liposomes

Cells were seeded in 24-well plates (5.0×10^4 cells/well) and incubated in an atmosphere of 5% CO₂ at 37 °C for 24 hr. Then cells were washed three times by DPBS and the medium was exchanged with 72 µg/mL Rho-GGLG- or Rho-M-GGLG-liposome solution in fresh DMEM or DMEM containing 10% FBS. Upon incubation at 37 °C for 2 hr, the cells were washed once with DPBS containing 20 U/mL heparin sulfate to remove membrane-bound liposomes and twice with DPBS, then added with 200 µL of 0.5% Triton X-100 buffer to lyse cells. The amount of liposomes internalized in the cells was fluorometrically determined from the lysate using a fluorescence spectrometer (excitation wavelength, 485 nm; emission wavelength, 590 nm). The protein concentration of the lysate was determined by a standard protein assay (660 nm Pierce Protein Assay, Pierce Biotechnology, Rockford, IL). The cellular uptake efficiency

of the liposomes was expressed as lipid- μg per cellular protein-mg.

4.3.1.2. Study for the influence of temperature block on the cellular uptake of liposomes

Cells were seeded in 24-well plates (5.0×10^4 cells/well) and incubated in an atmosphere of 5% CO_2 at 37 °C for 24 hr. Then cells were pre-cooled at 4 °C for 2 hr before exchanging the medium in the cell culture dish with 400 μL cold complete DMEM containing 72 $\mu\text{g}/\text{mL}$ Rho-liposomes. Upon further incubation at 4 °C for 2 hr, the cells were washed once with pre-cold DPBS containing 20 U/mL heparin sulfate and twice with pre-cold DPBS, then added with 200 μL of 0.5% Triton X-100 buffer to lyse cells.

4.3.2. Results

4.3.2.1. Study for the influence of serum on the cellular uptake of liposomes

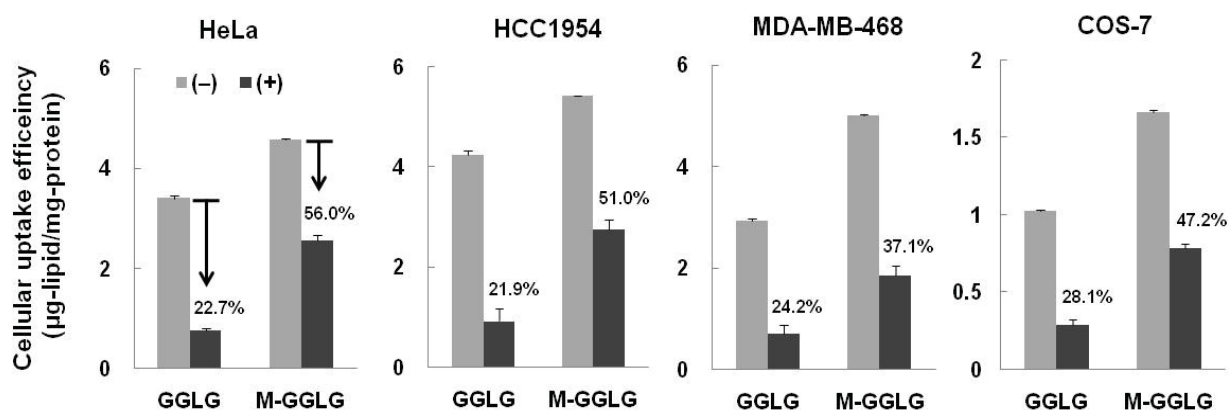


Fig. 4-5. Serum inhibition of the cellular uptake of liposomes in HeLa, HCC1954, MDA-MB-468, and COS-7 cells. Errors mean S.E. (n=6). Dark bars show the cellular uptake efficiencies of liposomes under co-incubation with 10% serum, and light bars show the cellular uptake efficiencies in the DMEM medium without serum.

The cooperation of a number of factors and proteins in serum often leads to the suppression of

the cellular internalization of nanoparticles in serum-containing medium. [28, 29] As shown in Fig.4-5, the cellular uptake efficiency of GGLG-liposomes in serum-containing medium was decreased to 20-30% by comparison to that in serum-free medium in HeLa, HCC1954, MDA-MB-468 and COS-7 cells. However, the inhibitory of serum addition for M-GGLG-liposomes was less severe, with the ratio of cellular uptake efficiency of 37.1-56.0% in serum-containing medium in the above cell lines.

4.3.2.2. Study for the influence of temperature block on the cellular uptake of liposomes

Endocytosis of nanoparticles is well known to be energy-dependent intracellular trafficking pathway. [30] Through temperature blocking at 4 °C, active endocytic membrane transport could be inhibited. Thus, the cellular uptake at 4 °C shows the passive transport of liposomes, well known as membrane fusion.

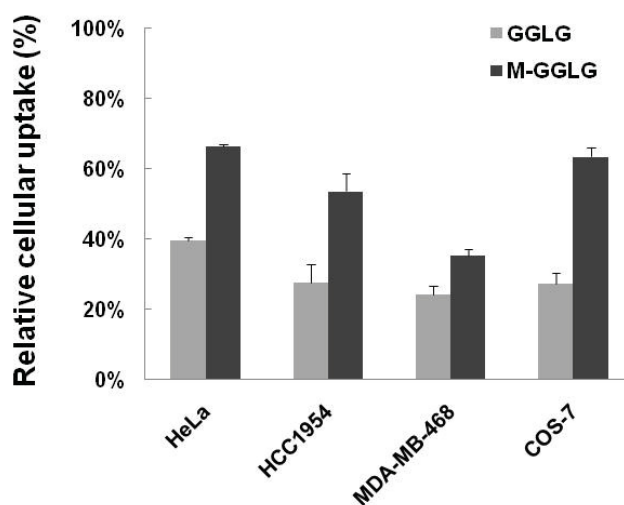


Fig. 4-6. Cellular uptake efficiency of GGLG- and M-GGLG-liposomes in HeLa, HCC1954, MDA-MB-468 cells after temperature block at 4 °C. Error bars mean S.E. (n=4).

As shown in Fig.4-6, temperature block at 4 °C caused the cellular uptake ratio of GGLG-liposomes to reduce 60-80% in HeLa, HCC1954, MDA-MB-468 and COS-7 cells. By comparison, M-GGLG-liposomes exhibited a less inhibition ratio (35-70%) at low

temperature in the above cell lines.

4.4. Summary

The composition and physical properties such as size and pH-sensitivity of M-GGLG- and GGLG-liposomes were the same as revealed in Chapter 1, and the only difference is the additional maleimide-moiety on M-GGLG-liposome surface instead of methyl on GGLG-liposome surface. Therefore, the different cellular uptake behavior of M-GGLG-liposomes was considered as the contribution of maleimide-moiety on the biological properties.

Unlike GGLG-liposomes, the cellular uptake of M-GGLG-liposomes was not significantly inhibited by conventional endocytosis inhibitors including single or mixed CME inhibitors CPZ, caveolae-mediated endocytosis inhibitors Nys and MBCD, and macropinocytosis inhibitors Cyto D and Wort in HeLa, MDA-MB-468 and COS-7 cells. (Fig.4-1 and Fig.4-2). However, confocal microscopic observation of the subcellular distribution of M-GGLG-liposomes showed a co-localization with lysosomes after the inhibition of these conventional endocytic pathways (Fig.4-3). Therefore, it was suggested that rather than the conventional endocytic pathways for M-GGLG-liposomes, maleimide-modification triggered a novel endocytic pathway, which is related to the functions of maleimide on the surface of M-GGLG-liposomes.

Serum consist a number of factors that could usually down regulate or suppress the functions of cell surface proteins/receptors, and it is considered as an inhibitory factor of cellular internalization of nanoparticles. By comparison to GGLG-liposomes, the inhibitory rate of cellular uptake of M-GGLG-liposomes in serum-containing medium to that in serum-free was alleviated (Fig.4-4) to a significant extent, suggesting the existence of a more potent cellular internalization pathway for M-GGLG-liposomes.

Generally, most of the active transport on cell membrane can be inhibited by temperature

Chapter 4

block at 4 °C. [31] Therefore, after washing off the liposomes which might attached to the cytoplasmic membrane, the cellular internalization at 4 °C reveals the passive transport of liposomes into the cells. As shown in Fig.4-5, maleimide-modification mitigated the suppression of temperature block to the cellular internalization of M-GGLG-liposomes by comparison to that of GGLG-liposomes, suggesting an enhanced ratio of cellular uptake of M-GGLG-liposomes through passive transport such as membrane fusion.

To sum up, the maleimide-modification of liposome surface has strengthened the interaction of liposomes and cell membrane, thus the cellular uptake of M-GGLG-liposomes was enhanced. Rather than conventional endocytosis, maleimide might have triggered other pathways, including enhanced passive trafficking, for enhanced cellular uptake of maleimide-modified liposomes.

References

- [1] Torchilin VP. Recent advances with liposomes as pharmaceutical carriers. *Nat Rev Drug Discov.* 2005;4:145-60.
- [2] Hoeller D, Volarevic S, Dikic I. Compartmentalization of growth factor receptor signalling. *Current opinion in cell biology.* 2005;17:107-11.
- [3] Marsh M, Helenius A. Virus entry: open sesame. *Cell.* 2006;124:729-40.
- [4] Doherty GJ, McMahon HT. Mechanisms of endocytosis. *Annual review of biochemistry.* 2009;78:857-902.
- [5] Roth TF, Porter KR. Yolk Protein Uptake in the Oocyte of the Mosquito *Aedes Aegypti*. *L. The Journal of cell biology.* 1964;20:313-32.
- [6] Rothberg KG, Heuser JE, Donzell WC, Ying YS, Glenney JR, Anderson RG. Caveolin, a protein component of caveolae membrane coats. *Cell.* 1992;68:673-82.
- [7] Mayor S, Pagano RE. Pathways of clathrin-independent endocytosis. *Nature reviews Molecular cell biology.* 2007;8:603-12.

Chapter 4

- [8] Kirkham M, Parton RG. Clathrin-independent endocytosis: new insights into caveolae and non-caveolar lipid raft carriers. *Biochimica et biophysica acta*. 2005;1745:273-86.
- [9] Frick M, Bright NA, Riento K, Bray A, Merrified C, Nichols BJ. Coassembly of flotillins induces formation of membrane microdomains, membrane curvature, and vesicle budding. *Current biology : CB*. 2007;17:1151-6.
- [10] Shao Y, Akmentin W, Toledo-Aral JJ, Rosenbaum J, Valdez G, Cabot JB, et al. Pincher, a pinocytic chaperone for nerve growth factor/TrkA signaling endosomes. *The Journal of cell biology*. 2002;157:679-91.
- [11] Orth JD, McNiven MA. Get off my back! Rapid receptor internalization through circular dorsal ruffles. *Cancer research*. 2006;66:11094-6.
- [12] Overholtzer M, Mailloux AA, Mouneimne G, Normand G, Schnitt SJ, King RW, et al. A nonapoptotic cell death process, entosis, that occurs by cell-in-cell invasion. *Cell*. 2007;131:966-79.
- [13] Conner SD, Schmid SL. Regulated portals of entry into the cell. *Nature*. 2003;422:37-44.
- [14] Marsh M, McMahon HT. The structural era of endocytosis. *Science*. 1999;285:215-20.
- [15] Parton RG, Richards AA. Lipid rafts and caveolae as portals for endocytosis: new insights and common mechanisms. *Traffic*. 2003;4:724-38.
- [16] Amyere M, Mettlen M, Van Der Smissen P, Platek A, Payrastra B, Veithen A, et al. Origin, originality, functions, subversions and molecular signalling of macropinocytosis. *International journal of medical microbiology : IJMM*. 2002;291:487-94.
- [17] Niedergang F, Chavrier P. Signaling and membrane dynamics during phagocytosis: many roads lead to the phagos(R)ome. *Current opinion in cell biology*. 2004;16:422-8.
- [18] Swanson JA, Watts C. Macropinocytosis. *Trends in cell biology*. 1995;5:424-8.
- [19] Wang LH, Rothberg KG, Anderson RG. Mis-assembly of clathrin lattices on endosomes reveals a regulatory switch for coated pit formation. *The Journal of cell biology*. 1993;123:1107-17.

Chapter 4

- [20] Rodal SK, Skretting G, Garred O, Vilhardt F, van Deurs B, Sandvig K. Extraction of cholesterol with methyl-beta-cyclodextrin perturbs formation of clathrin-coated endocytic vesicles. *Molecular biology of the cell*. 1999;10:961-74.
- [21] Dharmawardhane S, Schurmann A, Sells MA, Chernoff J, Schmid SL, Bokoch GM. Regulation of macropinocytosis by p21-activated kinase-1. *Molecular biology of the cell*. 2000;11:3341-52.
- [22] Mettlen M, Platek A, Van Der Smissen P, Carpentier S, Amyere M, Lanzetti L, et al. Src triggers circular ruffling and macropinocytosis at the apical surface of polarized MDCK cells. *Traffic*. 2006;7:589-603.
- [23] Montaner LJ, da Silva RP, Sun J, Sutterwala S, Hollinshead M, Vaux D, et al. Type 1 and type 2 cytokine regulation of macrophage endocytosis: differential activation by IL-4/IL-13 as opposed to IFN-gamma or IL-10. *Journal of immunology*. 1999;162:4606-13.
- [24] Araki N, Johnson MT, Swanson JA. A role for phosphoinositide 3-kinase in the completion of macropinocytosis and phagocytosis by macrophages. *The Journal of cell biology*. 1996;135:1249-60.
- [25] Nel AE, Madler L, Velegol D, Xia T, Hoek EM, Somasundaran P, et al. Understanding biophysicochemical interactions at the nano-bio interface. *Nature materials*. 2009;8:543-57.
- [26] Verma A, Stellacci F. Effect of surface properties on nanoparticle-cell interactions. *Small*. 2010;6:12-21.
- [27] Verma A, Uzun O, Hu Y, Han HS, Watson N, et al. Surface-structure-regulated cell-membrane penetration by monolayer-protected nanoparticles. *Nature materials*. 2008;7:588-95.
- [28] Zelphati O, Uyechi LS, Barron LG, Szoka FC, Jr. Effect of serum components on the physico-chemical properties of cationic lipid/oligonucleotide complexes and on their interactions with cells. *Biochimica et biophysica acta*. 1998;1390:119-33.
- [29] Johnstone SA, Masin D, Mayer L, Bally MB. Surface-associated serum proteins inhibit

Chapter 4

the uptake of phosphatidylserine and poly(ethylene glycol) liposomes by mouse macrophages. *Biochimica et biophysica acta*. 2001;1513:25-37.

[30] Mukherjee S, Ghosh RN, Maxfield FR. Endocytosis. *Physiological reviews*. 1997;77:759-803.

[31] Willingham MC, Rutherford AV, Gallo MG, Wehland J, Dickson RB, Schlegel R, et al. Receptor-mediated endocytosis in cultured fibroblasts: cryptic coated pits and the formation of receptosomes. *The journal of histochemistry and cytochemistry : official journal of the Histochemistry Society*. 1981;29:1003-13.

Chapter 5 Study of the functions of maleimide on the cellular uptake of liposomes

5.1. Introduction

5.1.1. Overview

5.1.2. Functions of protein disulfide isomerase

5.1.3. Membrane fusion

5.2. The functions of cell surface thiols on the cellular uptake of maleimide-modified liposomes

5.2.1. Methods

5.2.1.1. Cell culture

5.2.1.2. Confocal laser scanning microscopic observation of thiol distribution on cell surface

5.2.1.3. Study for the concentration of thiols on different cell surfaces

5.2.1.4. Study for the influence of serum on thiol expression on cell surface

5.2.1.5. Serum influence on thiol recovery after blocking by DTNB

5.2.1.6. Study for the influence of PDI inhibitors on cellular uptake of liposomes

5.2.2. Results

5.2.2.1. Confocal laser scanning microscopic observation of thiol distribution on cell surface

5.2.2.2. Study for the concentration of thiols on different cell surfaces

5.2.2.3. Study for the influence of serum on thiol expression on cell surface

5.2.2.4. Serum influence on thiol recovery after blocking by DTNB

5.2.2.5. Study for the influence of PDI inhibitors on cellular uptake of liposomes

5.3. The functions of maleimide on the enhanced cellular uptake of maleimide-modified liposomes

Chapter 5

5.3.1. Methods

5.3.1.1. Study for the influence of thiol-reactive compounds on cell surface thiols

5.3.1.2. Study for the influence of NEM on cellular uptake of liposomes

5.3.2. Results

5.3.2.1. Study for the influence of thiol-reactive compounds on cell surface thiols

5.3.2.2. Study for the influence of NEM on cellular uptake of liposomes

5.4. Summary

References

5.1. Introduction

5.1.1. Overview

Cellular thiols are well known to play an important role in redox regulation of cellular functions and response to endogenous and exogenous oxidative stress. Many proteins containing cysteine residues in their primary structures are capable to fold and stabilize the tertiary structure by forming internal disulfide bonds. Particularly in secreted proteins, which encounter strong oxidants in the extracellular milieu, disulfide bonding makes great contributions to protein stability. The thiol-expression moiety can be a reductive form or oxidative form in a mosaic or transmembrane protein/peptide. (Fig.5-1) The disulfide bonds present in mature proteins can be cleaved into thiols through dithiol–disulfide exchange, alkaline hydrolysis or acid-based assisted hydrolysis.[1] Thioredoxins, a ubiquitous protein (~12 KDa) with a dithiol/disulfide active site, are the major cellular protein disulfide reductases in cytosol, providing electrons for a number of reductases. [2] The Protein disulfide isomerase (PDI), a member of thioredoxin family catalyzing disulfide formation and isomerization and inhibiting aggregation, is responsible for reduction of disulfide bonds of macromolecular conjugates during endocytosis. [3] (Fig.5-2) Other redox enzymes such as GILT (Gamma-interferon-inducible lysosomal thiol reductase), also contribute to the reduction and redox regulation in the endosome/lysosome. [4]

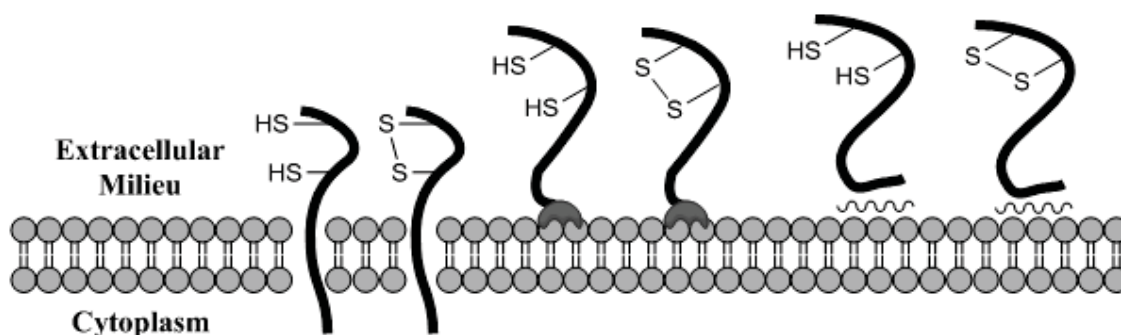


Fig. 5-1. Membrane proteins expose thiol groups to the extracellular milieu (exofacial thiols). The cellular plasma membrane is a lipid bilayer containing associated proteins. These proteins can be

Chapter 5

transmembrane proteins, glycosylphosphatidylinositol-linked proteins or non-covalently bound proteins. These thiols can be in reduced (-SH) or oxidized (S-S) form. [5]

The reversible nature of the disulfide bond has been exploited in a number of ways for advanced drug delivery via disulfide exchange between the substrates and cellular thiols. [6] For example, a protein kinase C peptide inhibitor which is cell-impermeant, could cross cell membranes when an activated cysteine was introduced into its sequence. [7] It is suggested that the peptides containing disulfides or thiols can cross-react with cell surface thiols, and then might be either trapped in the membrane or further internalized. Not only peptides, but also other synthetic biomolecules such as oligonucleotides, nanoparticles, polymers, fluorescent dyes or probes that present thiol-reactive moieties, can exhibit an enhanced cellular association and internalization. [5] However, it is still unclear of the exact mechanism of thiol-mediated cellular uptake. Thiolated biomolecules could interact with exofacial thiols followed by the standard endocytosis pathways to pass through the plasma membrane. There is also another supposition that the thiol-mediated uptake of nanoparticles is independent from the widely known receptor-mediated endocytotic routes such as clathrin-dependent endocytosis (CME), caveolae-mediated endocytosis, clathrin- and caveolae-independent endocytosis or macropinocytosis. [8]

In this research, I developed a thiol-reactive liposome M-GGLG with a small amount of maleimide-PEG, which showed remarkable increased drug delivery efficiency both *in vitro* and *in vivo* by comparison to the unmodified liposome GGLG. Herein, the possible cellular uptake mechanisms of maleimide-modified liposomes are disclosed. Moreover, the biological functions of cell surface thiols on the cellular internalization of thiol-reactive nanoparticles are also investigated.

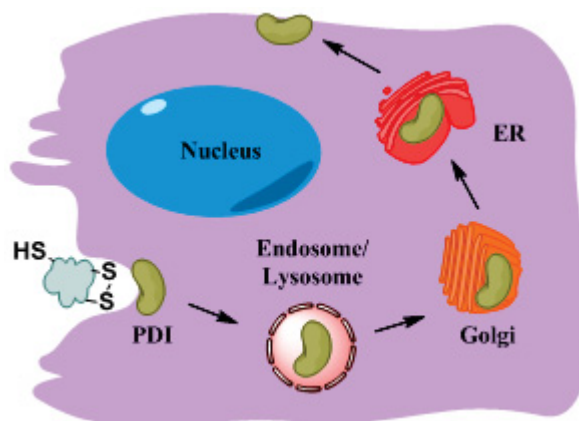


Fig. 5-2. Illustration of thiol-mediated cellular uptake of thiol-reactive nanoparticles and the recycle of cell membrane PDI (protein disulfide isomerase). PDI catalyzes the disulfide exchange between the substrates and cell surface thiols/disulfides, which is recognized as one of the promoters that facilitated the cellular uptake of thiol-reactive compounds.

5.1.2. Functions of protein disulfide isomerase

The cross-link of disulfide bonds to specific cysteines functions the stabilization of a protein or the conjugation to other proteins during the maturation of extracellular proteins. A structural change of the proteins occurs as the protein forms disulfide bond and folds into its three-dimensional structure. One of these folding assistants is protein disulfide isomerase (PDI), which is a member of a large family of dithiol/disulfide oxidoreductases, the thioredoxin superfamily. [9] It is an enzyme that catalyzes disulfide formation and isomerization (Fig.5-3), and also a chaperone that inhibits aggregation of proteins. In addition to its major site of location at ER, PDI also considerably exists in plasma membrane. [10]

Recent researches have reported that plasma membrane-associated PDI indeed plays specific and important roles at the cell surface. For example, Couet [11] has suggested that PDI catalyses the partial shedding of the thyrotropin (TSH) receptor in human thyroid cells; based on these conclusions, shedding can be suppressed by membrane-impermeant sulfhydryl blockers or anti-PDI antibodies. Furthermore, it has been revealed by Feinman [12] that PDI

is necessary for the blood platelet activation at the level of $\alpha\text{IIb}\beta_3$ which contains free sulfhydryl groups. It has been also found by Bjerkvig [13] that PDI expression is related to the invasive properties of malignant glioma. Other functions of PDI include the mediation of integrin-dependent adhesion, [14] and membrane fusion for virus entry such as Newcastle disease virus [15], Sindbis virus, [16] Moloney murine leukemia virus, [17] retrovirus, [18] mouse polyoma virus [19] and human immunodeficiency virus type 1(HIV-1). [20, 21]

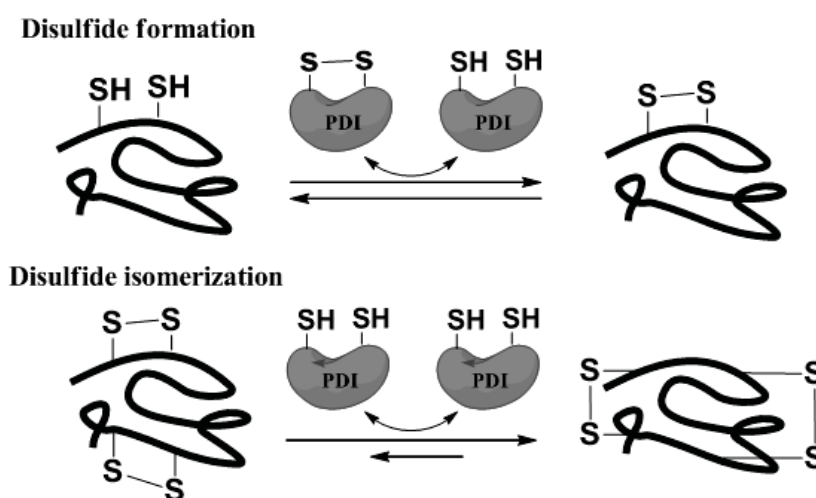
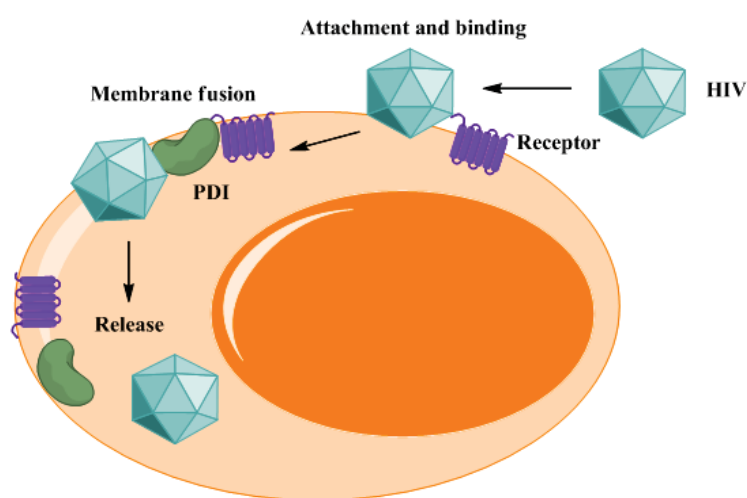


Fig. 5-3. Schematic illustration of PDI-catalyzed disulfide formation and isomerization. PDI-catalyzed disulfide formation occurs when the oxidizing equivalents are transferred from the disulfide of the oxidized PDI active site to the reduced PDI. Conversely, the reduction of a disulfide substrate results in the oxidation of PDI reductive site. On the contrary, disulfide isomerization requires PDI in the reduced form and does not lead to any oxidation of PDI.

During the virus infection, cell entry of enveloped viruses is mediated by viral fusion proteins, which induces the fusion of the viral envelope with host cell membranes. Thiol/disulfide exchange of various cell entry proteins such as diphtheria toxin, has been proved necessary for the cell entry of viruses. [22, 23] In vaccinia virus infection, the disulfide bonds in core proteins are reduced during entry into the host cell. [24] Generally, the reduction, rearrangement or isomerization of disulfide bonds of virus core or envelop proteins

is involved in the membrane fusion for virus entry. For example, as shown in Picture 5-1, PDI is required for the fusion of membranes mediated by HIV-1 Envelop (Env). Upon gp120 on virus envelop binding to the host cell receptors such as CD4, thiol/disulfide isomerase cleaves disulfide bonds in Env, facilitating its refolding which is required for membrane fusion. The inhibitors of PDI such as bacitracin, 5,5'-dithiobis-(2-nitrobenzoic acid) (DTNB) and monoclonal antibodies, can reduce or inhibit the entry of these viruses by blocking the initial phase of disulfide cleavage and exofacial thiols. [7]



Picture 5-1. Schematic diagram of the HIV invasion into host cell mediated by PDI. Blue polygon, HIV model; green crescent, PDI; purple complex, HIV receptors such as CD4 and CCR5 receptors on cell surface.

5.1.3. Membrane fusion

Membrane fusion is one of the most widespread and fundamental processes in mammalian cells, which describes the conformation of one single continuous bilayer merged from two separate lipid membrane. Although all fusion reactions possess common features, they are catalyzed by different proteins during each step of fusion. For example, there are enzymes to mediate the recognition of the membranes, or to drag the membranes getting close and destabilize the lipid/water interface, or to initiate the mixing of the lipids. [25]

SNARE (soluble NSF attachment protein receptor where NSF stands for *N*-ethyl-maleimide-sensitive fusion protein) proteins have been proposed to be involved in all intracellular membrane fusion events that have been studied so far. There are more than 30 SNARE family members, which regulate the fusion process in nearly all the distinct subcellular compartments, including endosome/lysosome, Golgi, endoplasmic reticulum (ER) and plasma membrane. It is likely that SNAREs control at least partially the specificity of membrane transport. However, the mechanism of this specificity remains controversial. Some functional studies have provided exciting insights into the molecular mechanisms of SNAREs interaction which generates the driving force to fuse separate lipid bilayers. (Fig.5-4)

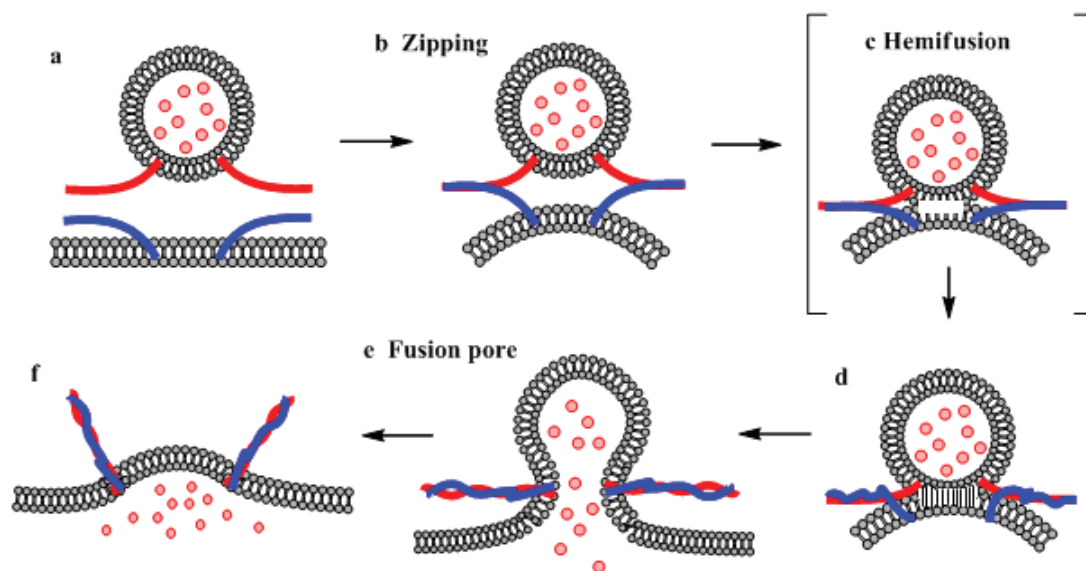


Fig. 5-4. Schematic illustration of SNARE-mediated lipid fusion. [26] a) The two separate membranes (v-SNAREs and t-SNAREs, referring to their vesicle or target membrane localization) are in the vicinity of each other before contact. b) SNARE complexes initiate zipping from the amino-terminal end and draw the two membranes coming towards each other. c) Zipping proceeds with increased curvature and lateral tension of the membranes to expose the bilayer interior. Spontaneous hemifusion occurs when the separation is reduced adequately. d) The highly unfavourable void space at the membrane junction in (c) leads to the construction of contact between the distal membrane leaflets on v-SNARE and t-SNARE. e) The lateral tension in the transbilayer contact region initiates membrane

disruption to produce a fusion pore. f) The fusion pore expands to both sides, and finally the membrane relaxes and become a single continuous bilayer.

5.2. *The functions of cell surface thiols on the cellular uptake of maleimide-modified liposomes*

5.2.1. *Methods*

5.2.1.1. *Cell culture*

HeLa, HCC1954, MDA-MB-468 and COS-7 cells were maintained in Dulbecco's Modified Eagle's Medium (DMEM) supplemented with 10% fetal bovine serum (FBS) and 1% penicillin-streptomycin. The cells were grown at 37 °C in an atmosphere containing 5% CO₂ and passaged by trypsinization with 0.1% trypsin-EDTA.

5.2.1.2. *Confocal laser scanning microscopic observation of thiol distribution on cell surface*

Alexa-C₅-maleimide, a membrane impermeable agent which can conjugate the thiols covalently was used to observe the distribution of thiols on cell surface. Cells were seeded in 6-well glass plates (5×10^4 cells/well) and incubated in an atmosphere of 5% CO₂ at 37 °C for 24 hr. To further prevent cellular internalization of Alexa-C₅-maleimide, cells were pre-cooled on ice for 30 min. After washing cells with pre-cooled DPBS, 10 μM Alexa-C₅-maleimide in fresh DMEM without FBS was added in cell culture plates for further incubation on ice for 15 s, 30 s, 1 min, 2 min, 3 min, 4 min, 5 min, 8 min and 10 min. To verify the thiol-conjugation was irreversible, cells were pre-incubated with 500 μM *N*-ethylmaleimide (NEM) for 5 min on ice, and then washed by pre-cooled DPBS three times following the further incubation with 10 μM Alexa-C₅-maleimide in fresh DMEM for 5 min on ice. Cells were fixed by 4% formalin solution for 15 min after washing by pre-cooled DPBS three times, and then observed under confocal laser scanning microscopy.

Chapter 5

5.2.1.3. Study for the concentration of thiols on different cell surfaces

Cells were seeded in 12-well plates (5×10^4 cells/well) and incubated in an atmosphere of 5% CO₂ at 37 °C for 24 hr. After cooling cells on ice for 30 min and washing by pre-cooled DPBS, 10 μM Alexa-C₅-maleimide in fresh DMEM was added in the cell culture plates for 5 min incubation on ice. Then the cells were washed and lysed by 0.5% Triton X-100, following the measurement of the concentration of Alexa- C₅-maleimide with an emission wavelength of 528 nm and an excitation wavelength of 485 nm using a fluorescence spectrometer. The protein concentration of the lysate was determined by standard protein assay (660 nm Pierce Protein Assay). The concentration of cell surface thiols was represented as thiols-nmol per protein-mg. The quantitation of cell surface thiols was conducted by measuring the fluorescent intensity of Alexa-maleimide bound to the surface thiols.

5.2.1.4. Study for the influence of serum on thiol expression on cell surface

HeLa cells (5×10^4 cells/well) were seeded in 12-well cell culture plates and incubated in an atmosphere of 5% CO₂ at 37 °C for 24 hr. Then the culture medium was exchanged with fresh DMEM medium containing different concentration of FBS (volume percentage such as 5%, 10% and 20%) for further 24 hr incubation. The cells were cooled at 4 °C for 2 hr and washed by DPBS twice. 5 μM Alexa 488-C₅-maleimide in DMEM was added for 10 min incubation on ice, following the lysis in 0.5% Triton X-100 DPBS buffer to measure the concentration of Alexa-maleimide and cell protein.

5.2.1.5. Serum influence on thiol recovery after blocking by DTNB

HeLa cells (5×10^4 cells/well) were seeded in 6-well glass plates and incubated in an atmosphere of 5% CO₂ at 37 °C for 48 hr. For the control groups, the cells were pre-incubated at 37 °C or 4 °C for 2 hr. Then the cells were washed by DPBS three times and surface thiols

Chapter 5

were measured by adding 5 μM Alexa-maleimide in fresh DMEM for 5 min, followed by the fixation with 4% formalin for 10 min. The fluorescence was observed under Confocal Laser Scanning Microscopy (CLSM). For the inhibition groups, 100 μM DTNB in fresh DMEM was first added for 5 min incubation after the 2 hr pre-incubation at corresponding temperature. Then the cells were washed by DPBS twice and added with 5 μM Alexa-maleimide in fresh DMEM for 5 min to conjugate the residual surface thiols. Finally, after cells were washed by DPBS twice, 4% formalin DPBS buffer was added for 10 min fixation and then cells were observed under CLSM. For the recovery groups, after the DTNB inhibition for 5 min (in the same condition mentioned above), culture medium was exchanged with fresh DMEM with or without 10% FBS for 2 hr incubation at corresponding temperature. Then the cell surface thiols were measured and observe using the same method mentioned above.

5.2.1.6. Study for the influence of PDI inhibitors on cellular uptake of liposomes

Cells were seeded in 24-well plates (5.0×10^4 cells/well) and incubated in an atmosphere of 5% CO_2 at 37 $^\circ\text{C}$ for 24 hr. For PDI inhibition, cells were pre-incubated with 1 nM DTNB or bacitracin in DMEM for 30 min at 37 $^\circ\text{C}$ under a 5% CO_2 atmosphere. Then the medium in the cell culture dish was exchanged with 400 μL fresh complete DMEM containing 72 $\mu\text{g}/\text{mL}$ Rho-liposomes. Upon incubation at 37 $^\circ\text{C}$ for 2 hr, the cells were washed once with DPBS containing 20 U/mL heparin and twice with DPBS, then added with 200 μL of 0.5% Triton X-100 buffer to lyse cells.

5.2.2. Results

5.2.2.1. Confocal laser scanning microscopic observation of thiol distribution on cell surface

Alexa Fluor 488- C_5 -maleimide is a membrane-impermeable compound which can conjugate

reduced thiols covalently. It was used here to imitate the thiol-reaction of maleimide moiety of M-GGLG-liposomes at the cell surface. As shown in Fig.5-5A&B, the conjugation of maleimide to the cellular thiols initiated within 15 s, and the reaction was completed in about 5 min. In Fig.5-5C, cell surface was dyed with Alexa-maleimide which disclosed the existence of a large number of free thiols on cell surface. The distribution of thiols also included the cell junctions and adhesions, where abundant thiol-related proteins are expressed such as PDI. [14] Moreover, the intracellular trafficking of cell surface thiol-related protein into cytoplasm was also observed in weak fluorescence.

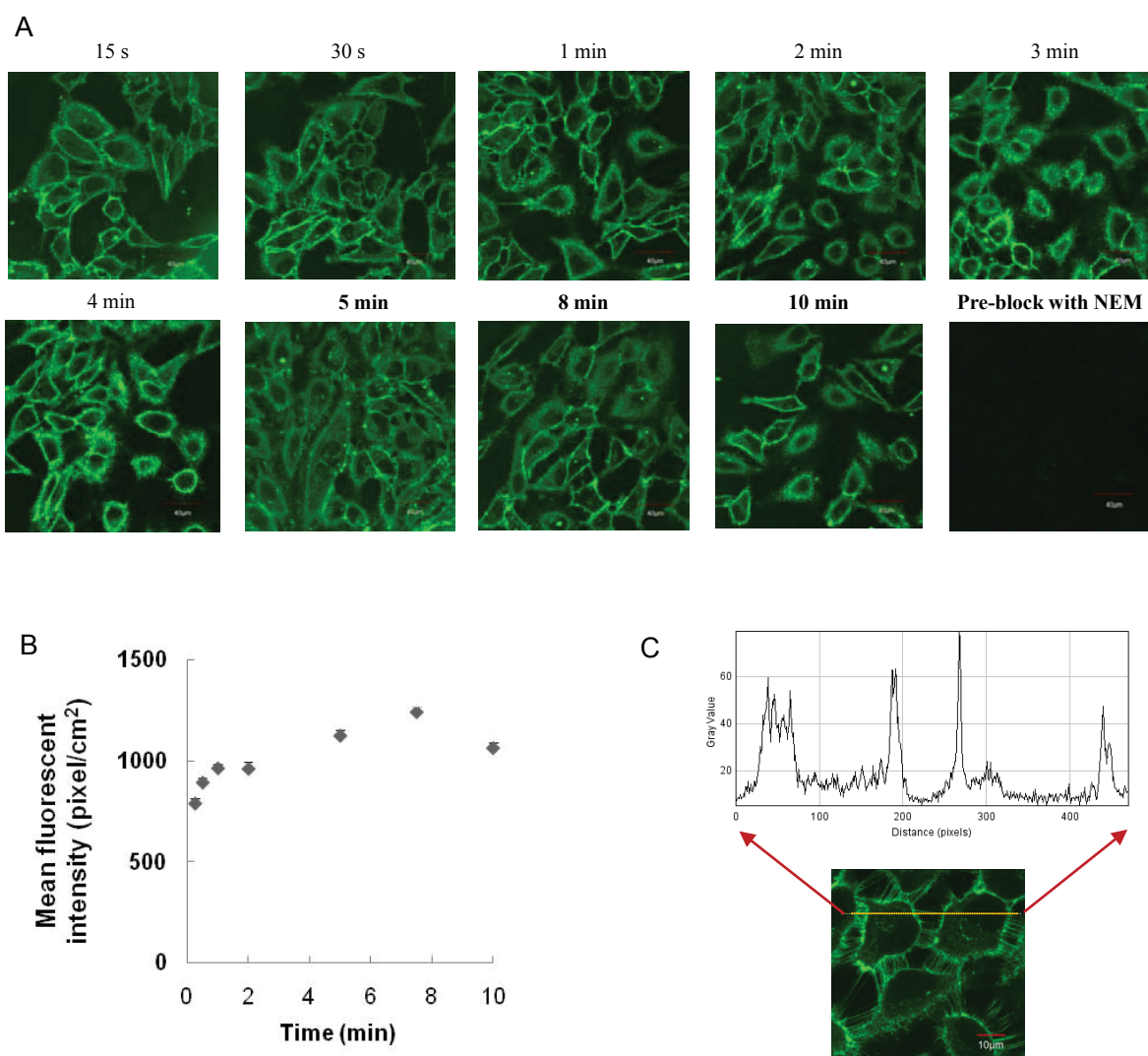


Fig. 5-5. (A) Conjugation of Alexa-C₅-maleimide (10 μ M) to cell surface thiols in HeLa cells for

different time incubation at 4 °C observed under CLSM and (B) calculation of the fluorescent intensity by using ImageJ software. Errors mean SEM. n=20; (C) Confocal microscopic observation of thiol-conjugation with Alexa-C₅-maleimide for 30 s incubation with HeLa cells at 4 °C. (λ_{em} 519 nm/ λ_{ex} 473 nm)

5.2.2.2. Study for the concentration of thiols on different cell surfaces

Fig.5-6 revealed the concentration of cellular surface thiols was varied in different cell lines. HeLa cells shown the highest surface thiol density among the tested cell lines.

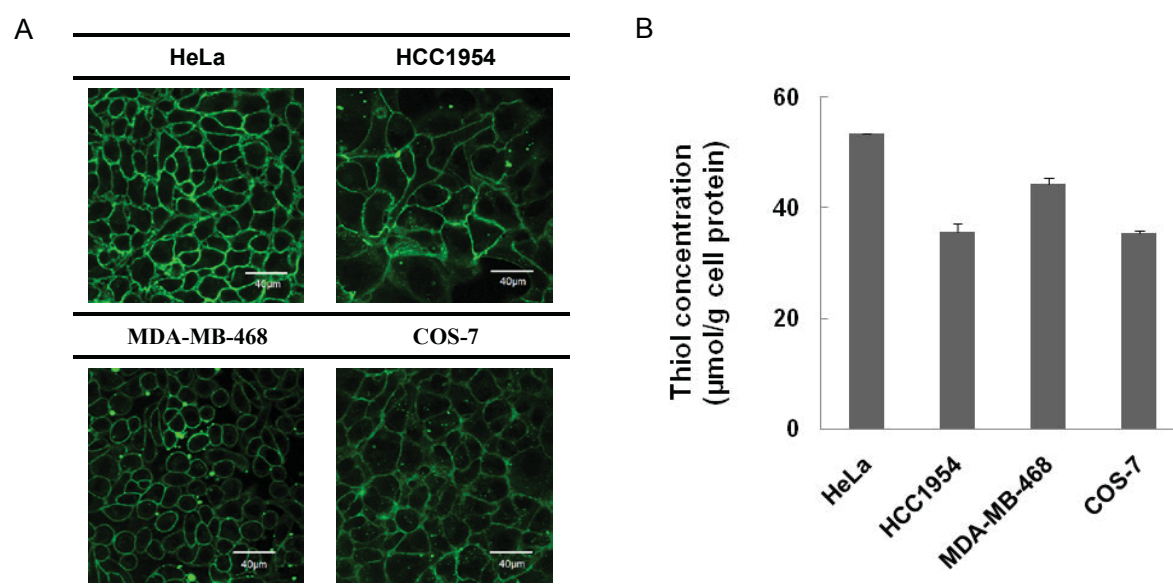


Fig. 5-6. (A) Confocal microscopic observation of thiols on cell surface using Alexa-C₅-maleimide incubation with HeLa, HCC1954, MDA-MB-468 and COS-7 cells for 5 min on ice; (B) Concentration of cell surface thiols. Error bars mean S.E. n=4.

5.2.2.3. Study for the influence of serum on thiol expression on cell surface

As shown in Fig.5-7, the serum starvation has influenced the expression of cell surface thiols. The surface thiols were apparently decreased by increasing the concentration of serum from 5% to 20%, which indicated the protein/peptides in serum are oxidative stress to cells and

they can oxidize the surface thiols and/or inhibit the function of membrane reductases. This phenomenon also reflects the decrease of cell activity under serum condition, which caused decreased cellular uptake efficiency of GGLG- and M-GGLG-liposomes in serum containing medium as revealed in Fig.4-5 of Chapter 4.

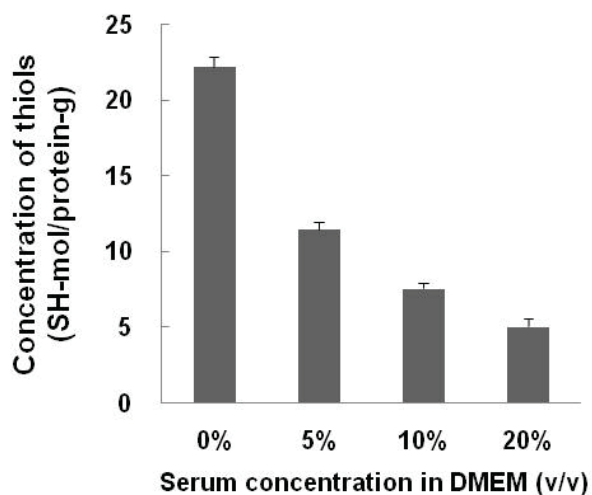


Fig. 5-7. The influence of serum on cell surface thiol expression. HeLa cells were incubated with DMEM medium containing different concentration of FBS (volume percentage) for 12 hr and the thiols were quantified by Alexa 488-C₅-maleimide. Error bars mean S.E. (n=6)

5.2.2.4. Serum influence on thiol recovery after blocking by DTNB

The conjugation of DTNB to surface thiols is covalent but reversible. As shown in Fig. 5-8, the cell surface thiols could recover to 60-80% after 2 hr incubation at 37 °C, which suggested that the surface reductase such as PDI can protect the cell from oxidative stress. It was also revealed that the enzyme function is temperature-dependent. At low temperature such as 4 °C, the expression of free thiols was significantly reduced and the recovery rate was also as low as around 10%. Therefore, the recovery of surface thiols was temperature-dependent, and the addition of serum at least did not impede the recovery of thiols in a relatively short period (2 hr).

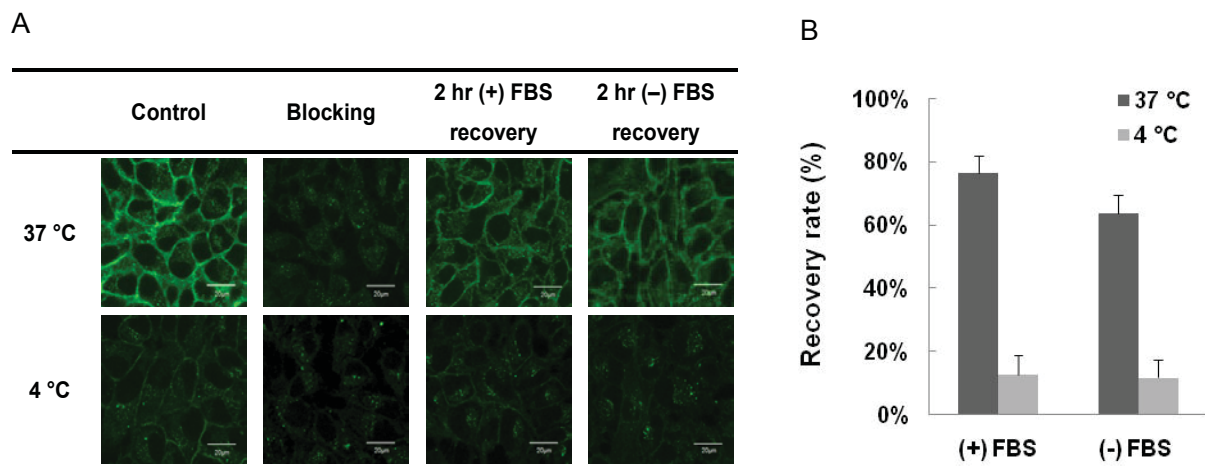


Fig. 5-8. (A) Confocal microscopic observation of the recovery of cell surface thiols after PDI inhibition at 37 °C and 4 °C. Alexa-C₅-maleimide (2 μM) was used to conjugate with membrane thiols for 5 min incubation with HeLa cells; (B) Thiol recovery rate after 2 hr incubation in DMEM medium with/without 10% FBS. Errors mean SEM. n=30.

5.2.2.5. Study for the influence of PDI inhibitors on cellular uptake of liposomes

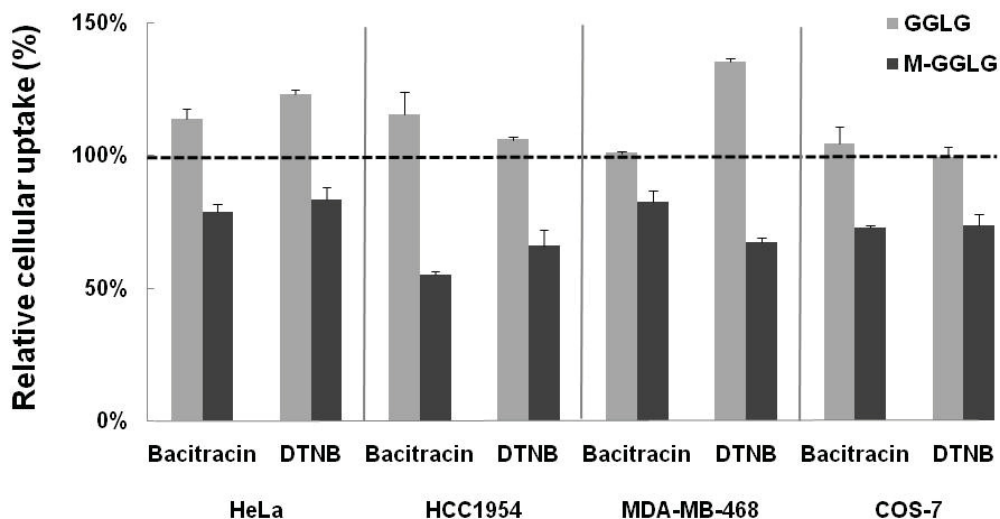


Fig. 5-9. Relative cellular uptake of liposomes after pre-incubation with PDI inhibitors bacitracin and DTNB at 37 °C. Error bars mean S.E. n=4.

PDI is a key factor that regulates the thiols on cell surface. Well know inhibitors are bacitracin and DTNB, which block the reductive functions of PDI. [27, 28] As shown in Fig.7, the cellular uptake of M-GGLG-liposomes was inhibited by bacitracin and DTNB to 50%-80% in HeLa, HCC1954, MDA-MB-468 and COS- 7 cells, while no inhibition was verified for GGLG-liposomes.

5.3. The functions of maleimide on the enhanced cellular uptake of maleimide-modified liposomes

5.3.1. Methods

5.3.1.1. Study for the influence of thiol-reactive compounds on cell surface thiols

HeLa cells were seeded in 24-well plates (5.0×10^4 cells/well) and incubated in an atmosphere of 5% CO₂ at 37 °C for 24 hr. Then cells were pre-incubated with 10 pM, 100 μM DTT or 10 pM, 10 nM or 100 μM NEM in fresh DMEM for 10 min at 4 or 37 °C under a 5% CO₂ atmosphere. (For 4 °C groups, cells were pre-cooled for 2 hr.) Then the medium in the cell culture dish was exchanged with 400 μL fresh complete DMEM containing 72 μg/mL Rho-liposomes. Upon incubation at 4 or 37 °C for 2 hr, the cells were washed once with DPBS containing 20 U/mL heparin sulfate and twice with DPBS, and then added with 200 μL of 0.5% Triton X-100 buffer to lyse cells.

5.3.1.2. Study for the influence of NEM on cellular uptake of liposomes

Cells cells were seeded in 24-well plates (5.0×10^4 cells/well) and incubated in an atmosphere of 5% CO₂ at 37 °C for 24 hr. For the influence of NEM, cells were pre-incubated with 0.01 nM or 100 μM NEM in fresh DMEM for 10 min at 37 °C under a 5% CO₂ atmosphere. Then the medium in the cell culture dish was exchanged with 400 μL fresh complete DMEM containing 72 μg/mL Rho-liposomes. Upon incubation at 37 °C for 2 hr, the cells were washed once with DPBS containing 20 U/mL heparin sulfate and twice with DPBS, and then

added with 200 μ L of 0.5% Triton X-100 buffer to lyse cells.

5.3.2. Results

5.3.2.1. Study for the influence of thiol-reactive compounds on cell surface thiols

At 4 °C, the activity of enzymes can be inhibited, thus an increasing thiol number was observed after DTT reduction. However, this reductive property was limited and thiol number reached the maximum at 10 μ M DTT. By comparison, the thiol number did not influenced significantly at 37 °C, which indicated the oxidation is a fast process and the equilibrium of thiol/disulfide is quickly recovered when the enzymes are active.

On the other hand, the oxidation/conjugation of maleimide to cell surface thiols is covalent and irreversible. As shown in Fig.5-10, the NEM conjugation was potent at both 37 °C and 4 °C, which suggested the thoroughly inhibition of surface thiols.

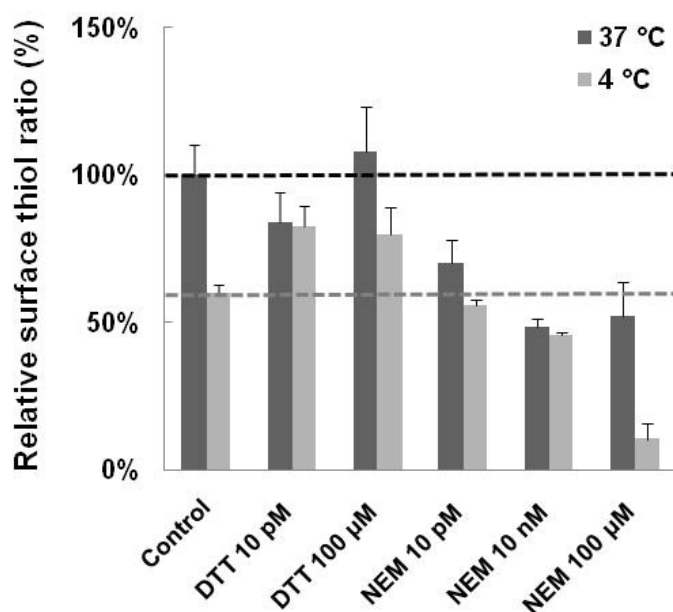


Fig. 5-10. The influence of thiol-reactive DTT and NEM on the concentration of cell surface thiols. HeLa cells were incubated with different concentrations of the above reagents for 5 mins and then the residual thiols were quantified by the Alexa 488-C₅-maleimide. Error bar mean S.E. (n=4)

5.3.2.2. Study for the influence of NEM on cellular uptake of liposomes

As shown in Fig.5-11, in low concentration of NEM (i.e., 0.01 nM), the decreased cellular uptake of M-GGLG-liposomes was observed to around 70% in HeLa, HCC1954, MDA-MB-468 and COS-7 cells, while no significant inhibition was observed for GGLG-liposomes in the above cell lines. In high concentration of NEM (i.e., 100 μ M), the cellular uptake of both GGLG- and M-GGLG-liposomes were increased to 120%~250% in the cell lines tested.

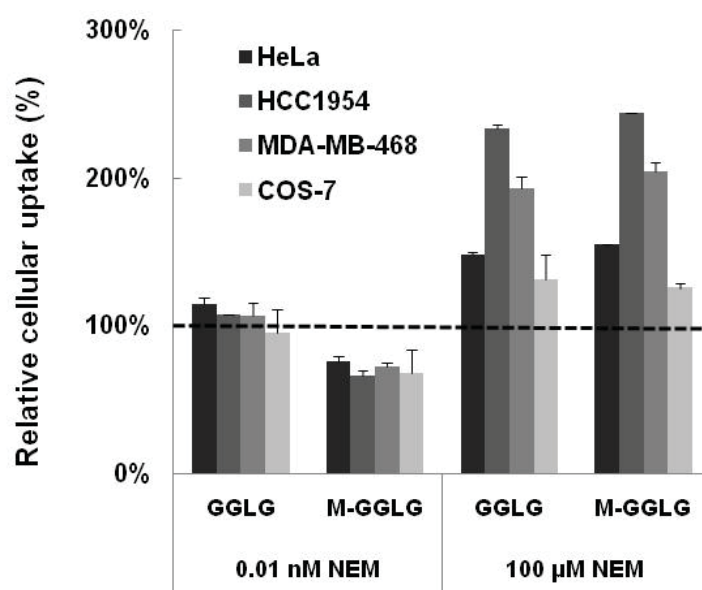


Fig. 5-11. The influence of *N*-ethylmaleimide (NEM) on the cellular uptake of liposomes at 37 °C. NEM was pre-incubated with cells for 10 min, following the incubation with liposomes. Errors mean S.E. (n=3).

5.4. Summary

Cell surface thiols are important functional groups for self-protection against extracellular oxidative stress, which numerous (Fig.5-5) and extensively exist (Fig.5-6) in different cell lines. It is reported that cell surface thiols are involved in the enhanced membrane fusion between some viral envelopes and host cell membrane during virus infection process, [15, 20] and they are highly expressed during tumor cell invasion. [13] PDI (protein disulfide

isomerase), a member of thioredoxin family, is considered as one of the keys factors that regulate these processes. It is also emphasized that the oxidoreductase activity of PDI superfamily is important to facilitate the cellular uptake of a series of thiol-reactive compounds or particles. [5]

NEM (*N*-ethylmaleimide) is a membrane-impermeable compound that could conjugate with thiols covalently. We utilized a small amount of this low molecular weight compound (e.g. 0.01 nM) to pre-block the thiol sites on cell surface, so that the cellular uptake of M-GGLG-liposomes were decreased while that of GGLG-liposomes was not (Fig.5-11). It is suggested that the conjugation between cell surface thiols and maleimide is necessary for the enhanced cellular uptake of M-GGLG-liposomes.

Thus, the inhibition of surface thiols such as PDI inhibition by DTNB and bacitracin, significantly decreased the cellular internalization of M-GGLG-liposomes while GGLG-liposomes was not affected (Fig.5-9).

The influence of maleimide on cell surface was not only as an inhibitor of surface thiols but also could be as a stimulator of cellular uptake of both maleimide-modified and non-modified liposomes in a relative high concentration (e.g., 100 μ M in Fig.5-11). It was considered that at low concentration of NEM, it first interacted with thiol-relative enzymes such as PDI and inhibited the cellular uptake of thiol-reactive liposomes (e.g., M-GGLG-liposome). However, after the functions of PDI were completely blocked, a relatively high concentration of NEM might disturb other membrane proteins which lead membrane fusion or poration on cell membrane to give an enhanced permeability for all kinds of nanoparticles that have a proper size. It should be noted that the cell surface thiols are variable according to the cell species, generations, concentration and culturing condition and time. Thus, unfortunately, the circumscription of the inhibitory and stimulatory effect of NEM for cellular internalization of M-GGLG-liposomes was ambiguous to define. There was no doubt that at relatively high concentration (e.g., 100 μ M) of NEM for long time (e.g., 24 hr)

Chapter 5

incubation, the cell viability was almost zero and morphological changes in HeLa, HCC1954, MDA-MB-468 and COS-7 cells were observed. Therefore, we suggested that high concentration of NEM would lead formation of membrane pores so that liposomes with a proper diameter could flow into the cytoplasm, resulting in an increased cellular uptake.

References

- [1] Hogg PJ. Disulfide bonds as switches for protein function. *Trends Biochem Sci.* 2003;28:210-4.
- [2] Arner ES, Holmgren A. Physiological functions of thioredoxin and thioredoxin reductase. *European journal of biochemistry / FEBS.* 2000;267:6102-9.
- [3] Wilkinson B, Gilbert HF. Protein disulfide isomerase. *Bba-Proteins Proteom.* 2004;1699:35-44.
- [4] Arunachalam B, Phan UT, Geuze HJ, Cresswell P. Enzymatic reduction of disulfide bonds in lysosomes: Characterization of a Gamma-interferon-inducible lysosomal thiol reductase (GILT). *P Natl Acad Sci USA.* 2000;97:745-50.
- [5] Torres AG, Gait MJ. Exploiting cell surface thiols to enhance cellular uptake. *Trends in biotechnology.* 2012;30:185-90.
- [6] Saito G, Swanson JA, Lee KD. Drug delivery strategy utilizing conjugation via reversible disulfide linkages: role and site of cellular reducing activities. *Advanced drug delivery reviews.* 2003;55:199-215.
- [7] Aubry S, Burlina F, Dupont E, Delaroche D, Joliot A, Lavielle S, et al. Cell-surface thiols affect cell entry of disulfide-conjugated peptides. *FASEB journal : official publication of the Federation of American Societies for Experimental Biology.* 2009;23:2956-67.
- [8] Sahay G, Alakhova DY, Kabanov AV. Endocytosis of nanomedicines. *Journal of Controlled Release.* 2010;145:182-95.
- [9] Ferrari DM, Soling HD. The protein disulphide-isomerase family: unravelling a string of

Chapter 5

folds. *Biochem J.* 1999;339 (Pt 1):1-10.

[10] Noiva R. Protein disulfide isomerase: the multifunctional redox chaperone of the endoplasmic reticulum. *Seminars in cell & developmental biology.* 1999;10:481-93.

[11] Couet J, de Bernard S, Loosfelt H, Saunier B, Milgrom E, Misrahi M. Cell surface protein disulfide-isomerase is involved in the shedding of human thyrotropin receptor ectodomain. *Biochemistry.* 1996;35:14800-5.

[12] Essex DW, Li M, Miller A, Feinman RD. Protein disulfide isomerase and sulfhydryl-dependent pathways in platelet activation. *Biochemistry.* 2001;40:6070-5.

[13] Goplen D, Wang J, Enger PO, Tysnes BB, Terzis AJ, Laerum OD, et al. Protein disulfide isomerase expression is related to the invasive properties of malignant glioma. *Cancer research.* 2006;66:9895-902.

[14] Lahav J, Gofar-Dadosh N, Luboshitz J, Hess O, Shaklai M. Protein disulfide isomerase mediates integrin-dependent adhesion. *FEBS letters.* 2000;475:89-92.

[15] Jain S, McGinnes LW, Morrison TG. Thiol/disulfide exchange is required for membrane fusion directed by the Newcastle disease virus fusion protein. *Journal of virology.* 2007;81:2328-39.

[16] Abell BA, Brown DT. Sindbis virus membrane fusion is mediated by reduction of glycoprotein disulfide bridges at the cell surface. *Journal of virology.* 1993;67:5496-501.

[17] Pinter A, Kopelman R, Li Z, Kayman SC, Sanders DA. Localization of the labile disulfide bond between SU and TM of the murine leukemia virus envelope protein complex to a highly conserved CWLC motif in SU that resembles the active-site sequence of thiol-disulfide exchange enzymes. *Journal of virology.* 1997;71:8073-7.

[18] Wallin M, Ekstrom M, Garoff H. Isomerization of the intersubunit disulphide-bond in Env controls retrovirus fusion. *The EMBO journal.* 2004;23:54-65.

[19] Gilbert J, Ou W, Silver J, Benjamin T. Downregulation of protein disulfide isomerase inhibits infection by the mouse polyomavirus. *Journal of virology.* 2006;80:10868-70.

Chapter 5

- [20] Fenouillet E, Barbouche R, Courageot J, Miquelis R. The catalytic activity of protein disulfide isomerase is involved in human immunodeficiency virus envelope-mediated membrane fusion after CD4 cell binding. *The Journal of infectious diseases*. 2001;183:744-52.
- [21] Markovic I, Stantchev TS, Fields KH, Tiffany LJ, Tomic M, Weiss CD, et al. Thiol/disulfide exchange is a prerequisite for CXCR4-tropic HIV-1 envelope-mediated T-cell fusion during viral entry. *Blood*. 2004;103:1586-94.
- [22] Hogg PJ. Disulfide bonds as switches for protein function. *Trends Biochem Sci*. 2003;28:210-4.
- [23] Wouters MA, Lau KK, Hogg PJ. Cross-strand disulphides in cell entry proteins: poised to act. *BioEssays : news and reviews in molecular, cellular and developmental biology*. 2004;26:73-9.
- [24] Locker JK, Griffiths G. An unconventional role for cytoplasmic disulfide bonds in vaccinia virus proteins. *The Journal of cell biology*. 1999;144:267-79.
- [25] Jahn R, Lang T, Sudhof TC. Membrane fusion. *Cell*. 2003;112:519-33.
- [26] Chen YA, Scheller RH. SNARE-mediated membrane fusion. *Nature reviews Molecular cell biology*. 2001;2:98-106.
- [27] Dickerhof N, Kleffmann T, Jack R, McCormick S. Bacitracin inhibits the reductive activity of protein disulfide isomerase by disulfide bond formation with free cysteines in the substrate-binding domain. *The FEBS journal*. 2011;278:2034-43.
- [28] Mandel R, Ryser HJ, Ghani F, Wu M, Peak D. Inhibition of a reductive function of the plasma membrane by bacitracin and antibodies against protein disulfide-isomerase. *Proc Natl Acad Sci U S A*. 1993;90:4112-6.

Chapter 6 Conclusions and prospect

6.1. Conclusions

6.1.1. Physical and biological evaluation of maleimide-modified liposomes

6.1.2. Mechanisms of maleimide-mediated advanced drug delivery

6.2. Prospect

6.2.1. Application of thiol-reactive moieties on advanced drug delivery system

6.2.2. Further investigation of the biological function of cellular thiols

6.1. Conclusions

Maleimide is a thiol-reactive compound/moiety which contains unsaturated imide. Its NH group can be substituted by alkyl or aryl groups such as methyl or phenyl. Maleimide can also be linked to polymer such as polyethylene glycol chains, which is widely used to conjugate with the cysteine residues of proteins.

In my research, maleimide-PEG lipid was utilized for the surface modification of liposomes (from pH-sensitive GGLG-liposomes to obtain M-GGLG-liposomes) served as an advanced drug delivery system. (Fig.6-1)

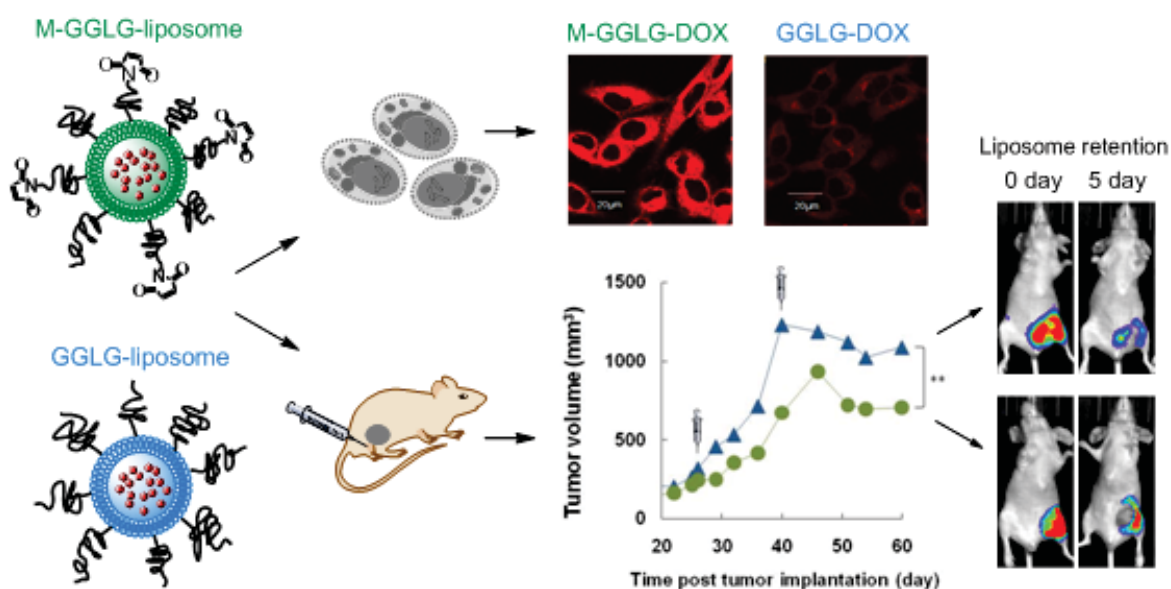


Fig. 6-1. Graphic abstract of the experimental design and applications of maleimide-modified liposomes on advanced drug delivery.

6.1.1. Physical and biological evaluation of maleimide-modified liposome

With a small amount of maleimide-modification (0.3 mol%), the physical properties such as size distribution, dispersibility, drug encapsulation efficiency, drug/lipid ratio, drug leakage rate and pH-sensitivity were not significantly influenced by comparison of M-GGLG-liposomes to GGLG-liposomes. However, M-GGLG-liposomes were more rapidly

(i.e., ≥ 2 -fold) internalized into HeLa, HCC1954 and MDA-MB-468 cells by comparison to GGLG-liposomes. Moreover, the saturation of the cellular uptake of M-GGLG-liposomes was also significantly increased. On the other hand, the cytotoxicity experiments showed that empty liposomes of both GGLG and M-GGLG were biocompatible in all the cell lines tested under all the experimental conditions. Thus the significantly increased cytotoxicity of DOX-encapsulating M-GGLG-liposomes indicates an efficient cellular uptake and subsequently intracellular drug delivery of DOX from M-GGLG-liposomes. *In vivo*, M-GGLG-liposomes encapsulating doxorubicin (M-GGLG-DOX-liposomes) showed a more potent antitumor effect than GGLG-DOX-liposomes and the widely used DPPC-DOX-liposomes after two subcutaneous injections around breast cancer tissue in mouse. The biodistribution of liposomes in this model was observed using an IVIS imaging system, which showed that M-GGLG-liposomes were present for significantly longer at the injection site by comparison with GGLG-liposomes.

6.1.2. Mechanisms of maleimide-mediated enhanced drug delivery

Because the lipid composition and physical properties of M-GGLG- and GGLG-liposomes was similar, the maleimide modification is supposed to be the key factor that led the enhanced drug delivery efficiency of M-GGLG-liposomes both *in vitro* and *in vivo*. Maleimide specifically conjugates the thiol of cysteine residues, thus the interaction of maleimide and thiols during the cellular internalization played an important role in the improved biological properties of M-GGLG-liposomes by comparison with GGLG-liposomes.

The intracellular trafficking of M-GGLG-liposomes was independent from the conventional endocytic pathways such as clathrin-mediated endocytosis, caveolae-mediated endocytosis and macropinocytosis since the inhibitors of these endocytotic pathways did not significantly suppressed the cellular uptake of M-GGLG-liposomes in comparison with that of GGLG-liposomes. However, the cellular thiols are relatively necessary for the enhanced

cellular uptake of M-GGLG-liposomes. By the treatment of thiol blockers and PDI inhibitors such as *N*-ethylmaleimide, bacitracin and DTNB, the cellular uptake of M-GGLG-liposomes was inhibited while that of GGLG-liposomes was not. Meanwhile, the confocal microscopic observation of the subcellular distribution of liposomes after cellular internalization suggested the location of both GGLG- and M-GGLG-liposomes being in lysosomes. Therefore, it was indicated that thiol-mediated cellular internalization of maleimide-modified liposomes is a novel endocytosis which is independent from the conventional endocytic pathways.

On the other hand, the biological studies also hinted an additional function of maleimide analogue NEM as a stimulator of membrane fusion/poration. With a high concentration (e.g., 100 μ M) of NEM incubation with cells, the cellular uptake of both GGLG- and M-GGLG-liposomes was increased. Because NEM is reactive to the membrane fusion proteins (e.g., SNARE-mediated membrane fusion), it is likely that maleimide analogues interfere with the fusion proteins so that the cell membrane permeability is increased. However, at low concentration of NEM (e.g., 0.01 nM), it functions as an inhibitor of the cellular uptake of M-GGLG-liposomes for the reason that redox-regulating enzymes such as PDI widely exist to protect the cell from external oxidative stress. Hence, NEM first encounters these thiol-related enzymes rather than other proteins. In this instance, NEM blocks the active sites for enhanced cellular uptake of M-GGLG-liposomes and further causes the decreased cellular internalization of M-GGLG-liposomes. Following the concentration of NEM increasing, the thiol-related reductive enzymes/sites are gradually saturated or blocked, which subsequently allows NEM to interfere with other membrane proteins such as fusion proteins SNAREs.

In conclusion, the functions of maleimide moiety are dual, i.e., at low concentrations as a blocker of surface thiols and at high concentrations as a stimulator of membrane fusion/poration. For M-GGLG-liposomes, the maleimide moiety could conjugate with cellular thiols which facilitate the cellular internalization of M-GGLG-liposomes, and may also

increase the membrane fusion potency at a relatively high concentration to increase the membrane permeability of M-GGLG-liposomes.

6.2. Prospect

6.2.1. Application of thiol-reactive moieties on advanced drug delivery system

In this research, maleimide was first utilized to practice the novel strategy of enhanced cellular uptake on 'smart' liposomes mediated by cell surface thiols. Maleimide specifically conjugates thiols in reductive form, thus it is supposed to be an excellent model to study the enhanced cellular uptake effect and the mechanisms of intracellular trafficking. However, maleimide is an exogenous compound, the biological function of which is still not thoroughly investigated. Therefore, endogenous thiols such as glutathione and cysteine are considered to be more preferable to be intensively employed, especially in clinical applications with high biocompatibility and easy and safe metabolism.

The *in vivo* application of maleimide-modified liposomes was also discussed by using sc administration for the reason that sc environment contains much less active factors or proteins that express free thiols and inactivate maleimide than iv environment. Unfortunately, it should be noted that this application is still limited to solid tumor, and intravenous (iv) administration is more often used clinically for anticancer therapy, especially in metastatic carcinomas. Even though, sc administration should not be underestimated since it can at the same time deliver anticancer drugs to local lymph nodes which benefit the suppression of tumor diffusion into circulatory system and further invasion to other tissues. Therefore, sc administration is considered as an adjuvant therapy to consolidate the efficacy after tumor resection or iv treatment of anticancer drugs.

For the application of thiol-reactive nanoparticles by iv administration, further investigation of inactivation is needed. It is also supposed that in the blood circulatory system, the free thiols on proteins are hidden in the inner side or sheltered in the groove section of

protein so as to avoid the oxidation from stressful milieus. Therefore, it is not that easy for maleimide to attach and bind to the proteins in circulatory system indeed. In case of the unexpected binding, oxidative form of thiols are recommended such as disulfide, because it has been reported that disulfide modification can also be facilitated by PDI and increase the cellular uptake of some peptides and nanoparticles.

6.2.2. Further investigation of the biological function of cellular thiols

Cell thiols are numerous and extensively exist in cell surface. By utilizing the cellular thiols, enhanced cellular uptake can be obtained. Therefore, it is beneficial to study the distribution of surface thiols in different cell lines in order to discover appropriate targets for thiol-reactive nanoparticles in advanced drug delivery.

In this study, I revealed the maleimide-mediated enhanced cellular uptake is a novel endocytic pathway which is independent from the conventional endocytic pathway, i.e., clathrin-mediated endocytosis, caveolae-mediated endocytosis and macropinocytosis. However, the key proteins that directly facilitate or relate to the endocytosis of thiol-reactive compounds need to be further investigated. These proteins have a great potential to become novel targets for enhanced cellular uptake of drug carriers.

Moreover, the biological functions of maleimide on fusion proteins also needs to be further studied. For example, the determination of the fusion protein that conjugates maleimides or other thiol-reactive compounds, and its function in different cell lines; and the dose-effect relationship of maleimide. The fusion proteins that play important roles in enhanced permeability are thought to be applicable in the target design of drug carriers to improve the drug delivery efficiency. And membrane fusion-mediated drug delivery is also promising to become a novel strategy in DDS.

Academic Achievements

List of Publications

1. Tianshu Li, Shifang Lu, Lei Xing, Guichun Lin, Zhu Guan, Zhenjun Yang. “A new strategy for the synthesis of 3-deazaneplanocin A”, *J. Chin. Pharm. Sci.* 19 (2010) 436-442.
2. Tianshu Li, Shinji Takeoka. “A novel application of maleimide for advanced drug delivery: *in vitro* and *in vivo* evaluation of maleimide-modified liposomes”, *Int. J. Nanomedicine*, accepted.

Symposiums

1. Tianshu Li, Shifang Lu, Zhenjun Yang. “Synthesis and evaluation of Neplanocin A analogues as anticancer and antiviral drugs”, 6th National Organic Chemistry Conference of Chinese Chemical Society, *oral presentation*. 2009.08.
2. Tianshu Li, Takuya Amari, Shinji Takeoka. “Preparation and evaluation of amino acid-containing liposomes”, 33rd Annual Meeting of Japan Biomaterial Society, *poster presentation*. 2011.10.
3. Tianshu Li, Shinji Takeoka. “Preparation and evaluation of amino acid-containing liposomes”, Germany-Japan Joint Symposium for Diamond Researchers on Sustainable Life Science Innovation, *oral presentation*. 2011.12.
4. Tianshu Li, Shinji Takeoka. “Preparation and evaluation of amino acid-containing liposomes”, Japan-India Joint Workshop on “Biomedical Research”, *poster presentation*. 2012.02.
5. Tianshu Li, Shinji Takeoka. “Using maleimide-modification to improve the properties of liposomes for advanced drug delivery”, 6th Shinjuku Biomaterial Conference, *oral presentation*. 2013.01.

6. Tianshu Li, Shinji Takeoka. “Preparation and biological evaluation of maleimide-modified liposomes for advanced drug delivery”, 2nd International Conference on Biomaterial Science in Tsukuba, *poster presentation*. 2013.03.

7. Tianshu Li, Shinji Takeoka. “*In vitro* and *in vivo* evaluation of maleimide-modified liposome for drug delivery”, 245th American Chemical Society Meeting & Exposition, *oral presentation*. 2013.04.

Acknowledgement

The presented thesis is the collection of the studies which have been carried out under the guidance from Professor Dr. Shinji Takeoka, Department of Life Science and Medical Bioscience, Graduate School of Advanced Science and Engineer in Waseda University from September, 2010 to July, 2013. The author expresses the greatest acknowledgment to Professor Dr. Takeoka for his valuable suggestions and continuous instruction and encouragement during her Ph.D. study. The author also expresses her sincere gratitude to Professor Dr. Yasuo Ikeda and Professor Dr. Nobuhito Goda for their precious and constructive advice on this study and their great effort as judging committees of this doctoral thesis.

The author acknowledges to Dr. Keitaro Sou for his valuable suggestions on the preparation and evaluation of liposomal drug delivery system. The author also acknowledges Dr. Takuya Amari for his considerable help on the early stage of her laboratory work. Moreover, the author would like to show gratitude to Dr. Yosuke Okamura, Dr. Toshinori Fujie, Dr. Satoshi Arai, Dr. Atsushi Murata, Dr. Satya Ranjan Sarker, Dr. Hong Zhang, Mr. Akihiro Saito, Miss Sunyun Tan, Mr. Chen-Yu Hsieh, Miss Yumiko Aoshima, Mr. Shota Hirosawa and Miss Risa Yasumi for their precious advice and friendly encouragement. In addition, the author would like to appreciate the kindness help from all the other members in Takeoka Laboratory, including Mr. Kabuto Iida, Mr. Keisuke Ito, Mr. Norihiko Kato, Mr. Takuya Tajima, Miss Mami Doi, Mr. Gen Noguchi, Mr. Atsushi Fujiyama, Mr. Ryosuke Shiraishi, Mr. Kenta Kakiuchi, Mr. Shoichiro Suzuki, Miss Mao Fujii, Mr. Ryosuke Hokama, Mr. Mitsumasa Homma, Mr. Kento Yamagishi, Mr. Zehui Yang, Mr. Yuya Ishiduka, Miss Aiko Oue, Mr. Katsuhiko Sato, Mr. Kazuaki Sawaki, Mr. Takuya Miyagawa and Miss Urara Watanabe.

Finally, the author would like to express her great gratitude to China Scholarship Council for financial support on her daily life, and her family for their emotional support on her continuous study/research life. The author also would like to thank all her friends that used to help her with any difficulty, who are priceless treasure in her life.

July 2013
Tianshu Li